Journal of Polymer Science: Part C, Polymer Symposia, No. 3

Morphology of Polymers

American Chemical Society Symposium

Held at Los Angeles, California, April 4-5, 1963

edited by *T. G. Rochow*

American Cyanamid Company, Stamford, Connecticut

published by INTERSCIENCE PUBLISHERS a division of John Wiley & Sons, Inc.

No. 3

Journal of Polymer Science, Part C, POLYMER SYMPOSIA

Morphology of Polymers

edited by T. G. ROCHOW

American Cyanamid Company,
Stamford, Connecticut

American Chemical Society Symposium
Held at Los Angeles, California, April 4–5, 1963

published by INTERSCIENCE PUBLISHERS,
a division of John Wiley & Sons, Inc.

JOURNAL OF POLYMER SCIENCE, PART C, *Polymer Symposia*

Editorial Board: R. M. Fuoss, J. J. Hermans, H. Mark, H. W. Melville, C. G. Overberger, G. Smets

Published at irregular intervals by Interscience Publishers, a Division of John Wiley & Sons, Inc. Publication Office at 20th and Northampton Streets, Easton, Pennsylvania. Executive, Editorial, and Circulation Offices at 605 Third Avenue, New York 16, New York. Subscription price, $154.00 per volume (including Part A: General Papers; and Part B: Polymer Letters). Foreign postage, $3.50 per volume (including Parts A and B).

Copyright © 1963, by John Wiley & Sons, Inc., Printed in U.S.A.

Introduction

In 1958 the former A.C.S. Division of Paint, Plastics, and Printing Ink Chemistry, with A. L. Alexander as chairman, suggested a symposium on the microscopy and optical properties of coatings. At the time, we felt that the morphology of coatings had not been sufficiently studied and correlated with composition and properties. Since then, however, interest and activity have increased markedly. By 1962 the present Division of Organic Coatings and Plastics Chemistry, W. O. Bracken, Chairman-Elect proposed a symposium on "the effect of molecular weight, macromolecular weight distribution, polymer structure, and polymer composition on morphology of plastics." Obviously "morphology" is taken broadly, as authors Chen and Grabar express it in their paper, "to include a range of characteristics from external shape of large objects to submicrographic features, extending to dimensions of the crystalline lattice" (or amorphous network).

We proceeded to organize the symposium on the basis of a previously published framework.* Within this framework the parameters of morphology, composition, and properties are considered on four levels of *macromolecular organization:*

Level	Morphology	Composition	Properties
I	Discrete molecule	Atoms in space	Chemical substance
II	Molecules in 2 dimensions	Molecules in interfaces	Latex, fiber, film
III	Molecules in 3 dimensions	Single phase	Amorphous or crystalline
IV	Whole material	System of phases	Practical article

Both ranks and files are not always distinctly defined. And the beginning as well as the end of the classification is open. For example, W. O. Statton began this symposium with a discussion of parts of macromolecules. Proceeding on Level I were papers by V. G. Peck and L. D. Moore, Jr. and by M. J. Richardson on electron microscopically observed morphology of macromolecular domains in polymers. T. Gillespie concluded the first session with an assessment of molecular configuration and entanglement by measurements and interpretation of viscosity.

The second session, moderated by F. R. Eirich, was about the morphology of macromolecules associated chiefly in a surface. E. B. Bradford and

* Rochow, T. G., Resinography of High Polymers, part of the A.C.S. Symposium on Analysis of High Polymers, sponsored by the Analytical Division (J. Mitchell, Jr.), St. Louis, March, 1961; *Anal. Chem.*, **33**, 1816 (1961).

J. N. Vanderhoff discussed the colloidal interfaces in synthetic lattices. E. H. Erath and M. Robinson described the colloidal particles in thermosetting resins and H. P. Wohnsiedler discussed the particulate morphology of molded melamine-formaldehyde resin. J. P. Berry tied this session with the next one by correlating the morphology of fracture surfaces with treatment and properties of three dimensional pieces.

R. S. Stein moderated the third session, which was concerned with the crystalline phase. H. P. Wohnsiedler read the paper by C. S. Hsia Chen and D. G. Grabar, which pertained to polymorphism in a crystalline monomer and its effects on polymerization. N. K. J. Symons discussed the morphology of single crystals either grown from solution or from the melt. F. P. Price and H. D. Keith divided the discussion of a special type polycrystalline aggregate, the spherulite.

W. O. Bracken, Chairman-Elect of the Division, introduced the fourth and final session. There has been so much progress in studying crystalline polymers that there were two more papers in the area. One was by F. R. Anderson who studied brittle fractures of isothermally bulk-crystallized polyethylene. The other was by K. Sasaguri and R. S. Stein on the relationship between morphology and deformation of polyolefins. Then C. W. Hock spoke on the importance of producing a polyphase "alloy" by interaction of two components in order to obtain optimum strength in adhesives. T. G. Rochow concluded the symposium by reading M. C. Botty's paper on the morphology of some other polyphase solids.

T. G. Rochow

Central Research Division
American Cyanamid Co.
Stamford, Connecticut

Contents

MACROMOLECULAR DOMAINS

W. O. Statton: Studies of Matrix Rigidity to Determine Intimate Morphology . . 3

Virgil G. Peck and Louis D. Moore, Jr.: Morphology of Large Molecules in Polyethylene 19

M. J. Richardson: Molecular Weights of Amorphous Polymers by Electron Microscopy 21

T. Gillespie: The Use of Viscosity Data to Assess Molecular Conformation and Entanglement in Dilute Polymer Solutions 31

MORPHOLOGY OF SURFACES

E. B. Bradford and J. W. Vanderhoff: The Morphology of Synthetic Latexes . . 41

Edward H. Erath and Morton Robinson: Colloidal Particles in the Thermosetting Resins 65

H. P. Wohnsiedler: Morphology of Molded Melamine-Formaldehyde 77

J. P. Berry: The Morphology of Polymer Fracture Surfaces 91

THE CRYSTALLINE PHASE

C. S. Hsia Chen and D. G. Grabar: Morphological Aspects of Polymerization in the Solid State 105

N. K. J. Symons: The Morphology of Crystalline Polymers, with Especial Reference to Single Crystals Grown from the Molten State 109

Fraser P. Price: Kinetics of Spherulite Formation 117

H. D. Keith: Mechanisms and Kinetics of Spherulitic Crystallization in High Polymers 121

Franklin R. Anderson: Fracture Studies of Isothermally Bulk-Crystallized, Linear Polyethylene 123

Kiichiro Sasaguri and R. S. Stein: Relationship between Morphology and Deformation Mechanisms of Polyolefins 135

POLYPHASE SYSTEMS

Charles W. Hock: The Morphology of Pressure-Sensitive Adhesive Films 139

M. C. Botty: Morphology of Polyphase Solids 151

Author Index 163

Subject Index 164

MACROMOLECULAR DOMAINS

JOURNAL OF POLYMER SCIENCE: PART C NO. 3, PP. 3–8

Studies of Matrix Rigidity to Determine Intimate Morphology

W. O. STATTON, *E. I. du Pont de Nemours and Co., Inc., Carothers Research Laboratory, Wilmington, Delaware*

I. INTRODUCTION

When we think of "polymer morphology," our minds usually bring up a variety of semantic references. We may have a jumble of ideas about techniques of study, models of order and disorder, surfaces, replicas, spheres, fractures, spherulites, lamellae, birefringence, magnification, diffraction, absorption. All of these terms and others are somehow involved in polymer morphology. The problem is to sort out the differences in the techniques or tools of study from the results or knowledge that these techniques can provide. At the risk of confusing the situation even more, this paper will present still another technique for the study of polymer morphology and some typical results which it can provide. This risk is worth taking, I believe, because a new type of information is gained which can be useful in rounding out our complete understanding of polymer morphology.

The technique to be described briefly is nuclear magnetic resonance (NMR) of the solid state of polymers.[1–4] It will be shown that NMR is a technique to measure the local environment of polymer molecules and therefore provides a valuable new approach to the study of polymers. This approach can be given the designation intimate morphology or near neighbor morphology.

II. PRINCIPLES OF THE TECHNIQUE

NMR can be described in the frame of reference of either a physicist or chemist. Most likely the physicist's accurate description will convey very little to us without prolonged study on our part. As chemists, however, it is possible to think of NMR as another form of spectroscopy, like ultraviolet or infrared spectroscopy. The essential difference of NMR is implicit in the three words of its name: nuclear magnetic resonance.[5–7]

Instead of energy levels of electrons that chemists usually consider, we are studying energy levels in *nuclei*. Only certain nuclei with the correct spins are subjects for study; protons are fortunately one of the best and easiest to study and give some of the most informative results. The discussion in this paper will involve only proton magnetic resonance.

These protons will have energy level gaps only if they are put in a very strong *magnetic* field; we must create the energy level difference. This principle is similar to that described years ago by Zeeman for electrons. We can then perform the standard spectroscopic experiment of shining a beam of electromagnetic energy of the correct frequency (or wavelength) on the nuclei and get an absorption and emission as the nuclei change their energy levels. Thus, this is no different from classical spectroscopic studies with which all chemists are familiar. Unfortunately, the number of nuclei in the activated state at one time is so fantastically small (about 5 nuclei/million) that we could never detect the absorption or emission signal. Another principle can be used in order to build this signal to measurable strength. The energy which is used is at a frequency corresponding to a natural precessional frequency of the nucleus. If the energy is applied as a rotating current in a coil surrounding the sample at right angles to the large magnetic field direction, a smaller magnetic field is created which is just right to activate all of nuclei at one time, providing a *resonance* effect. Thus, NMR is a study of the energy absorption at certain natural frequencies by certain nuclei when they are in a strong magnetic field. The usual experiment in IR or UV spectroscopy is to vary the wavelength and to plot emission or absorption; in NMR it usually is easier experimentally to vary the magnetic field strength. Since the field strength is synonymous with frequency by a simple relationship, one usually sees a plot of a spectrum with gauss as the abscissa even though this is somewhat foreign to our thinking. An up-to-date commercial instrument uses an applied magnetic field of about 14,000 gauss and a frequency of electromagnetic radiation of 60 Mcs/sec., which is in the radio frequency range.[8]

At a particular field strength there will be the characteristic absorption line for protons. With the high resolution techniques for studying liquids and solutions, this absorption line is shown to be actually many lines very close together. However, when liquids are frozen into the solid state, the line becomes very, very broad since now there is a local dipolar field caused by neighboring protons. This local field around a proton has an effect on the total magnetic field strength felt by the proton. The greater this dipolar interaction, the greater broadening there is to the resonance line. This is the key to the discussion here; by measuring this broadening effect, we can learn about the near neighbor interaction and the intimate morphology. There is a simple generality that the broader the line, the more rigid is the matrix surrounding the segment; the narrower the line, the more fluidlike is the matrix.

Another way to visualize the cause of differences in spectra is to think of the constraints on segment motion that the surroundings provide. If the matrix offers many constraints on segment mobility, the rigidity is high and the NMR line is broad. If the matrix offers no constraint on segment mobility, the NMR line is narrow like that of a liquid; in fact, the solid is behaving in this motional test like a liquid.

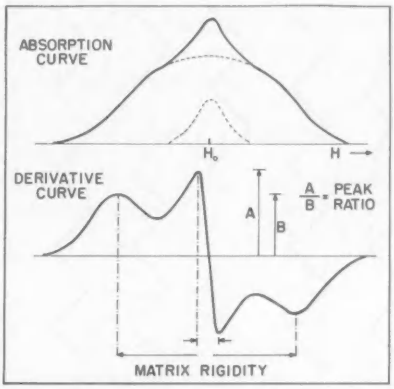

Fig. 1. Complex resonance curve for solid polymers.

Thus, a new sort of information is now obtainable which gives a morphological detail of the highest magnification. Instead of thinking of aggregations of fibrils or lamellae or groups of molecules, one now thinks in terms of the immediate environment around each segment of the molecule. For instance, in linear polyethylene one visualizes a particular CH_2 segment and then asks about the CH_2 segments which are nearest neighbors (the adjacent ones on the same chain and the nearest ones on adjacent chains). As physicists, we would probably not consider this to be morphology and would prefer to talk about relaxation times or correlation times. As chemists, however, we do consider this to be a type of morphology. It is the "end of the line" as we take smaller and smaller portions of the polymer and ask about the shape and form within that portion. We end up with a dynamic view of the environment, but this dynamic view probably is the only one that is significant as we study the morphology of regions approaching atomic dimensions.

The instrumental technique used to obtain the spectra from polymers is complicated and beyond the scope of this paper. Figure 1 shows a typical broad line spectrum at the top and its derivative at the bottom. The usual instrument normally produces this latter derivative curve. The peaks of the derivative curve allow an easy calculation of the width of the broad peak at its maximum slope. This breadth is usually taken as the "half width" or "line width." This is the measure which provides the concept of matrix rigidity discussed above.

An additional, more fluidlike mode of motion is also shown in Figure 1 by the narrow peak at the center of both absorption and derivative curves. Such bi-modal spectra with fused peaks indicate that two modes of motion exist simultaneously in the solid polymer: one motion is constrained and rigid, and the other motion unconstrained and fluidlike. The exact nature of the morphology which can allow such liquidlike fluidity in the solid state is speculative. The existence of the fluidity tells us how the seg-

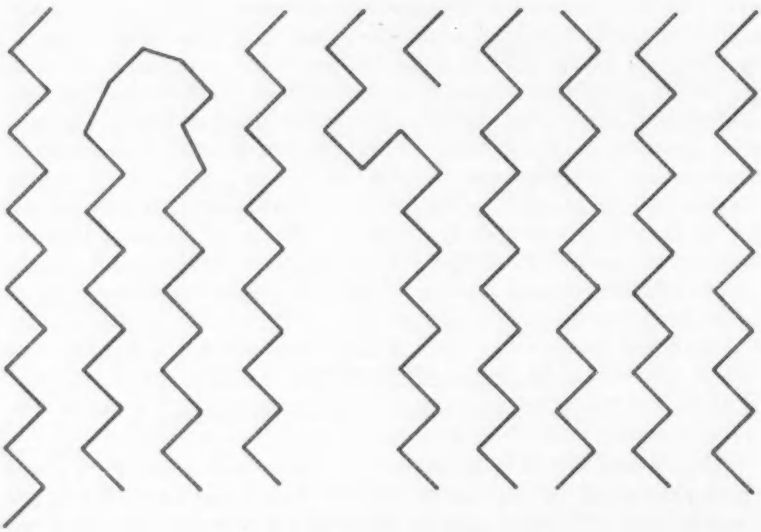

Fig. 2. Possible defect structures in polymer lattices. The zigzag represents the CH_2 groups in a simple polymer chain.

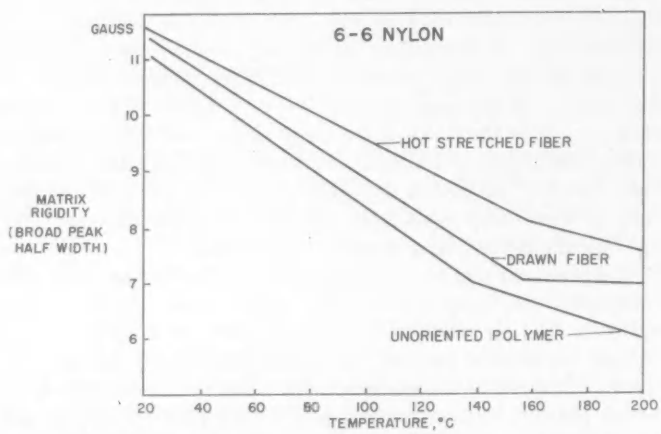

Fig. 3. Matrix rigidity data for unoriented (flake) polymer of 6,6 nylon and fibers drawn from it.

ments do *not* exist; it does not, unfortunately, give us a definite statement of how the segments do exist. However, some clues may be found if we compare polymer NMR spectra to similar spectra from metals and other low molecular weight solids in which the narrow peak is interpreted as due to defects.[9] As sketched in Figure 2, possible defects are shown for portions of simple polyethylene chains. The segments surrounding these

defect areas could have greatly different motion than the ones within a perfect, constrained lattice. Such interpretation is speculative, but it perhaps approximates the actual situation.

III. TYPICAL RESULTS

Studies at elevated temperatures have been especially informative.[10] Figure 3 shows matrix rigidity data for unoriented (flake) polymer of 6,6 nylon and fibers drawn from it. It is obvious that at all temperatures the

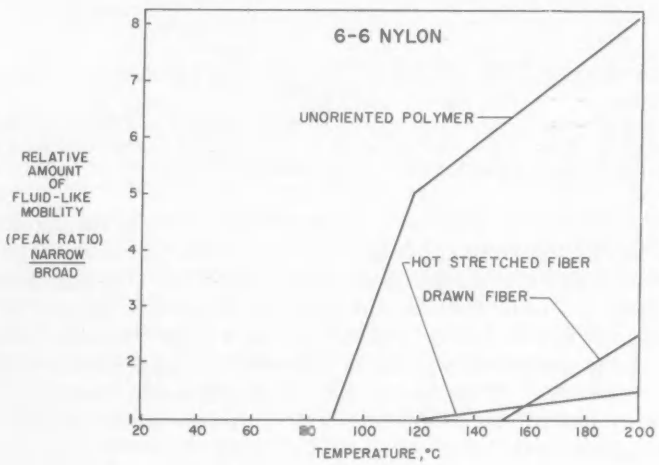

Fig. 4. Measure of the relative amount of the fluidlike mobility of unoriented (flake) polymer of 6,6 nylon and fibers drawn from it.

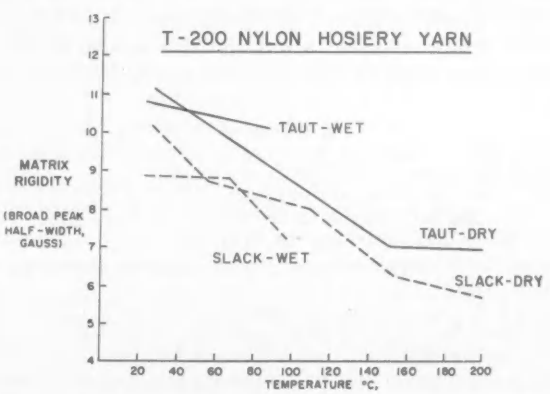

Fig. 5. Difference in the matrix rigidity of T-200 nylon hosiery yarn when fibers are kept at constant length (taut) compared to when they are free to shrink or grow (slack) during heating. Dry or immersed in D_2O.

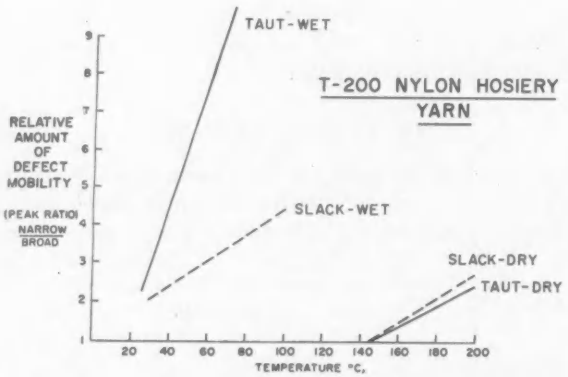

Fig. 6. Difference in the relative amount of defect mobility of T-200 nylon hosiery yarn when fibers are kept at constant length (taut) compared to when they are free to shrink or grow (slack) during heating. Dry or immersed in D_2O.

matrix rigidity of the oriented material is higher than for the unoriented (even though the x-ray crystallinity is lower when oriented). The hot stretching is shown to tighten up the system still more. The same samples are shown in Figure 4 where a measure of the relative amount of the fluidlike mobility is shown. Again, there is a great difference between oriented and unoriented material in amount of fluidlike mobility and its onset temperature. Thus, both measurements tell us that the deformation process to convert from the unoriented to the oriented state is an operation which tightens up the whole system.

The influence of water on hydrogen bonded polyamides has long been known. The data in Figures 5 and 6 show the drastic differences in the two parameters of near neighbor morphology when the fibers are studied wet compared to dried. Figures 5 and 6 also show the difference in results when fibers are kept at constant length (taut) compared to when they are free to shrink or grow (slack) during the heating in the NMR experiment.

References

1. Powles, J. G., *Polymer*, **1**, 219 (1960).
2. Slonim, I. Ya., *Usp. Khim.*, **31**, 609 (1962).
3. Sauer, J. A., and A. E. Woodward, *Rev. Mod. Phys.*, **32**, 88 (1960).
4. Slichter, W. P., *Makromol. Chem.*, **34**, 67 (1959).
5. Jackman, L. M., *Applications of Nuclear Magnetic Resonance Spectroscopy*, Pergamon, N. Y., 1959.
6. Roberts, J. D., *Nuclear Magnetic Resonance*, McGraw-Hill, N. Y., 1959.
7. Varian Associates, *NMR and EPR Spectroscopy*, Pergamon, N. Y., 1960.
8. E.g., Model V-4302, DP-60, Varian Associates, Palo Alto, Calif.
9. Pound, R. V., *J. Phys. Chem.*, **57**, 743 (1953); B. A. Dunnell, L. W. Reeves, and K. O. Strømme, *Trans. Faraday Soc.*, **57**, 372 (1961).
10. Details of these and other results are being submitted for publication.

JOURNAL OF POLYMER SCIENCE: PART C NO. 3, PP. 9–19

Morphology of Large Molecules in Polyethylene*

VIRGIL G. PECK and LOUIS D. MOORE, JR., *Research Laboratories, Tennessee Eastman Company, Division of Eastman Kodak Company, Kingsport, Tennessee*

Long-chain branching in polyethylene has been of considerable interest to a number of investigators in the past several years. However, Billmeyer was the first to describe a method for studying long-chain branching in polyethylene.[1] He determined the weight-average molecular weight of the polyethylene by light scattering and the intrinsic viscosity by the usual means. From the weight-average molecular weight, he calculated the intrinsic viscosity for a linear polyethylene of the same molecular weight. Since chain branching reduces the spatial extension of a molecule of given molecular weight,[2] the intrinsic viscosity is also reduced. Therefore, comparison of the measured viscosity with that calculated for a linear polymer allowed the degree of long-chain branching to be estimated.

Using this method, Billmeyer found that high-pressure polyethylenes, in general, were extensively branched and possessed very broad molecular weight distributions. Since his original measurements were made only at an angle of 90°, no measurements could be made of the angular dependence of scattering. Therefore, no molecular sizes could be calculated from the light-scattering data.

Since this initial work, several papers[3–7] reporting measurements at a number of angles have been published. These studies revealed the presence of very large particles in polyethylene solutions. The results of such a study are shown in Figure 1, which is a Zimm[8] plot of light-scattering data obtained at 11 angles and 5 concentrations of polyethylene.[3] The ordinate of each experimental point is proportional to the concentration divided by the intensity of light scattered at that particular angle and that particular concentration. The abscissa is equal to $\sin^2\theta/2$, where θ is the angle of observation, plus $100\times$ the concentration. The data obtained at each angle are extrapolated to infinite dilution in order to eliminate the effects of interactions between polymer molecules. The infinite dilution data are then extrapolated to zero angle to eliminate the effects of destructive interference of the scattered waves. The intercept of this infinite dilution curve is equal to the reciprocal of the weight-average molecular weight, which, in this case, is equal to 1,410,000.

* Presented at the 144th National Meeting of the American Chemical Society, Los Angeles, California, March 31–April 5, 1963.

The initial slope of the infinite dilution curve is proportional to the Z-average mean square radius of gyration of the particles in solution divided by the weight-average molecular weight.[2,8] In other words, this initial slope is a measure of the spatial dimensions of the scattering particles. This particular sample has a root-mean square radius of 1220 A. It can be seen that plots of this kind give measures of the molecular weight and the size of the particles in solution.

The Zimm plot shown in Figure 1 has a feature which is not usually found in graphs of this type; that is, the initial slopes of the constant angle curves decrease considerably with decreasing angle, the slopes changing by a factor of almost five on going from 135 to 0°. This feature may be interpreted[3,4] as an indication that the particles responsible for the majority of

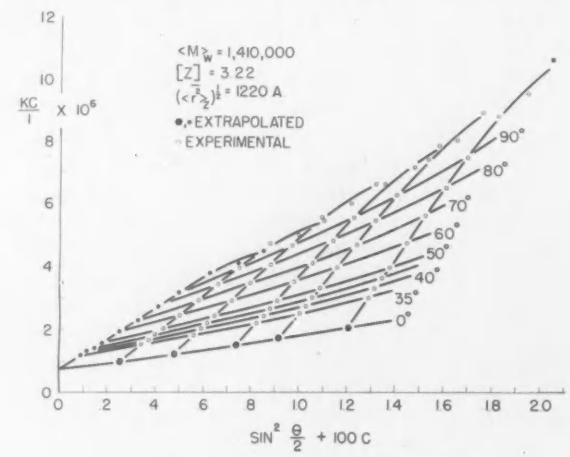

Fig. 1. Zimm plot: polyethylene 1.

the scattering at forward angles are more compact and do not interact as strongly with the solvent as the particles which contribute predominantly to the backward scattering.

Another typical Zimm plot is shown in Figure 2, which is a plot of data for a second polyethylene.[3] Here the scattering pattern shows a pronounced curvature in the infinite dilution curve. This somewhat unusual feature may be interpreted as evidence of a very broad molecular weight distribution.[3,9,10] However, Muus and Billmeyer[7] attributed this unusual curvature and change of slope with angle to the presence of an "insoluble" fraction which is made up of "particles large relative to the wavelength of visible light."

If the particles responsible for this scattering behavior are not truly molecules of polyethylene, they should probably be removed before the solutions are studied in order to avoid an erroneous interpretation of the light-scattering data. If, however, they are molecules of polyethylene,

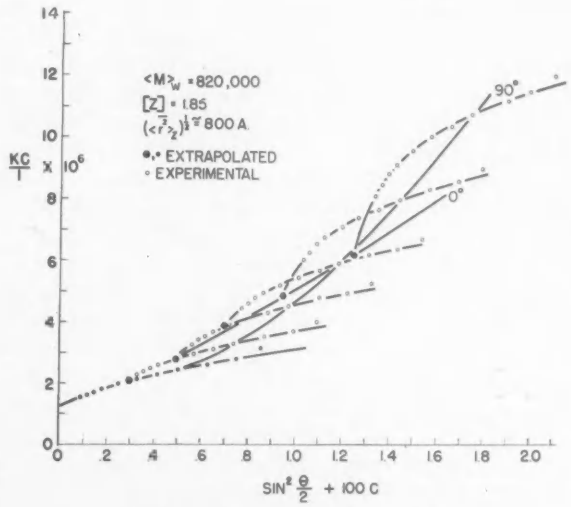

Fig. 2. Zimm plot: polyethylene 2.

they should not be excluded from study as the results would not truly be representative of the sample.

In 1957, we first reported our studies on the particles in some high-pressure polyethylenes. This work involved both light-scattering measurements and electron microscopy. We demonstrated that the particles could be observed in the electron microscope if the appropriate techniques of sample preparation were utilized. The purposes of that study were to gain a deeper insight into the nature of these intensely scattering particles and to determine whether or not they should be removed from the solutions of polyethylenes before study by light scattering. The purpose of the work reported in this paper was to learn more about these particles by concentrating them and studying their behavior in bulk polyethylene.

The origin of the particles which are responsible for these scattering patterns is not well established. However, there are at least four possibilities which we have attempted to investigate. The first possibility is that the particles may be foreign material. Trementozzi[5] found that very large particles were still present in solutions of polyethylene fractions obtained by a fractional precipitation procedure. Fractions of polyethylene have been obtained in our laboratory by an extraction method similar to that of Desreux and Spiegels.[11] Light-scattering measurements on this solution indicated that very large particles with a Z-average size of 1150 A. were present. The infinite dilution curve also showed an initial upward curvature, indicating the presence of high-molecular-weight molecules of extreme branching.

The presence of the large particles in fractions obtained by these two entirely different methods seems to eliminate the possibility that they are

foreign matter, for one would certainly not expect foreign material to be so similar to polyethylene in its solubility characteristics.

The second possibility is that the particles are actually aggregates of molecules. However, this does not seem to be an adequate explanation. Heating the solutions for three days at 125°C. did not appreciably change the scattering. Nicolas[4] made studies of polyethylene in 1-chloronaphthalene, a polar solvent, and in tetralin, a nonpolar solvent, at temperatures ranging from 80 to 125°C. All samples gave consistent scattering patterns. These experiments tend to rule out the possibility of aggregation by simple van der Waals forces or any normal polar forces.

The third possibility, suggested by Muus and Billmeyer, is that there is an "insoluble" fraction of the polymer in the solution. A look at the Zimm plot of one of the samples reported by these workers to have this insoluble fraction, however, indicates a Z-average size which is of the same order as the wavelength of the light used. Furthermore, experiments in our laboratories indicate that with the polyethylene used for the Zimm plot in Figure 1 the large particles were not removed by filtration through filters with a rated pore size of 0.45 μ. A similar filtration of a solution of the polyethylene used for the Zimm plot in Figure 2 resulted in very little change of its scattering envelope. Since the particles are mostly in the range of a few hundred Angstroms in size, as we will later show, they should probably not be referred to as insoluble microgel.

Very high molecular weight molecules are undoubtedly formed by a long-chain-branching mechanism[12,13] in the high-pressure polymerization of ethylene to high conversions. This offers the fourth possibility; namely, that the particles may be highly branched individual molecules. We believe this is the true case.

The particles were first observed several years ago with the electron microscope.[14] Films of high-pressure polyethylene were cast on a glass slide and treated with *m*-xylene at temperatures ranging from room temperature to 80°C. This treatment tended to remove the lower molecular weight fractions and leave the particles exposed. Figure 3 shows the particles as originally observed in these films. They were always found in aggregates such as shown in the figure. The large particles are approximately 500 A. in diameter, and although smaller particles can be observed, it is impossible to measure the lower limit of size.

Pyrolysis of a sample such as this indicated that the particles are actually polyethylene. The sample was heated to 300°C. for up to 168 hr. and checked for number of spheres, intrinsic viscosity, molecular weight, and light-scattering dissymmetry several times during this treatment. It was found that molecular weight and dissymmetry decreased rapidly, as did the number of particles observed in the films. However, the intrinsic viscosity decreased only slightly. This is exactly what might be expected from highly branched molecules of high molecular weight.

Since the number of particles in any of the films were too few to be usable for study of bulk polyethylene, it appeared desirable to concentrate the

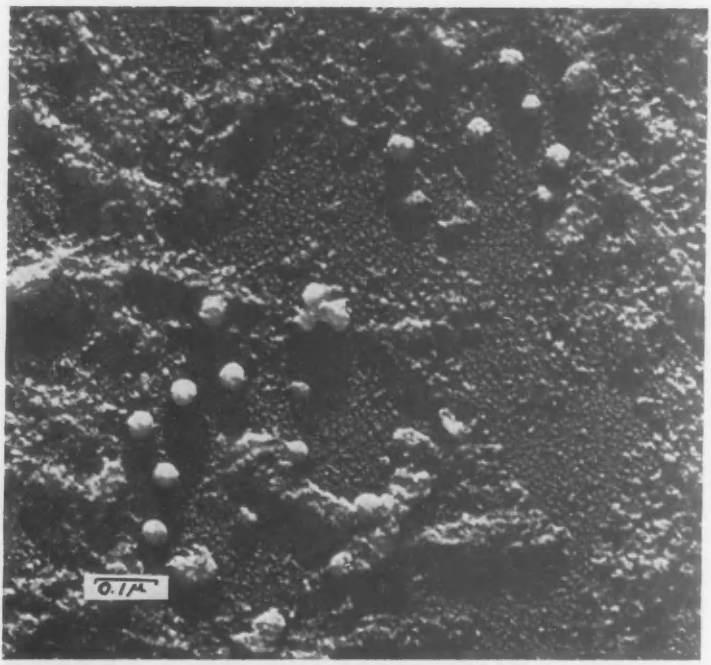

Fig. 3. Etched film of polyethylene.

spheres. Our first attempts involved fractionation, but we were unable to increase the number of particles to any great extent. We also observed that we were unable to etch the resulting films because of the narrow solution temperature range. Consequently, our next efforts were with the ultracentrifuge. Some concentration resulted by the flotation method, but it still was insufficient to be beneficial. The third method involved filtration through millipore filters and proved to be acceptable.

Three solutions of the polyethylene used for the Zimm plot in Figure 1 were made up in 1-chloronaphthalene at different concentrations. These were filtered successively through filters with pore sizes of 0.45, 0.3, 0.22, and 0.1 μ. After each filtration, dissymmetry measurements were made on the filtrate and the filtered material was examined in the electron microscope. The latter was accomplished by washing the filters in hot xylene and spraying this solution onto substrates of polyethylene before shadowing. Solution etching proved useless because of the very narrow fraction of molecular weight, but the spheres were readily observable. Figure 4 shows the material taken from the 0.22-μ filter.

Investigation of the 0.45-μ filter produced insufficient material for examination in the electron microscope. However, when material from the other three filters was examined, it was found that the particles removed by

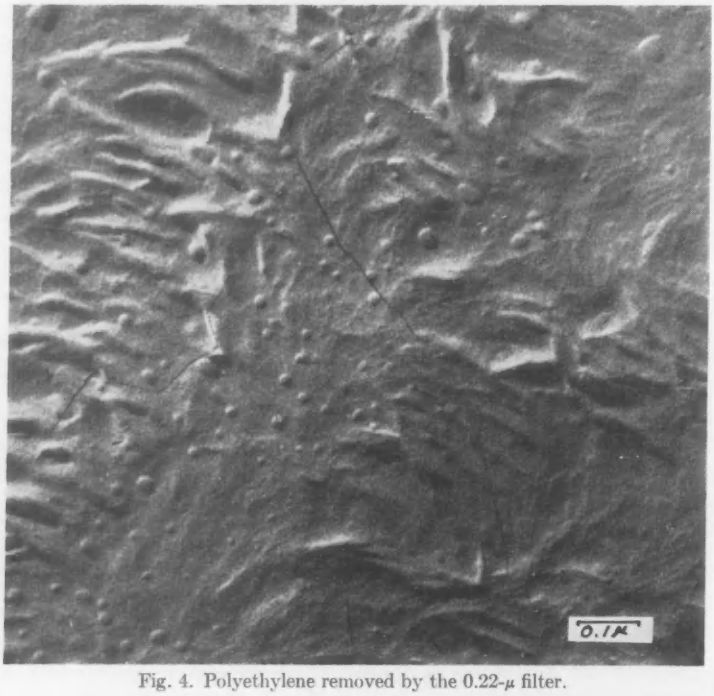

Fig. 4. Polyethylene removed by the 0.22-μ filter.

the 0.3-μ filter ranged from approximately 700 to 800 A. in diameter; those particles on the 0.22-μ filter were approximately 500–700 A.; and those on the 0.1-μ filter were approximately 300–500 A. These sizes generally appear to be three to four times smaller than the pore size of the filter, probably because the particles are swollen when in solution.

TABLE I
Light-Scattering Results after Filtration

Light-scattering results			Concentration after filtration through 0.10-μ filter		
Pore size of filter used, μ	Scattering dissym-metry, Z	Mol. wt. estimated from scattering at 45°, 90°, 135°	Original solution	Amt. found in 5 ml. of soln., G.	Amt. calcd. from orig. soln., G.
Before filtration	3.39	1.52×10^6	Most dilute	0.0073	0.0083
0.45	3.18	1.06×10^6	Intermediate	0.0147	0.0149
0.30	3.04	1.04×10^6	Most concentrated	0.0217	0.0212
0.22	2.84	0.90×10^6			
0.10	2.38	0.50×10^6			

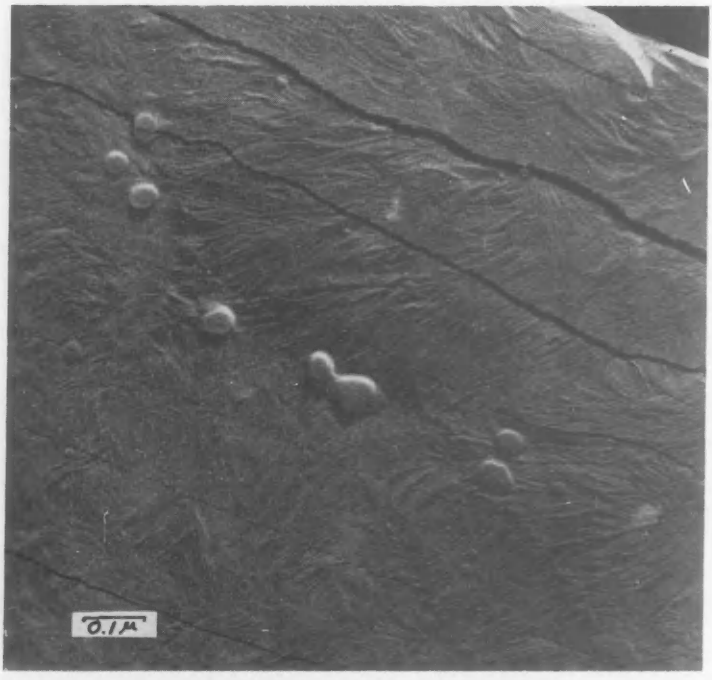

Fig. 5. Polyethylene film calendered and drafted.

Table I summarizes the light-scattering data and gives a measure of the concentration of polymer after the last filtration. This concentration is expressed as the weight of residue after evaporation of solvent from 5 ml. of solution and is compared to that calculated from the original concentration. With the possible exception of the sample of lowest concentration, an insignificant weight of polymer was removed by filtration. Even though very little polymer was removed, there was a progressive change in the light-scattering properties with filtration, the largest change occurring after filtration through the 0.1-μ filter. The Zimm plot for this final filtrate revealed a weight-average molecular weight of 500,000, only a little greater than one-third that of the unfiltered polymer.

Since we were able to concentrate the particles, we decided to add the particles from all filters for study in bulk material so that it would be more representative of the original material. These were placed in hot xylene, and then a small amount of the original polyethylene ($\sim$10% by weight) was added to this solution. A thin film was cast from this solution and picked up on a thick polyethylene film. This composite film was then melted on a glass slide, producing a thick film with an intimate mixture of the spheres concentrated close to one surface. Replication of these surfaces did not show spheres; they were all imbedded in the film.

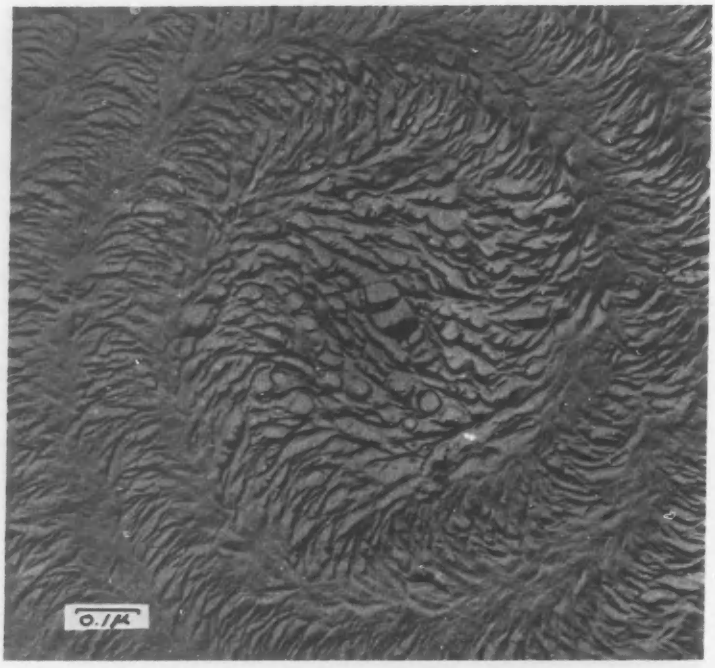

Fig. 6. Spherulite plus spheres in cast polyethylene film.

These films were then submitted to mechanical treatments, such as calendering and drafting. Examination of the surface of a film that had been calendered only still did not reveal any spheres, but after solution etching, a few flat areas which may have been spheres were observed. However, after calendering a film to 3:1 reduction and then drafting approximately 200%, we found flattened spheres, as shown in Figure 5. Calendering flattened the spheres, whereas drafting tended to separate them from the base polymer. They have acted as complete entities within the base polymer in all of our investigations.

We next wondered how the particles would behave when in bulk polymer cast into a film. We, therefore, cast a thin film from a xylene solution of polyethylene plus some of the particle concentrate. This film was shadow cast and examined in the electron microscope. The typical structure of spherulites was found, but at the center of many spherulites there were concentrations of the particles, much as we had observed in our original work several years ago. Figure 6 shows a typical group of spheres at the center of a spherulite. They are partially covered, since this film was unetched.

This work indicated that the spheres tend to aggregate for some still unknown reason. Therefore, results might be different if they could be

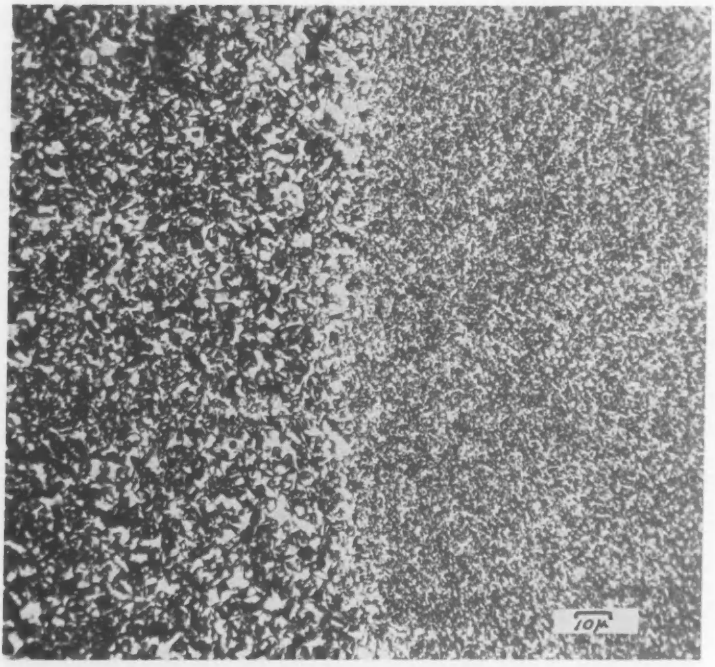

Fig. 7. Effect of ultrasonics on polyethylene containing many spheres.

separated in solution before being used. Treatment in solution with an ultrasonorator proved useful for this purpose. The spheres became well separated and did not reaggregate.

When the previous experiment of casting a film was repeated using an ultrasonorated solution, no aggregates were observed. However, there were indications, in a limited manner, that there were more and smaller spherulites formed. It could not be ascertained whether a particle was associated with each spherulite. For this reason we made a set of films for comparing light transmission data. Figure 7 shows the results. On the left is a film cast from a drop of the solution containing spheres which had been given no ultrasonic treatment. On the right is a film made from the same solution after ultrasonic treatment. These films were heated together on the slide to the melt and then cooled at the same rate so that spherulite formation would be expected to be the same. However, when the spheres are separated there are many more nucleii present to form many small spherulites and, therefore, produce a clear film. The same polyethylene film not containing any added spheres looked like the hazy one on the left.

Single crystals of polyethylene may be easily grown from dilute solutions. Since the spheres always behaved as entities in the bulk polymer, it ap-

peared desirable to observe their action in solution as crystals were grown. Figure 8 shows a single crystal of polyethylene grown from a solution of *m*-xylene which contained some of the concentrated particles. You can see that the crystal grew quite normally, but did not include the spheres as a part of the growth. Once again they were either entrapped or left outside entirely. This indicates that the highly-branched molecules never uncoil in solution; therefore they cannot join in the folded structure of the crystal.

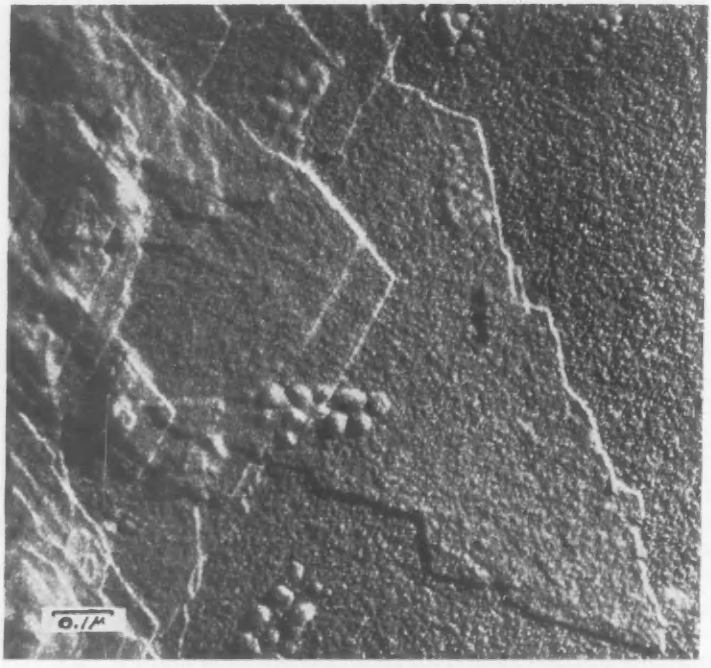

Fig. 8. Single crystal of polyethylene plus spheres.

Finally, we wished to repeat the pyrolysis experiments using the concentrated particles. For this experiment, we sprayed a solution of the particles onto a carbon substrate. Several samples were made, and each examined in the electron microscope after a specified time in the oven at 300°C. The control, which was not heated, contained the spheres. As the samples were heated, the spheres gradually decreased in number, and finally, after 200 hr., had disappeared almost completely, leaving a nearly uniform film of polyethylene on the substrate.

Inasmuch as the spheres behave as separate entities in polyethylene but still have the characteristics of the polymer, we believe that we are studying individual highly branched large molecules of polyethylene. The molecular

weights appear to be one to several millions. The particles should be considered a part of the original polyethylene even though they are there in very few numbers.

References

1. Billmeyer, F. W., Jr., *J. Am. Chem. Soc.*, **75**, 6118 (1953).
2. Zimm, B. H., and W. H. Stockmayer, *J. Chem. Phys.*, **17**, 1301 (1949).
3. Moore, L. D., Jr., *J. Polymer Sci.*, **20**, 137 (1956).
4. Nicolas, L., *Compt. Rend.*, **244**, 80 (1957).
5. Trementozzi, O. A., *J. Polymer Sci.*, **23**, 887 (1957).
6. Kobayashi, T., A. Chitale, and H. P. Frank, *J. Polymer Sci.*, **24**, 156 (1957).
7. Muus, L. T., and F. W. Billmeyer, Jr., *J. Am. Chem. Soc.*, **79**, 5079 (1957).
8. Zimm, B. H., *J. Chem. Phys.*, **16**, 1099 (1948).
9. Benoit, H., *J. Polymer Sci.*, **11**, 507 (1953).
10. Benoit, H., A. M. Holtzer, and P. Doty, *J. Phys. Chem.*, **58**, 635 (1954).
11. Desreux, V., and M. C. Spiegels, *Bull. Soc. Chim. Belges*, **59**, 476 (1950).
12. Roedel, M. J., *J. Am. Chem. Soc.*, **75**, 6110 (1953).
13. Beasley, J. K., *J. Am. Chem. Soc.*, **75**, 6123 (1953).
14. Moore, L. D., Jr. and V. G. Peck, *J. Polymer Sci.*, **36**, 141 (1959).

JOURNAL OF POLYMER SCIENCE: PART C NO. 3, PP. 21–29

The Molecular Weight of Amorphous Polymers by Electron Microscopy

M. J. RICHARDSON,* *Physics and Chemistry of Solids, Cavendish Laboratory, Cambridge, England*

Many physical properties of polymers, both in bulk and in solution, are determined by the molecular weights of the constituent macromolecules. Methods of determining these weights and their distribution are thus of fundamental importance. Normally a number-, weight-, or more complicated average molecular weight is obtained. The full distribution may only be found after many tedious fractionations, the resolution of which decreases as the average molecular weight increases. In addition, molecular weights of the order of a million and above are not easy to determine with accuracy.[1] Such large molecules should, however, be readily visible in the electron microscope in which 5–6 A. resolution may be obtained with suitable specimens. A compact spherical polymer molecule of unit density and molecular weight one million has a diameter of some 150 A.; larger molecules, of course, become progressively easier to see. Thus, if suitable conditions can be found for the deposition of individual, well-defined polymer molecules, a method is available that will extend the range over which accurate molecular weight determinations may be made and which is probably limited only by solubility considerations at the highest molecular weights. This paper will describe an experimental investigation of the conditions needed.

For a number of years now, the electron microscopical observation of various natural macromolecules, such as viruses and proteins, has been a well-established and valuable technique.[2] On the other hand little work has been carried out on synthetic organic polymers. The first important results were obtained by Siegel et al.[3] who looked at several metal-shadowed polystyrene fractions obtained by spraying a solution in a θ solvent on to the supporting film. Particles of approximately the correct size were found. Nasini et al.[4] obtained similar results with polymethyl methacrylate deposited from a mixed solvent. In neither case was the absolute accuracy high due to the limitations imposed by the techniques available at the time. However, recent improvements, both in techniques and instrumentation, suggest that this approach is now one of great promise and worth investigating in some detail. In the work to be described a spray

* Present address: Basic Physics Division, National Physical Laboratory, Teddington, Middlesex, England.

technique was again used. Basically the ideal conditions sought were such that the combination of spray droplet size and polymer concentration gave droplets containing either one or no polymer molecules.

EXPERIMENTAL

Precipitant was added to a solution of the polymer in a good solvent and the mixture sprayed, using a Vaponefrin Nebulizer, onto an evaporated carbon film backed by mica. After metal shadowing, the carbon film was floated off on to copper microscopical grids in the usual way. The shadowing angle was obtained from the length of the shadow cast by polystyrene latex particles, which are known from the shadow-geometry to be true spheres, sprayed on after the polymer.

Occasionally, to investigate the effect of the substrate, the polymer was sprayed on to mica, metal shadowed, backed by evaporated carbon, and finally floated off. For convenience, most preliminary observations on the effects of the various parameters such as solvent composition, substrate, or temperature, were carried out at polymer concentrations of 10^{-3}%. Measurements on individual molecules were made on polymer from 10^{-4} %, or more dilute, solutions. Specimens were examined in a Siemens Elmiskop I microscope operating at 80 Kv. The microscope was calibrated by using the platinum phthalocyanine $(20\bar{1})$ planar spacing of 11.94.

POLYSTYRENE

The change in configuration of a polymer in solution as the solvent power is decreased is well reflected in Figures 1–3. Figure 1 shows polystyrene sprayed from solution in benzene only. The swollen coils collapsed onto the substrate to give a shapeless deposit. As nonsolvent (*n*-butanol) was added the loose coils contracted to eventually give relatively rigid spheres (Fig. 2). In a very poor solvent these spheres themselves agglomerated

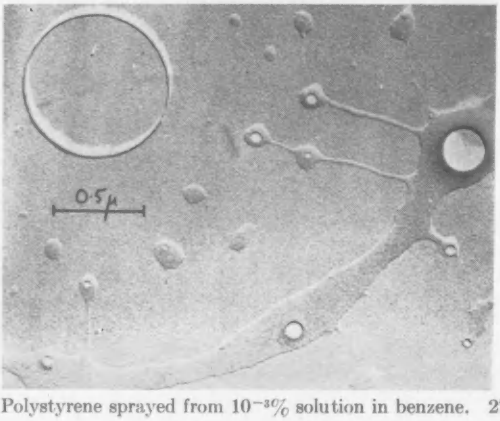

Fig. 1. Polystyrene sprayed from 10^{-3}% solution in benzene. 27,000×.

(Fig. 3). The smaller spheres seen in Figure 2 were shown to be individual molecules by decreasing the polymer concentration but keeping the solvent/nonsolvent ratio constant. On dilution the larger spheres rapidly decreased in size but the diameter of the smaller ones remained constant—although they naturally appeared less often (Fig. 4). The composition of the solvent/nonsolvent mixture required to form individual molecules in this

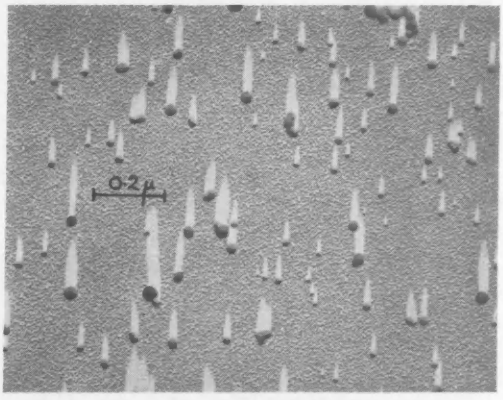

Fig. 2. Polystyrene sprayed from $10^{-3}\%$ solution in benzene(67%)/*n*-butanol. 55,000×.

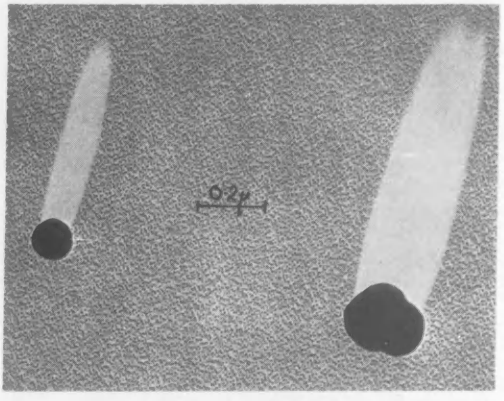

Fig. 3. Polystyrene sprayed from $10^{-3}\%$ solution in benzene(40%)/*n*-butanol. 55,000×.

way was not very critical, a variation of some $\pm 5\%$ having no observable effect. Agglomeration in the region of poorer solvents could be avoided by working at higher dilution. The number of molecules per micrograph was then so small, however, that the number of plates needed to give significant results became inconveniently large.

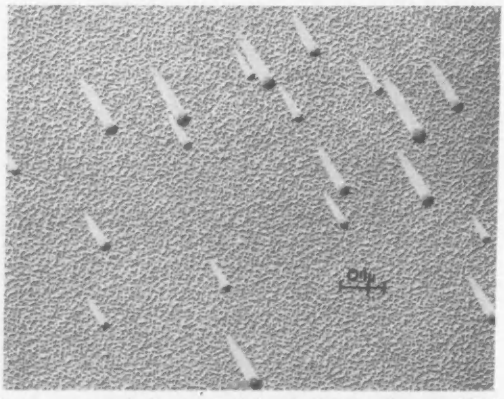

Fig. 4. Polystyrene sprayed from $10^{-4}\%$ solution in benzene(67%)/*n*-butanol. Gold palladium shadowed at $\cot^{-1}$ 6.2. 68,000×.

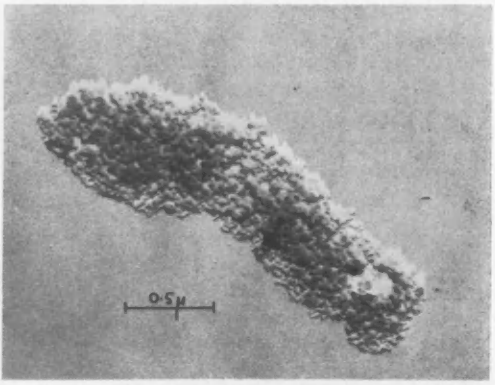

Fig. 5. Same as Figure 2 but sprayed onto mica. 27,000×.

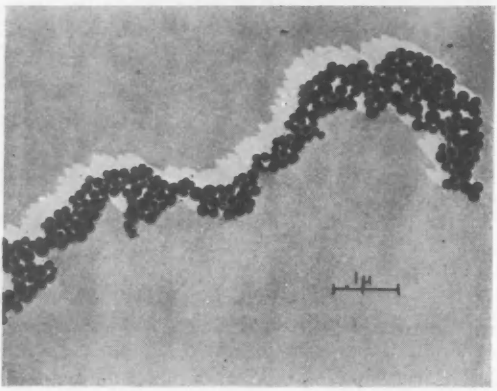

Fig. 6. Same as Figure 3 but sprayed onto mica. 10,000×.

EFFECT OF SUBSTRATE

When the substrate was a mica surface, rather than a carbon film, and conditions were otherwise the same as those in Figures 2 and 3, the results shown in Figures 5 and 6 were obtained. The solvent systems did not wet mica as well as carbon and the droplets, though evaporating rapidly, still had time, on landing, to run together and coalesce to produce islands that were aggregates of individual (Fig. 5) or agglomerated (Fig. 6) polymer molecules.

SOLVENT EFFECTS

Replacement of benzene by chloroform or carbon tetrachloride did not change the general behavior discussed above. Again, involatile nonsolvents behaved similarly to *n*-butanol. However, when the precipitant had a vapor pressure similar to, or higher than, that of the solvent no suitable solvent/nonsolvent combination was ever found which led to the *exclusive* formation of molecular spheres of the type shown in Figure 4. Aggregates were always present to some extent.

In general, therefore, polystyrene sprayed at a concentration of the order of 10^{-4}% from solution in mixed solvents appeared as film, a mixture of individual molecular spheres and large aggregates, or large aggregates only, as the power of the solvent mixture was progressively decreased. Exclusive formation of single spherical polymer molecules only occurred when three conditions were satisfied. First, the composition of the bulk solution had to be such that it was still "good" only in the sense that polymer–solvent interactions were *just* favored relative to those between polymer segments. Polymer molecules thus had a slightly expanded configuration but little tendency to aggregate. Secondly, the solution had to wet the substrate so that if a droplet contained several molecules these were immediately well dispersed from each other on hitting the substrate. Thirdly, the nonsolvent component in the dispersed droplet had to be less volatile than the solvent so that on drying a progressively poorer solvent remained. It was only in this drying stage that polymer molecules assumed the required compact configuration.

OTHER GLASSY POLYMERS

The preceding remarks seem to apply to glassy amorphous polymers as a whole although, as would be expected, various detail differences have been found. The case of polyacrylonitrile will illustrate this. Good solvents for this polymer, such as dimethyl formamide, are rather involatile. Polyacrylonitrile from most dimethyl formamide/nonsolvent combinations looked very similar to that of Figure 7. In a sense the situation was similar to that occurring in Figure 5. The solvent phase was so involatile that the droplets formed a liquid film on the substrate. As it dried this film merely left a few large islandlike aggregates of polymer. If, however, the

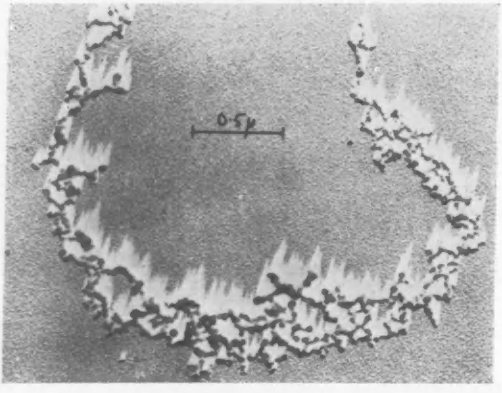

Fig. 7. Polyacrylonitrile sprayed from 10^{-3}% solution in dimethyl formamide(50%)/3-heptanone. 27,000×.

carbon film was heated to 80°C. to speed up the rate of evaporation the behavior of polyacrylonitrile exactly paralleled that of polystyrene on changing the power of the solvent.

RUBBERY POLYMERS

So far only glassy polymers have been discussed. Attempts to observe molecules of rubbery polymers by techniques similar to any of the above were totally unsuccessful. Indeed, attempts to produce even large spherical aggregates failed. In every case all that was obtained was a filmy coating on the carbon film with, at most, a few surface dimples to hint at any fine structure. The contrast between glassy and rubbery polymers was immediate and striking.

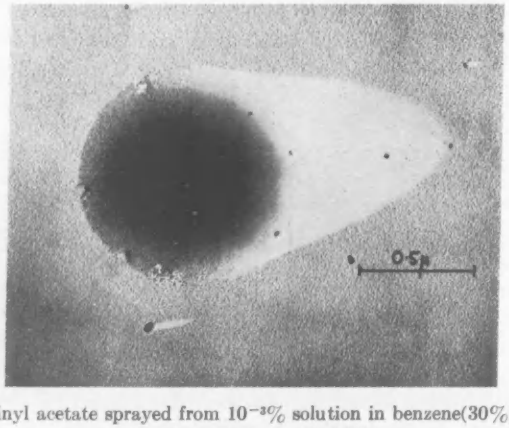

Fig. 8. Polyvinyl acetate sprayed from 10^{-3}% solution in benzene(30%)/*n*-butanol at room temperature. 34,000×.

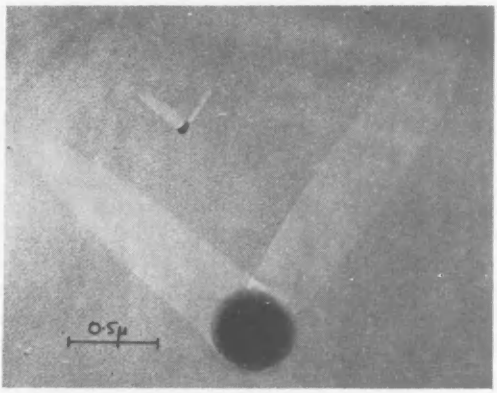

Fig. 9. Same as figure 8 but cooled to −10°C. before spraying. 27,000×. Longer shadow: immediately after spraying; shorter shadow: after examination in electron beam.

By suitably adjusting the temperature a glassy polymer may of course be brought into the rubbery condition and vice versa. This is particularly easily done with polyvinyl acetate for which the glass temperature is about 30°C. This polymer was therefore used to investigate the effect of a temperature change through the glass–rubber transition on the structure observed in the electron microscope. A benzene(30%)/*n*-butanol solution was expected to be a very poor solvent for polyvinyl acetate and thus should have given spherical agglomerates in the glassy region. Figure 8 shows that what, in fact, was observed was something resembling the cap of a sphere. A preparation with the solution initially at 40°C. was quite shapeless. By contrast, on cooling the solution to 0°C., or below, before spraying, well-defined spheres were obtained which, however, collapsed in the electron beam (Fig. 9) to give something resembling Figure 8. Of course, the decrease in temperature from 20° to 0°C. was equivalent to adding much nonsolvent which might reasonably account for the changes observed. This was not the case here as however much nonsolvent was present at 20°C. no objects of definite shape were ever observed using the normal technique. On the other hand, if the same solution giving Figure 8 was sprayed on to a substrate cooled by liquid nitrogen and then freeze-dried the polymer remaining appeared very similar to that of Figure 9. This showed that in solution the polymer existed as spherical aggregates as would be expected, but a combination of the rubbery nature of the polymer with surface tension forces on drying led to the collapsed structure typical of all rubbers prepared by the simple spray technique. Attempts to obtain better results by spraying on to surfaces energetically unfavorable to polyvinyl acetate led to only slight improvement.

Although the freeze-drying technique clearly demonstrated the need to operate below the glass transition temperature it was not suitable for the

production of single molecules, further evidence for the mechanism postulated for the formation of these in an earlier section (Solvent Effects). Freeze-drying prevented the normal all-important change in polymer configuration as the liquid droplets dried to a progressively poorer solvent. Thus it would seem that the only satisfactory method of producing well-defined single molecules of rubbery amorphous polymers is to cool the substrate some degrees below the glass transition temperature and to use a solvent system that remains liquid at the operating temperature. In addition, to avoid creep the polymer thus obtained must be maintained at this temperature until the metal shadowing process is complete (subsequent changes are then immaterial as the geometry of the shadow effectively defines the initial shape of the polymer). The importance of this step cannot be too strongly emphasized. Even polyvinyl acetate creeps at room temperature, a few degrees below its normally accepted glass transition. Thus an aggregate like that of Figure 9 composed of polymer of molecular weight 33,000 transforms to the cap-like structure of Figure 8 in a few hours. If the molecular weight is 1,500,000 the change takes a few days. The mobility of polymers, kept at room temperature but having glass transitions well below this, in the fifteen minutes or so required to pump out the bell jar before metal shadowing can be readily appreciated.

MOLECULAR WEIGHT MEASUREMENT

Having found the requisite conditions for the deposition of individual, tightly-coiled polymer molecules the molecular weight may easily be found if the important assumption, that the density of the isolated molecule is the same as that of the bulk polymer, is true. For the high molecular weights considered here this indeed seems a reasonable assumption but it can only be verified by comparing results obtained electron microscopically with those found by more conventional methods. A well-characterized polymer is essential. The sample used was a fraction of molecular weight 1,500,000 of an anionic polystyrene which *before* fractionation had a weight- to number-average molecular weight ratio of only 1.02. The polymer was sprayed at a concentration of $5.10^{-5}\%$, in a mixture of benzene (67%)/isobutanol and the nebulizer pumped only once. Otherwise the cooling effect caused by the vaporization of the liquid in the spray might have led to aggregation.

Samples were shadowed with platinum to give a calculated metal thickness of some 8 A. This figure is only very approximate since the assumption of a spherically symmetrical distribution of metal with respect to the shadowing source is a highly idealized one. Some indication of the metal thickness is needed, however, as the cap of metal deposited on the polymer molecule may considerably distort the true dimensions. The problem was carefully investigated using polystyrene latex and tobacco mosaic virus (TMV). Contrary to the observations of Misra et al.[5] it was found that the size, nominally 880 A. but apparently nearer to 750 A., of the shadowed

latex particles compared well with that of the unshadowed ones, provided measurements were made of the shadow width at the point where this was a maximum.

The exposed ends of TMV rods lying parallel to the direction of shadowing gave definite signs of an increase in width. However, the diameter (170 A.) of TMV could always be accurately estimated from the shadow lengths. Similar results were obtained with haemoglobin molecules of the order of 200 A. in diameter. Distortion by shadowing material of the true particle dimensions in a direction normal to the direction of shadowing thus seems to be quite general if the particles are less than some 300 A. in diameter. Reflection of shadowing material from off the substrate may well be responsible. Whatever the explanation, particles of the type shown in Figure 4 were assumed to be true spheres the diameters of which could be obtained from the shadow lengths. In this way the polystyrene sample discussed above was found to have number- and weight-average molecular weights of 1,250,000 and 1,340,000. An accuracy of better than 20% is estimated at this molecular weight so these figures are in good agreement with the viscosimetric average weight of 1,500,000. Molecular weights as low as 500,000 can be estimated by this technique although here the method is not very satisfactory as gross distortion of particle dimensions by shadowing material occurs. Conversely, when molecular weights of the order of three million and above are being determined excellent accuracy may be expected.

I should like to thank Dr. T. G. Rochow of the American Cyanamid Company and Dr. F. Wenger for gifts of polyacrylonitrile and anionic polystyrene, respectively, Dr. F. P. Bowden for his interest in this work and the Natural Rubber Producers' Research Association for a Research Fellowship.

Leave of absence to attend this conference was given by kind permission of the Director, National Physical Laboratory.

References

1. McIntyre, D., in *Unsolved Problems in Polymer Science*, National Academy of Sciences, National Research Council Publication, 995, Washington, D. C., 1962, p. 71.

2. See C. E. Hall, *J. Biophys. Biochem. Cytol.*, **1**, 613 (1960).

3. Siegel, B. M., D. H. Johnson, and H. Mark, *Polymer Sci.*, **5**, 111 (1950).

4. Nasini, A. G., G. Ostacoli, G. Maldifassi, G. Saini, and L. Trossarelli, *Ric. Sci., Suppl.*, **25**, 432 (1955).

5. Misra, D. N., N. N. Das Gupta, P. Sadhukhan, *Fifth International Congress for Electron Microscopy*, Volume 2, Academic Press, New York, 1962.

JOURNAL OF POLYMER SCIENCE: PART C NO. 3, PP. 31–37

The Use of Viscosity Data to Assess Molecular Entanglement in Dilute Polymer Solutions

T. GILLESPIE, *Plastic Fundamental Research, The Dow Chemical Company, Midland, Michigan*

INTRODUCTION

We would like to know a great deal more about the manner in which molecules interact in polymer systems in order to solve more quickly a wide range of problems associated with the manufacture and use of plastics. As an indication of our ignorance of this vital subject one has only to consider the vast amount of work that has been done on dilute solutions and how little information it has yielded about what happens when two polymer molecules come in contact. The work described below was an attempt to do something about this by looking at viscosity data to see if they reveal anything about entanglement on collision.

One of the equations which seems to fit viscosity data on dilute polymer solutions and on dilute suspensions is

$$\ln \eta_r = [\eta]\, c + k_2\, [\eta]^2\, c^2 + \ldots \tag{1}$$

where η_r is the viscosity of the disperse system divided by the viscosity of the suspending fluid and c is the concentration in g./ml. of solution or suspension. $[\eta]$ is the Staudinger index.[1] The surprising fact about the constant k_2 is that it is positive for suspensions while it is usually negative for polymer solutions. This is illustrated in Figure 1 where k_2 is the slope of the plots suggested by eq. (1).

When two rigid spherical particles collide in a suspension they form a dumbbell (Fig. 1) and we would expect them to contribute more to the viscosity than when they are apart. When two polymer molecules collide in solution there is a good chance that they may entangle because of their loose structure (Fig. 1) and it would not be surprising if this molecular aggregate contributed less to the viscosity of the solution than two separate molecules. It is shown in what follows that this essential difference between polymer molecules and rigid particles is sufficient to account for the fact that k_2 is negative for polymer solutions and positive for suspensions of rigid particles.

In discussing the viscosity of polymer solutions it is somewhat more common to use the equation

$$\eta_r = 1 + [\eta]\, c + k'\, [\eta]^2\, c^2 + \ldots \tag{2}$$

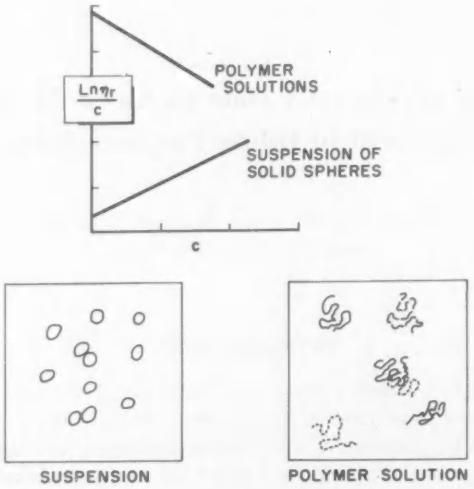

Fig. 1. An illustration of the differences between the behavior of suspensions of solid particles and polymer solutions.

where k' is the Huggins constant. It is known empirically that k' depends upon branching, goodness of solvent, etc. The major result of the present work is to explain these observations in terms of the molecular mechanism of entanglement.

THEORETICAL CONSIDERATIONS

Brinkman[2] has shown that Einstein's equation for the viscosity of an infinitely dilute suspension can be extended to higher concentrations by using a technique developed by Onsager[3] in a similar problem in dielectric theory. Brinkman's result may be expressed in the general form,[4,5]

$$\eta_r = \left(\frac{1}{1 - s\phi}\right)^k \tag{3}$$

where ϕ is the solids volume fraction and s is the change in volume of the suspension when unit volume of solid is added. k may be a function of the concentration and is given by

$$k = \frac{2.5\phi_{\text{eff}}}{\phi} \tag{4}$$

where ϕ_{eff} is the effective solids volume fraction. Both eqs (3) and (4) should apply to polymer solutions as well as to suspensions.

In the interest of a clear presentation of the essential features of such an application we may consider the rather crude model of a dilute uniform

molecular weight polymer solution consisting of only single molecules and doublets. In this case, if we take s equal to unity

$$\ln \eta_r = k\phi + \frac{k\phi^2}{2} + \ldots \tag{5}$$

If there are n molecules/cc.

$$\phi_{\text{eff}} = n\bar{v} \tag{6}$$

where $\bar{v}$ is the average hydrodynamic volume of a molecule.

$$n\bar{v} = nv_1 + n_2(v_2 - 2v_1) \tag{7}$$

where v_1 and v_2 are the hydrodynamic volumes of a single molecule and a doublet, respectively, and n_2 is the number of doublets per cc.

Simple kinetic arguments lead to

$$n_2 = \frac{K_1 n^2 t_c}{2} \tag{8}$$

where K_1 is "the orthokinetic collision rate constant at unit shear rate"[6] and t_c is the lifetime of a doublet at unit shear rate, n is given by

$$n = \phi/v_s \tag{9}$$

where v_s is the volume of a molecule when it is compacted so as to have the same density as the solid polymer from which the solution was made.

Combining eqs. (4–9)

$$\ln \eta_r = 2.5\frac{v_1}{v_s} - \phi + 2.5\frac{v_1}{v_s} - \left[\frac{1}{2} + \frac{K_1 t_c (v_2 - 2v_1)}{2v_s v_1}\right]\phi^2 + \ldots \tag{10}$$

by definition

$$2.5\frac{v_1}{v_s} = [\eta]\rho \tag{11}$$

and

$$\phi = c/\rho \tag{12}$$

where ρ is the density of the solid polymer.

Hence

$$\ln \eta_r = [\eta]c + (k_2[\eta]^2c^2) + \ldots \tag{13}$$

which corresponds to eq. (1).

$$k_2 = \frac{1}{5v_1}\left[v_s + K_1 t_c\left(\frac{v_2}{v_1} - 2\right)\right] \tag{14}$$

This equation indicates that k_2 may be positive or negative depending upon the ratio of the hydrodynamic volume of a doublet to the hydrodynamic volume of a single molecule (i.e., v_2/v_1).

It is convenient to discuss this result in more detail by considering the Huggins constant k', since it is used more often in the polymer literature than k_2. It is easy to show that

$$k' = \frac{1}{2} + k_2 \tag{15}$$

Introducing the Staudinger index,

$$k' = \frac{1}{2}\left[1 + \frac{1}{[\eta]\rho} + \frac{K_1 t_c N}{[\eta] M}\left(\frac{v_2}{v_1} - 2\right)\right] \tag{16}$$

where M is the molecular weight and N is Avogadro's number.

According to the previous work on dilute solutions which has been summarized and amplified by Flory,[7]

$$[\eta] = 0.603 \frac{N}{M} (\overline{r^2})^{3/2} \tag{17}$$

where $\overline{r^2}$ is the mean square value of the end-to-end distance of a polymer molecule.

At this time estimates of K_1 and t_c for polymer molecules are likely to be rather inaccurate. However, for the present purposes, we may take t_c equal to π which is the value for large particles which roll around each other without sticking.[8] According to Smolochowski's analysis for spherical particles[6]

$$K_1 = \frac{32\, r^3_{\text{eff}}}{3} \tag{18}$$

where r_{eff} is the effective collision radius. For polymer molecules one reasonable assumption would be that

$$r_{\text{eff}} = \sqrt{\overline{s^2}} \tag{19}$$

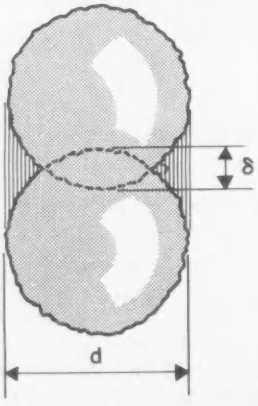

Fig. 2. Schematic diagram of a doublet composed of two loosely coiled molecules.

TABLE I
Estimated Entanglement in Typical Systems

Polymer	Solvent	$\bar{M}_w \times 10^{-4}$	T, °C.	$[\eta]$	k'	δ/d	Reference
Polystyrene	Toluene	1.05	25	7.7	0.51	0.33	11
		2.05	25	13.7	0.44	0.35	11
		12.5	25	51.5	0.36	0.38	11
		120.0	25	272.0	0.36	0.38	11
Polystyrene	Benzene	—	25	40.0	0.38	0.37	12
Polystyrene (0.0063% D.V.B.)	Benzene	—	25	557.0	0.46	0.35	12
Polystyrene (0.025% D.V.B.)	Benzene	—	25	234.0	0.61	0.30	12
Polystyrene (0.10% D.V.B.)	Benzene	—	25	93.0	0.82	0.23	12
Polystyrene (0.140% D.V.B.)	Benzene	—	25	73.0	0.44	0.35	12
Polystyrene	15% Acetone 85% Methyl-cyclohexane	100.0	25	81.0	1.22	0.09	13
Polystyrene	30% Acetone 70% Methyl-cyclohexane	100.0	25	153.0	0.53	0.32	13
Polystyrene	40% Acetone 60% Methyl cyclohexane	100.0	25	174.0	0.39	0.37	13
Polystyrene	60% Acetone 40% Methyl-cyclohexane	100.0	25	143.0	0.49	0.34	13
Polystyrene	75% Acetone 25% Methyl-cyclohexane	100.0	25	90.0	0.83	0.22	13

where $\sqrt{\bar{s}^2}$ is the radius of gyration of the polymer molecule.[7]

Using the relation

$$\sqrt{\bar{s}^2} = \sqrt{\bar{r}^2}/\sqrt{6} \tag{20}$$

eqs. (16–19) lead to

$$k' = \frac{1}{2} + 1.88\left[\frac{v_2}{v_1} - 2\right] \tag{21}$$

This equation states that the Huggins constant for dilute polymer solutions is a function of hydrodynamic volume of a doublet divided by the hydrodynamic volume of a single molecule (i.e., v_2/v_1). The weakest point

in the derivation of the equation is the assumption that the radius for collision is equal to the radius of gyration. Until this point has been checked more thoroughly there would be little point in attempting to solve the relatively complex problem of deriving an equation for v_2/v_1 on first principles.

To get a rough idea of what is going on when collisions between molecules occur, it is interesting to consider the collision of two spheres of volume v_1 to form an aggregate which is of the form illustrated in Figure 2. If we introduce Vand's useful concept of occluded liquid[9] which is indicated by the shaded portion of the diagram in Figure 2, then the degree of entanglement may be estimated in terms of δ/d, where both δ and d are as illustrated in Figure 2.

$$\frac{\pi d^3}{6} + \left(\frac{\pi d^2}{4}\right)(d - \delta) = \frac{v_2}{v_1}\left(\frac{\pi d^3}{6}\right) \tag{22}$$

Therefore

$$\frac{\delta}{d} = \frac{5}{3} - \frac{2}{3}\left(\frac{v_2}{v_1}\right) \tag{23}$$

Putting this in terms of k' which can be determined experimentally

$$\frac{\delta}{d} = \frac{1}{2} - \frac{k'}{3} \tag{24}$$

ANALYSIS OF EXPERIMENTAL DATA

Table I summarizes an attempt to estimate the entanglement in some typical polymer molecule collisions from published viscosity data. $\bar{M}_w$ refers to the weight-average molecular weight and T is the temperature.

The first four entries in Table I indicate that above a molecular weight of about 10^5, Huggins' prediction that k' should be constant[10] is sound. However, at low molecular weights, as pointed out by McCormick[11] k' increases. The values of the degree of entanglement as calculated from eq. (24) suggest that smaller molecules are more compact which is in agreement with the theory of polymer molecule configuration in solution.[1,7]

The second group of entries in Table I illustrates the effect of branching and crosslinking which would be expected to occur when styrene was copolymerized with divinylbenzene.[12]

Branching and crosslinking should make a polymer molecule more compact and reduce the degree of entanglement as indicated by the steadily decreasing values of δ/d up to about 0.10% divinylbenzene.

Above 0.10% divinylbenzene there is a sharp decrease in k'. The calculated value of δ/d indicates an increase in the degree of entanglement. This suggests the formation of "insoluble" particles which flocculate into irregular permanent aggregates which can inter-penetrate to some extent on collision. We have considerable viscosity data on partially flocculated latex which can be explained qualitatively on this basis and, apart from

some difference in the size of the individual particles which form the aggregates, the two systems would seem to be quite similar.

The last group of entries illustrate the conclusion of Palit, Colombo, and Mark[13] that k' diminishes as one passes to better solvent. The molecular entanglement as measured by δ/d increases as the molecules become looser and is a maximum in the best solvent.

DISCUSSION

Simple geometrical calculations indicate that in the solid state or in the melt the degree of entanglement must be much larger than in dilute solution or the individual molecules contract considerably. It has been suggested by Weissberg, Simha, and Rothman[14] that such contraction would occur even in dilute solutions due to "the nonideal part of the osmotic pressure," and would account for the changes in Huggins' constant which have been explained above in terms of molecular entanglement. These two alternative approaches should be kept in mind in any attempt to discuss melts or the solid state.

With regard to the idea of molecular entanglement it should be remembered that while we describe polymer molecules in terms of an average configuration considerable deviation from this average probably occurs. In this case one might expect more than one molecule to occupy the same domain and to act as a unit in flow processes.

References

1. Huggins, M. L., *Physical Chemistry of High Polymers*, Wiley, New York, 1958.
2. Brinkman, H. C., *J. Chem. Phys.*, **20**, 571 (1952).
3. Onsager, L., *J. Am. Chem. Soc.*, **58**, 1486 (1936).
4. Gillespie, T., *J. Colloid Sci.*, **18**, 32 (1963).
5. Gillespie, T., *Symposium on Emulsion Rheology*, Harrogate, England (to be published by Pergamon Press, London).
6. Kruyt, H. R., *Colloid Science*, Elsevier, New York, 1949.
7. Flory, P. J., *Principles of Polymer Chemistry*, Cornell Univ. Press, Ithaca, New York, 1953.
8. Manley, R. St. J., and S. G. Mason, *Can. J. Chem.*, **32**, 763 (1954).
9. Vand, V., *J. Phys. Colloid Chem.*, **52**, 277 (1948).
10. Huggins, M. L., *J. Am. Chem. Soc.*, **64**, 2716 (1942).
11. McCormick, H. W., *J. Colloid Sci.*, **16**, 635 (1961).
12. Cragg, L. H., and J. A. Manson, *J. Polymer Sci.*, **9**, 265 (1952).
13. Palit, S. R., G. Colombo, and H. Mark, *J. Polymer Sci.*, **6**, 295 (1951).
14. Weissberg, S. G., R. Simha, and S. Rothman, *J. Res. Natl. Bur. Std.*, **47**, 298 (1951).

MORPHOLOGY OF SURFACES

JOURNAL OF POLYMER SCIENCE: PART C NO. 3, PP. 41–64

The Morphology of Synthetic Latexes

E. B. BRADFORD and J. W. VANDERHOFF,
Physical Research Laboratory, The Dow Chemical Company, Midland, Michigan

INTRODUCTION

The morphology of synthetic latexes is a broad subject integrating colloid chemistry, polymer chemistry, and physical chemistry. The electron microscope is used extensively in this field because of its broad range of magnification; particles as small as 20 A. and as large as 10 μ can be resolved. These magnifications encompass the entire range of particle sizes produced by emulsion polymerization. Since the electron microscope can also define the shape and size distribution of individual particles, it is the primary tool used in investigations of latex morphology. It is especially valuable when used in conjunction with other investigative techniques.

This paper considers the morphology of latexes from three aspects: (*1*) the morphology of individual latex particles; (*2*) the morphology of latex films; and (*3*) the morphology of pigmented latex films. In the first section, the various polymer compositions and their relation to particle size determination are discussed; also, several unusual latex morphological configurations are shown. The second section includes the structure of both continuous and discontinuous films, the mechanism of film formation, and the effect of experimental variables on the film formation process. In the last section, the morphology of both the paint and paper coating types of pigmented films is described.

MORPHOLOGY OF LATEX PARTICLES

A. Various Latex Types

Emulsion polymerization generally produces particles which are perfect spheres within the limits of resolution of the electron microscope. This spherical configuration arises from the surface tension forces determined by the concentration of emulsifier adsorbed on the particle surface, and is enhanced by the plasticization of the polymer particle by increased temperature or imbibition of monomer. This configuration is consistent with the results of many investigations of various polymer compositions, particle sizes, and particle size distributions by electron microscopy. A few exceptions to this general configuration will be discussed later.

The morphology of individual latex particles is dependent upon the poly-

mer composition; latexes may be prepared from a wide variety of monomers and monomer mixtures. The particles may be homogeneous or heterogeneous in composition according to the various monomers used, their solubilities in water, and their order of addition to the polymerization. For homogeneous particles, i.e., where there is no appreciable compositional gradient from the center of the particle to the surface, the morphology is

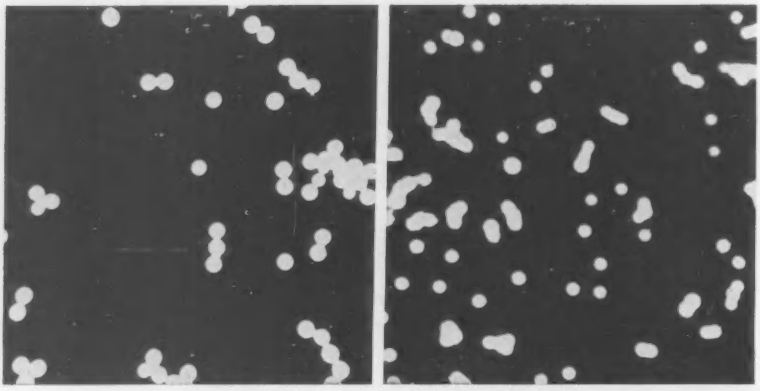

Fig. 1. Electron micrographs of latex particle dispersions: (*A*) polystyrene; (*B*) 60–40 styrene–butadiene copolymer.

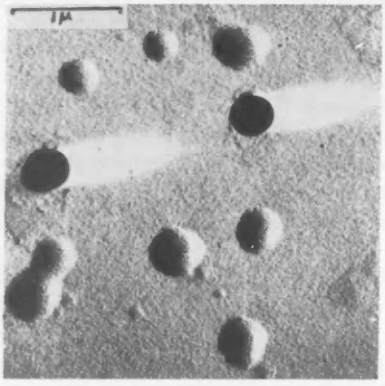

Fig. 2. Shadowed latex particles of polystyrene and a 75–25 isobutyl acrylate–styrene copolymer.

dependent upon the properties of the polymer itself. These different polymer types may be classified according to the ability of the latex to form a continuous film at room temperature; those which will form continuous films are called soft particle latexes and those which will not, hard particle latexes. In terms of this definition, some latexes fall somewhere between these two extremes. The latex type may be characterized more precisely

by the measurement of the minimum temperature at which it will form a continuous film.[1]

Hard and soft particles may be differentiated readily by electron microscopy. Figure 1 is an electron micrograph showing both hard (polystyrene) and soft (60–40 styrene–butadiene copolymer) particles; the latexes were diluted to ~20 ppm polymer and dried on specimen substrates;

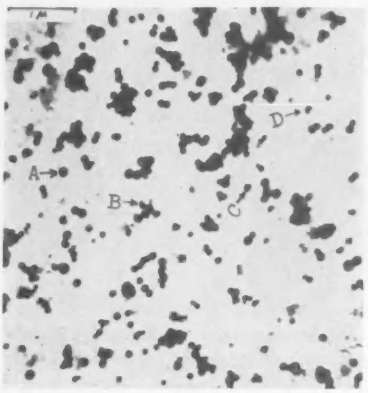

Fig. 3. Particles prepared by polymerizing styrene in a GR-S 1006 seed latex.

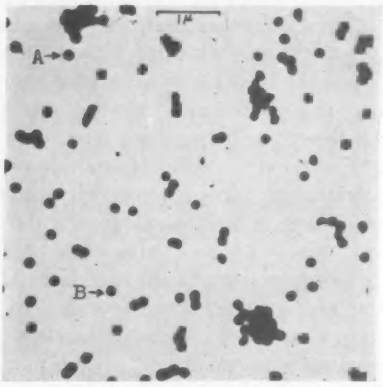

Fig. 4. Particles prepared by polymerizing a 70–30 vinyltoluene–butadiene mixture in a polystyrene seed latex.

the images of the hard particles (Fig. 1*A*) are distinct, while those of the soft particles (Fig. 1*B*) are hazy. To show the deformation of soft particles upon drying, similar specimens are shadowed with evaporated metal, e.g., chromium. Figure 2 shows a shadowed dispersion of polystyrene and 75–25 isobutyl acrylate–styrene copolymer particles in the same field. The polystyrene particles have not deformed appreciably during the drying process, as evidenced by their relatively long shadows, while the isobutyl

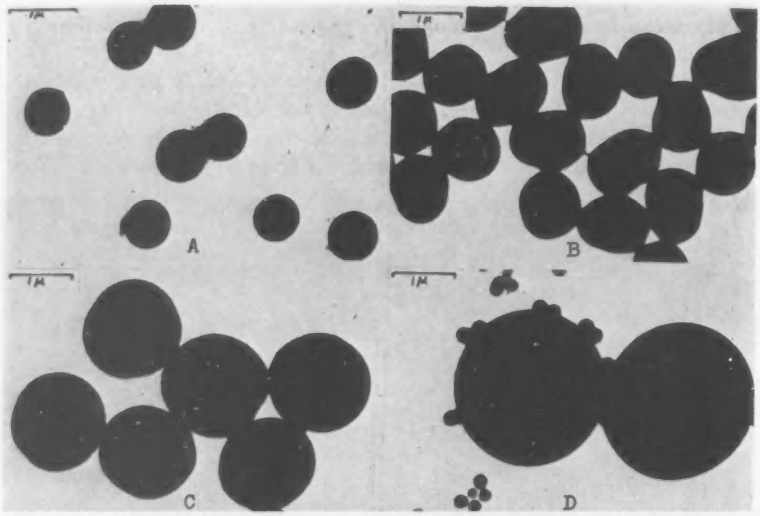

Fig. 5. Particles prepared by successive seeding polymerizations: (*A*) original seed; (*B*) distorted spheroids; (*C*) spheroids; (*D*) spheres.

acrylate–styrene copolymer particles have deformed considerably and display short shadows. This specimen was dried at room temperature; at higher temperatures, even the polystyrene particles would have deformed. Thus the morphological changes which occur upon drying are dependent upon the composition of the latex particles and the temperature.

The particles shown in Figures 1 and 2 are homogeneous in composition; however, it is possible to prepare heterogeneous particles by seeded emulsion polymerization, or by varying the order of addition of the monomers in a conventional polymerization. This heterogeneity can be observed in the electron microscope if there is a sufficient density difference between the two polymer species. Figure 3 shows particles prepared using GR-S 1006 butadiene–styrene copolymer latex as the seed latex (1 part polymer) for the polymerization of styrene monomer (3 parts). In these particles, the areas rich in polystyrene are more opaque in the electron beam than those rich in the butadiene–styrene copolymer. Some particles appear homogeneous, while others show definite compositional gradients; in some (arrow A), this compositional gradient is symmetrical about the particle center; in others (arrow B), the concentration of polystyrene is greater on one side of the particle, and the portion rich in the butadiene–styrene copolymer has deformed during the drying. A few particles (arrow C) appear to be spherical segments, and others (arrow D) display crescent-shaped images.

Figure 4 shows the converse, i.e., particles prepared using a polystyrene seed latex (1 part polymer) and a 70-30 vinyltoluene–butadiene monomer mixture (2 parts). Again some particles appear homogeneous, but others

show definite compositional gradients; in some particles (arrow A), this gradient is symmetrical about the particle center, but in others (arrow B), the vinyltoluene–butadiene copolymer is localized in one part of the particle. This compositional gradient is confirmed by the ability of this latex to form continuous films upon drying, while latexes comprised of homogeneous particles of the same overall composition form discontinuous films.

It should be emphasized that the foregoing examples were selected to show particles with compositional gradients; however, by varying the technique, it is possible to carry out similar polymerizations which yield homogeneous latex particles.

Figure 5 shows spheroidal particles prepared by seeded emulsion polymerizations in which the time allowed for the monomer to swell the seed particles was insufficient. In this series of polymerizations, each latex produced was used as a seed for the next step. The seed latex (1 part polymer) was heated for 3 hr. at 90–95°C. to decompose the residual persulfate initiator; after cooling to 70°C., the monomer (2.0–2.4 parts styrene containing 0.06% divinylbenzene) was added, and the mixture was agitated to allow the monomer to swell the seed particles; the persulfate initiator was then added, and the polymerization was carried out to a high conversion at 70°C. Figure 5*A* shows the particles of the initial seed latex, which was prepared previously by a seeded polymerization; these particles are monodisperse polystyrene spheres with an average diameter of 6600 A. This latex was used as a seed for a polymerization in which the monomer was mixed into the seed latex for only 1 hr. before the initiator was added; this produced distorted spheroids (Fig. 5*B*), ~11,000 A. in the longer dimension and ~9200 A. in the shorter dimension. In the next step, the monomer was mixed into the seed latex for 3 hr. before the initiator was added; the distorted spheroids were transformed into spheroids (Fig. 5*C*) with an average diameter of 15,300 A. In the last step, the monomer was again mixed into the seed latex for 3 hr. before the initiator was added; the spheroids were transformed into spheres (Fig. 5*D*); in addition, a new crop of small particles was initiated during this polymerization. Thus distorted spheroids were produced when the monomer mixing time was only 1 hr., but, when this time was increased to 3 hrs., the distorted spheroids were transformed gradually into spheres. Similar series of seeded polymerizations which used the longer monomer mixing times throughout produced spheres in each step. Apparently the shorter mixing times are not sufficient to allow a homogeneous distribution of the monomer in the seed particle. At these large particle sizes, two or more radicals can coexist in the particle without imminent termination;[2] this gives rise to separate polymerizations which are localized in a medium of high viscosity, causing the particle to grow into a distorted shape; this distortion develops despite the surface tension forces which generally force the particle to assume a spherical configuration.

Similar effects were observed in competitive growth polymerizations

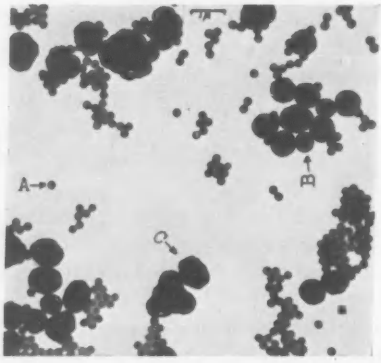

Fig. 6. Styrene–acrylonitrile copolymer particles prepared by a competitive growth seeding experiment.

where the monomer is a poor solvent for the seed polymer.[3] In these experiments, monomer is polymerized in a mixture of two monodisperse latexes of different particle size; these different-size particles compete for the available monomer and free radicals; the average particle sizes of each distribution are determined by electron microscopy before and after polymerization; the relative particle growth rates are then calculated from these measurements. For example, an 80–20 styrene–acrylonitrile mixture (5 parts) was polymerized in a seed latex (1 part polymer) comprised of a mixture of two monodisperse 70–30 styrene–acrylonitrile copolymer latexes with average diameters of 2600 and 4270 A.; during the polymerization, the larger particles, upon exceeding a critical size of ~6000 A., became irregular in shape, and their particle size distribution broadened considerably. Figure 6 shows the particles of the final latex; three distinct distributions of particle sizes can be observed; the smallest particles (arrow A) are the monodisperse polystyrene particles (2640 A. diameter) which were added to determine the magnification of the micrograph; the intermediate-size particles (arrow B), generally spherical and relatively narrow in particle size distribution, are the smaller styrene–acrylonitrile copolymer particles which did not exceed the critical size of ~6000 A.; the largest particles (arrow C), distorted and irregular in shape with a broad particle size distribution, are the larger styrene–acrylonitrile copolymer particles which exceeded the critical size during the polymerization. This last configuration is interpreted as the result of localized polymerizations in a medium of high viscosity; above the critical particle size, two or more radicals can coexist in the particle without imminent termination, and these separate polymerizations result in the formation of lumps on the particle surface.

The rhodium trichloride-initiated emulsion polymerization of butadiene produces polybutadiene comprised of 99+% of the *trans*-1,4 isomer.[4] This type of polymerization usually produces an unstable or partially co-

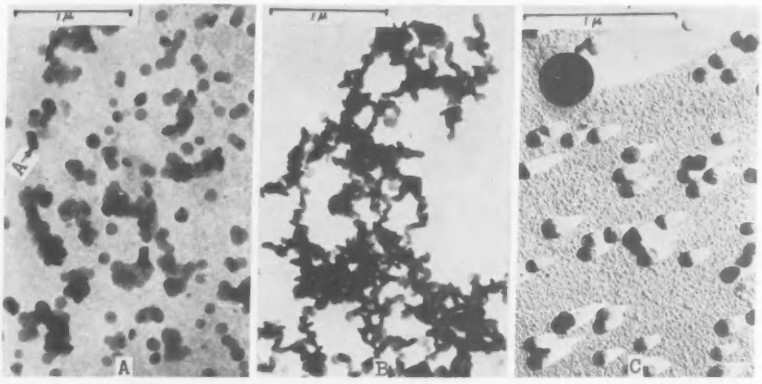

Fig. 7. Oblate spheroidal particles of *trans*-1,4-polybutadiene: (*A*) unbrominated; (*B*) brominated; (*C*) shadowed.

agulated latex which can, however, be examined by electron microscopy. It has been observed in our laboratory that, in certain of these latexes, the *trans*-1,4-polybutadiene particles are oblate spheroids rather than spheres. Figure 7*A* shows a dispersion of such a latex; most of the particle images are circular, but a few particles (arrow A), apparently deposited on edge, show the elliptical side projection of an oblate spheroid. Figure 7*B* shows a brominated dispersion of the same latex; the particles are aggregated by bromination, and many more particles are viewed on edge. Figure 7*C* shows a shadowed dispersion of the same latex; again a few particles are viewed on edge; the large sphere is a monodisperse polystyrene calibration particle (3650 A. diameter); micrographs such as this can be used to determine the particle dimensions assuming the particle configuration is that of an oblate spheroid.[5] It may be argued that the particles are spherical in the colloidal state and deform only upon drying; therefore, to demonstrate the oblate spheroidal configuration, the particle dimensions determined from both the unbrominated and brominated specimens were compared (bromine is used to harden butadiene-containing polymers for electron microscopy as shown in Figure 11). For the unbrominated sample, the average particle diameter was 1120 A. and the average particle height was 480 A.; the analogous values for the brominated sample were 1210 and 410 A.; the average height/diameter ratios, 0.43 and 0.34, were in acceptable agreement for this method of determination. Therefore it is concluded that these particles are oblate spheroids rather than spheres in the colloidal state. The formation of these nonspherical particles in an emulsion polymerization which produces a stereospecific polymer is additional evidence that this mechanism of polymerization differs considerably from the usual free radical type.

Electron microscopy may also be used to illustrate other aspects of latex morphology. For example, Figure 8 shows the effects of added nonpoly-

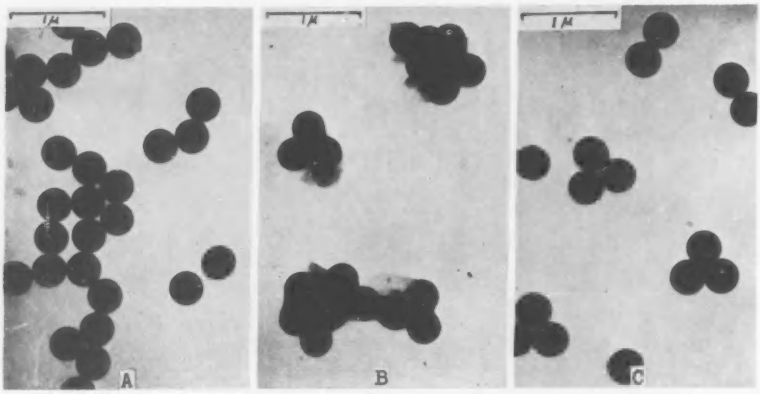

Fig. 8. Effect of latex additives: (*A*) original latex particles; (*B*) 10% potassium persulfate; (*C*) 10% Duponol ME.

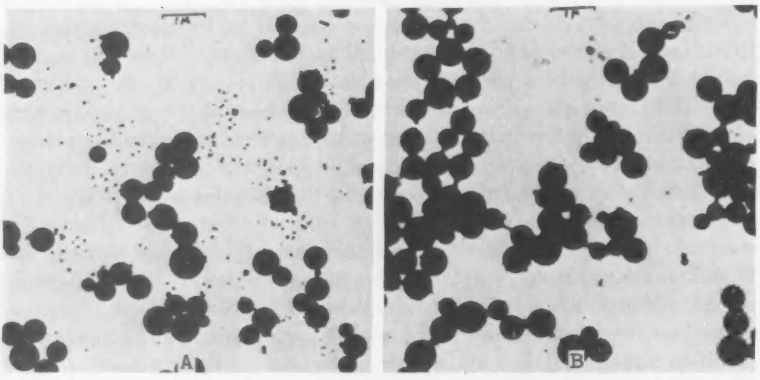

Fig. 9. Effect of mechanical shear on polyvinyl chloride particles: (*A*) before; (*B*) after.

meric substances. Figure 8*A* shows particles of the original monodisperse polystyrene latex; no contamination can be seen in the background. Figure 8*B* shows a similar dispersion containing an additional 10% potassium persulfate (based on polymer); the contaminant can be seen in the clusters of aggregated latex particles. Figure 8*C* shows a dispersion containing 10% Duponol ME (technical sodium lauryl sulfate); apparently the added emulsifier is adsorbed, at least in part, on the particle surfaces since their peripheries are less distinct, and the particle-particle contacts have an amorphous appearance not observed in the original latex. Thus, in sufficient concentrations, the presence of the nonpolymeric components of an emulsion polymerization recipe can be detected.

The effect of agitation on an experimental polyvinyl chloride latex is shown in Figure 9. A dispersion of the original latex particles is shown in

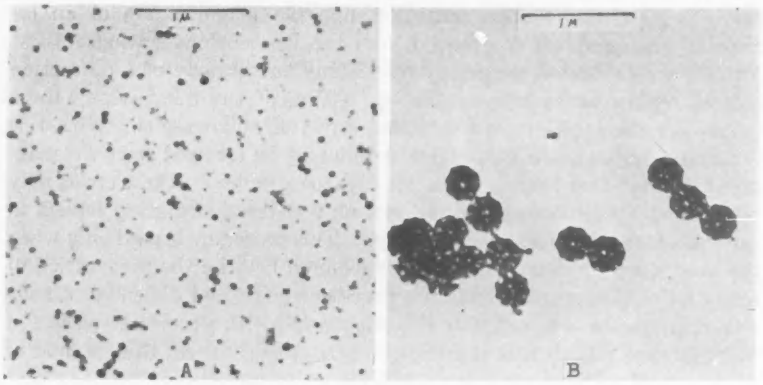

Fig. 10. Vinyl chloride–vinylidene chloride copolymer particles: (*A*) typical particles; (*B*) unusual configuration.

Figure 9*A*; the particle size distribution is very broad, with the particles ranging from ~300 to ~8000 A. in diameter. Figure 9*B* shows a dispersion of the same latex after intensive mechanical agitation in a Hamilton-Beach blender; the large particles are aggregated to a greater extent, and only a few individual small particles are seen; however, amorphous material is occluded between large particles in the clusters and, in many cases, forms tendrils connecting separated particles. The aggregation of particles as a result of mechanical shear is not unexpected, but the apparent deformation and extension of the small particles to form these interconnecting tendrils was not anticipated.

Another unusual particle configuration was observed in an experimental 80–20 vinyl chloride–vinylidene chloride copolymer latex. Figure 10*A* shows a typical dispersion of this latex; the particles have an average diameter of 550 A. Figure 10*B* shows an atypical particle configuration observed in another area of the specimen; the structure of the particles appears similar to that of a wheel, with amorphous material filling the spaces between the spokes. These unusual structures have been observed only in this latex, and the mechanism of their formation is not known.

B. Particle Size Determination

Many properties of commercial latex systems are dependent upon the particle size and particle size distribution of the latex. The electron microscope is unequaled for determining these parameters because it allows a direct visualization of the size of the individual particles. Two factors are important in the particle size determinations: (*1*) the calibration of the micrograph; and (*2*) the treatment of the particles to avoid aberrations which may arise from the sample preparation.

The calibration of the electron microscope is based either on diffraction grating replicas or some secondary standard, e.g., monodisperse latex

particles. For our routine measurements, the magnification of an individual micrograph is determined from the lens current settings; these settings are calibrated previously by making an exposure of a diffraction grating replica at each magnification setting of the microscope; these values are then used for an extended series of micrographs. With this technique, rather small and random errors may be incurred since the magnification may vary slightly from exposure to exposure.[6] These errors may be reduced by dispersing the particles on a diffraction grating replica to calibrate each micrograph individually.[6] This procedure is used only when the most accurate determinations are required because the preparation of many diffraction grating replicas is time-consuming and difficult. A suitable compromise is to calibrate the micrograph with previously-measured monodisperse polystyrene particles;[7] when properly used, this method of

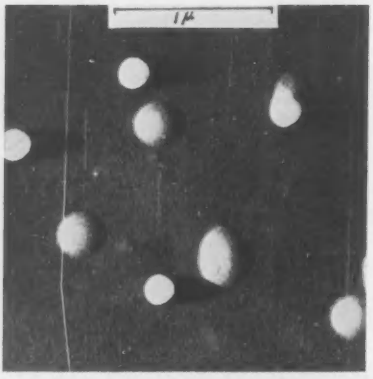

Fig. 11. Shadowed particles of a 60–40 styrene–butadiene copolymer latex before and after bromination.

calibration is almost as accurate and precise as that based on diffraction grating replicas. Polystyrene particles increase in apparent diameter upon prolonged exposure in the electron beam; this increase is dependent upon the metal comprising the specimen screen, e.g., it is negligible for stainless steel, but may be considerable for copper.[6] Under extreme conditions, polystyrene particles have even been observed to melt in the electron beam. Therefore, to obtain the most reliable particle size measurements, the latex particles should be dispersed on diffraction grating replicas supported by stainless steel grids, and the exposure to electron irradiation should be kept to a minimum; monodisperse polystyrene particles can be used for calibration in place of the diffraction grating replicas with only a small loss in accuracy and precision.

The techniques for the measurement of latex particle size must also take into account the polymer comprising the particles. As shown in Figure 2, the particles of latexes which form continuous films deform and coalesce with the substrate upon drying. Therefore, the measurement of these

particles cannot be carried out using the same methods employed for polystyrene particles.

Soft styrene–butadiene copolymer particles can be hardened for electron microscopy by bromination[8] or high-energy irradiation.[9] For example, Figure 11 shows a micrograph of shadowed brominated and unbrominated particles of a 60–40 styrene–butadiene copolymer latex; the brominated particles have not deformed appreciably upon drying, while the unbrominated particles have deformed and coalesced with the substrate. Although these particles are hardened satisfactorily by bromination, their particle diameters are affected by the amount of bromine absorbed. High-energy electrons can also be used to harden styrene–butadiene copolymer particles because the predominant reaction is crosslinking; similarly, this technique can be used for any other polymeric latex system which crosslinks predominantly upon exposure to high-energy electrons.

Some polymeric systems, e.g., those containing vinyl acetate, acrylate esters, vinyl chloride, or vinylidene chloride, do not respond to bromination since these polymers contain little or no residual unsaturation; some of these, e.g., those containing vinyl acetate, can be hardened by high-energy irradiation. However, when other polymers of practical interest in the coatings field, e.g., certain ethyl acrylate–methyl methacrylate copolymers, are exposed to high-energy electrons, the predominant reaction is degradation. For these systems (and all others which deform upon drying), the particle diameters can be determined from measurements of the deformed particles.[5] In this method, it is assumed that the configuration of the deformed particle is that of a spherical segment or an oblate spheroid. Monodisperse polystyrene particles are dispersed on the specimen substrate along with the deformed particles, and the specimen is shadowed; the calibration particles are used to determine the shadow angle and magnification of the exposure. From these data and measurements of the apparent diameter and shadow length of the deformed particles, the original spherical diameter can be calculated. This method has been demonstrated to be reasonably accurate and can be applied to any soft particle latex.

MORPHOLOGY OF LATEX FILMS

Upon drying, some latexes are transformed from a milky, colloidal dispersion to a transparent, tough film, and others, to a friable, white, opaque solid. The type of film obtained is dependent upon the properties of the polymer comprising the latex particles. As shown in the preceding section, hard particles such as polystyrene do not deform appreciably during drying; these latexes form white, opaque, discontinuous films. The soft particles, e.g., the styrene–butadiene and isobutyl acrylate–styrene copolymers, deform and coalesce with the substrate upon drying; these latexes form transparent, tough, continuous films.

The mechanism of latex film formation has been the subject of many investigations.[10] The generally-accepted mechanism follows. The latex

initially contains 30–50% by volume of latex particles. At this concentration, the particles move about freely, displaying their characteristic Brownian motion. As the water evaporates, the volume percent of polymer is increased until, at 50–75%, the particles are brought into contact with one another, and the particle motion ceases. The volume percent of polymer at this point is dependent upon the drying conditions, the latex stability at high concentrations, the average particle size, and the particle size distribution. Once the particles are in contact with one another, they are held in a more or less close-packed aggregate by the van der Waals' forces of attraction; the water remaining fills the interstices between the particles. As the water continues to evaporate, the capillary and surface tension forces are exerted on the particles; if these forces (which are of considerable magnitude) are sufficient to overcome the resistance of the particles to deformation, the particles are coalesced to form a continuous film; if they are not, a discontinuous film is formed. Once a continuous film is formed, its properties may be improved by "autohesion," i.e., the mutual interdiffusion of polymer chain ends across the particle-particle interfaces.

This paper treats the morphology of discontinuous and continuous films separately; in actual practice, the degree of coalescence may lie anywhere between these two extremes.

A. Morphology of Discontinuous Films

The opaque, white, friable, discontinuous films possess poor physical properties; they can be easily crushed to a powder between the fingers. These films were examined by replication of the polymer-air and polymer-substrate surfaces, and fracture cross sections.

The polymer-air surface replica of a film formed from a monodisperse polyvinyltoluene latex is shown in Figure 12*A*.[11] The latex was dried to form a film ~1 mm. thick; this film was placed in a vacuum evaporator, and silicon monoxide was evaporated onto the surface; the polymer was dissolved away, and the replica was recovered and examined in the electron microscope. It can be seen that the particles are arranged in a uniform hexagonally-packed array. Figure 12*B*[11] shows a similar replica viewed at lower magnification. Here the grain boundaries of the crystallites are visible; the order of packing of the center crystallite is square rather than hexagonal. These replicas show two-dimensional crystallites which are probably three-dimensional because of their high degree of uniformity. In a similar case, hexagonally-packed crystallites formed by a monodisperse polystyrene latex of larger particle size (1.2 μ as compared to 0.3 μ for the foregoing sample) were examined by optical microscopy; as the level of focus was lowered from the surface down through the crystallite, the grain boundaries were maintained (with the expected shifts) to as many as 24 layers. Thus the crystallites observed by surface replication as two-dimensional structures are in reality three-dimensional.

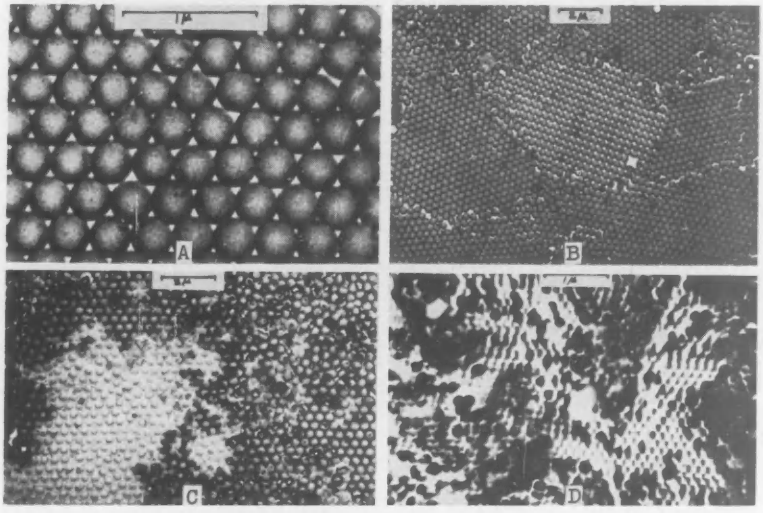

Fig. 12. Surface replicas of polyvinyltoluene latex films: (*A*) and (*B*) polymer-air surface; (*C*) polymer-substrate surface; (*D*) fracture cross section.

Figure 12*C* shows a replica of the polymer-substrate surface of a similar film. Some crystalline order is observed; however, the uniformity of packing is poorer, and the crystallites are smaller in size. Since the film dries from the upper surface, it is not unexpected that a less compact arrangement is observed more frequently in the lower surface. These discontinuous films are easily fractured; Figure 12*D* shows a replica of the surface structure of a fracture cross section. The square packing is more prevalent, and the uniformity of packing is not as great as in the upper surface.

The size of the crystallites formed is related to the conditions of drying.[12] When the latex is dried very slowly, e.g., in a desiccator over a saturated sodium chloride solution, so that several days or a week elapses before the film is dry, the size of the crystallites is increased. Smaller crystallites are formed when the latex is dried under room conditions, or at elevated temperatures (but still below the apparent second-order transition temperature of the polymer).

The presence of these crystallites is corroborated by other observations. For example, dried films of monodisperse latexes with particle sizes larger than ~1900 A. exhibit iridescent colors which vary with the angle of observation. In the particle size range 1900–3000 A., these colors are specific and can be used to identify smaller ranges, e.g., 2400–2700 A.; at particle sizes larger than 3000 A., the iridescent colors are rainbow-like rather than one specific color. These iridescent colors are also observed in the latexes; apparently the latex particles are arranged in crystallites which form on the walls of the container and on the latex surface. In some cases (for the

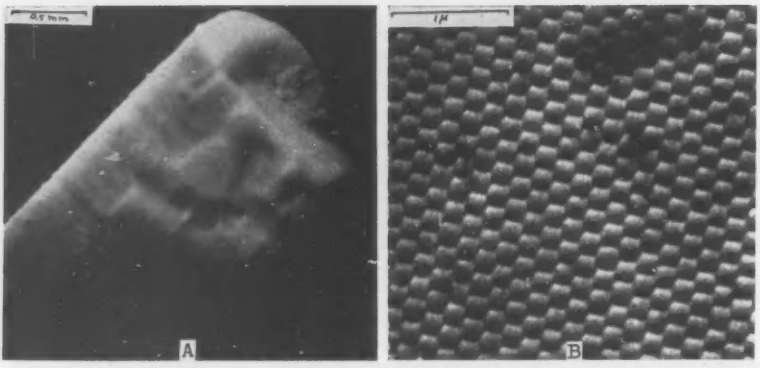

Fig. 13. Polyvinyltoluene latex "crystal:" (*A*) optical micrograph; (*B*) surface replica.

particle size range 1900–3000 A.), the colors exhibited by the latex are the same as those of the dried film. In other cases, however, the latex colors are indicative of a particle size larger than that of the dried film; apparently the particles in the latex align themselves in an ordered but less compact array than in the dried film.

The intensity of light diffracted by these latex particle crystallites has been examined quantitatively and used to calculate the particle size;[12] the values found were in good agreement with those determined by electron microscopy. The scattering was found to be that expected for two-dimensional crystallites; the opacity of the films obviates the diffraction from the second layer of packed particles.

In another experiment, a monodisperse polyvinyltoluene latex (average diameter 1320 A.) was centrifuged until a sediment was observed in the bottom of the tube. This sediment, after careful washing, was found to contain particles which outwardly resembled crystals; one of these is shown in Figure 13*A*. An electron micrograph of a surface replica of this "crystal" is shown in Figure 13*B*; the size of the crystallite is relatively large, and the uniformity of packing is very good. In addition, some deformation and coalescence of the hard particles are observed; this could be an artifact of the replication process, but it is more likely that some coalescence of the particles occurred because of the forces exerted upon them during the formation of the "crystal."

B. Morphology of Continuous Films

When the latex particles are soft, the forces exerted during drying are sufficient to cause particle coalescence. These continuous films can be examined by electron microscopy. Figure 14 shows a surface replica of a film cast from a 60–40 styrene–butadiene copolymer latex. To prepare this replica, a collodion solution was dried on the latex film to replicate the surface detail; this collodion replica was stripped off and coated with evaporated silicon monoxide; the collodion was then dissolved, leaving the

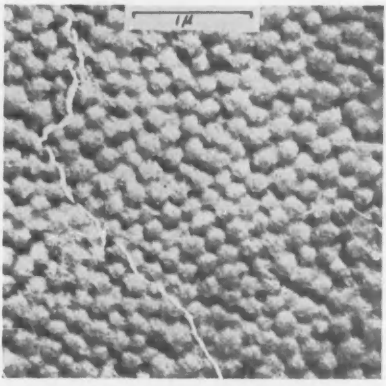

Fig. 14. Surface replica of a 60–40 styrene–butadiene copolymer latex film.

silicon monoxide replica which was recovered and examined in the electron microscope. This film was transparent, tough, and continuous; the particles have apparently coalesced, but their surface contours are still visible. The irregular white lines observed are cracks in the silicon monoxide replica which is very thin and fragile.

The film-forming characteristics of a latex are dependent upon the properties of the polymer comprising the particles. The resistance to deformation of a latex particle can be varied systematically and reproducibly by copolymerization, e.g., polystyrene latex forms a discontinuous film, but a

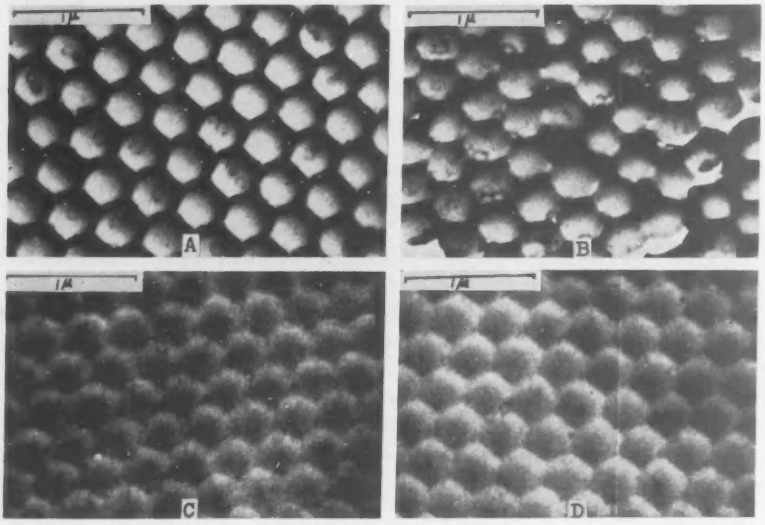

Fig. 15. Effect of 15 min. heating on polyvinyltoluene latex films: (*A*) original; (*B*) 202°F.; (*C*) 208°F.; (*D*) 214°F.

Fig. 16. Effect of Flexol 3GH plasticizer concentration on 75–25 vinyl chloride–vinylidene chloride copolymer latex films.

styrene–butadiene copolymer latex which contains more than ~30% butadiene forms a continuous film. The resistance to deformation can also be altered by heat or plasticization. For example, polyvinyltoluene latex films can be rendered continuous by heating;[13] Figure 15 shows the effects of heating dried films for 15 min. at various temperatures above the polymer softening temperature (~185°F.); Figure 15*A* shows a surface replica of the original film, while Figures 15*B*, *C*, and *D* show the effects of heating the dried films at 202, 208, and 214°F. The degree of coalescence is increased with increasing temperature. This correlates with the macroscopic appearance of the films; the opaque, friable film was transformed into one which was transparent and continuous.

Hard particle latexes can also be rendered film-forming by plasticization.[11] The effect of plasticizer concentration is shown in Figure 16 for a 75–25 vinyl chloride–vinylidene chloride copolymer latex plasticized with Flexol 3GH (triethylene glycol di-2-ethylbutyrate); without plasticizer, the film is opaque, white, and discontinuous; with increasing plasticizer concentration, the continuity and clarity of the film increases until, at 15% (based on polymer), the film is transparent, tough, and continuous. Figure 17 shows the surface replicas of the films shown in Figure 16. Without plasticizer (Fig. 17*A*), the particles are coalesced only slightly; with 5% plasticizer (Fig. 17*B*), the degree of coalescence is slightly greater, and, at 10% (Fig. 17*C*), still slightly greater, but still incomplete; with 15% plasticizer (Fig. 17*D*), the degree of coalescence is so great that the particles have lost their identity. Thus the film continuity was increased by increasing the plasticizer concentration.

Some plasticizer-latex combinations do not form a continuous film immediately after the plasticizer is added, but form a continuous film after aging. This phenomenon was analyzed theoretically, and the following mechanism was postulated for the plasticization process.[14] The emulsified plasticizer diffuses into the aqueous phase until a small, but saturated,

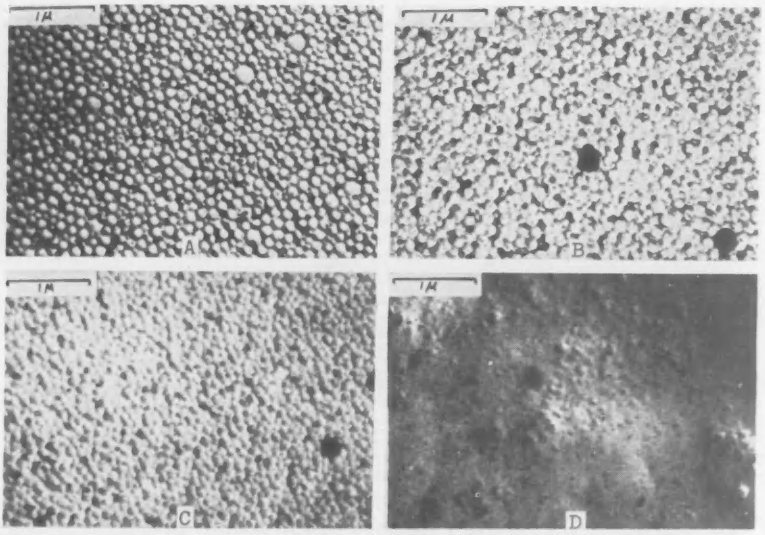

Fig. 17. Surface replicas of films shown in Fig. 16: (*A*) no plasticizer; (*B*) 5%; (*C*) 10%; (*D*) 15%.

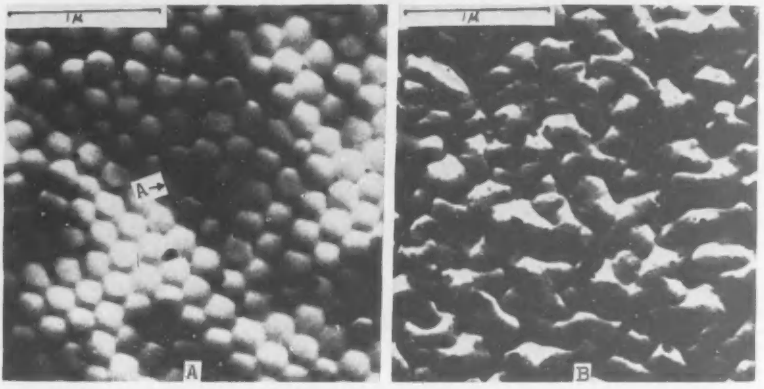

Fig. 18. Surface replicas of plasticized latex films: (*A*) post-plasticized polystyrene; (*B*) preplasticized polyvinyltoluene.

concentration is attained; the aqueous plasticizer slowly diffuses into the latex particles; as this occurs, the aqueous plasticizer is replenished by plasticizer diffusing from the emulsion droplets, and this diffusion process continues until all the plasticizer is in the latex particles. Since plasticizers are usually poor solvents for the polymer, the rate-controlling step is the absorption of plasticizer into the particle from the aqueous phase; consequently, the aging time required for this absorption is dependent upon the particular latex-plasticizer system. For example, when 15% Flexol

3GH was added to the 75–25 vinyl chloride–vinylidene chloride copolymer latex, the plasticizer could not be separated by centrifugation immediately after addition; however, when the plasticizer was 15% dioctyl phthalate, 23 days were required before the plasticizer could not be separated by centrifugation.

In another experiment,[11] a polystyrene latex (1 part polymer) was plasticized with 1 part V9 resin (a mixture of α-methylstyrene oligomers, average molecular weight 350–370) and allowed to age for 4 days; this film was soft, tacky, and opaque. A surface replica of this film is shown in Figure 18*A*; very little particle coalescence is observed; there are surface openings (arrow A) through which the plasticizer exuded to the film surface; the gray areas about the openings result from plasticizer which was not removed when the replica was rinsed. In another case, a polyvinyltoluene latex (3 parts polymer) was plasticized by adding 2 parts of an 88–12 mixture of V9 resin and plasticizer S. C. (triethylene glycol dipelargonate) to the monomer before polymerization; this composition formed a continuous film. Figure 18*B* shows a surface replica of this film; the surface appears wrinkled but continuous; this suggests that a surface skin, formed in the early stages of drying, wrinkled as the drying proceeded and the film shrank slightly.

MORPHOLOGY OF PIGMENTED LATEX FILMS

This section pertains to films formed from latexes which are formulated with pigments or fillers. These films can be divided into two general types according to the volume fraction of pigment, i.e., whether it is above or below the critical pigment volume concentration, CPVC.[15] Latex paints are examples of a system in which the CPVC is not exceeded, and latex paper coatings are examples in which the CPVC is exceeded.

A. Morphology of Latex Paint Films

Latex paints are colloidal dispersions containing both polymer and pigment particles. These compositions dry to form a dispersion of pigment particles in a matrix of coalesced polymer particles. Figure 19*A* shows a surface replica of a film cast from a 67–33 styrene–butadiene copolymer latex pigmented with titanium dioxide. The black particles in the micrograph (arrow A) are titanium dioxide particles which were extracted from the film when the collodion replica was stripped, and which subsequently adhered to the silicon monoxide replica when the collodion was dissolved. Similarly, a few latex particles (arrow B) which were removed in the same manner can be seen. A close inspection of the lighter areas of the replica shows the surface contours of both the coalesced latex particles and the pigment particles (arrow C) which were not removed during the replication process. It can be seen that many of the pigment particles are actually agglomerates of smaller particles; these agglomerates, as well as individual pigment particles, are dispersed throughout the film surface. Figure 19*B*

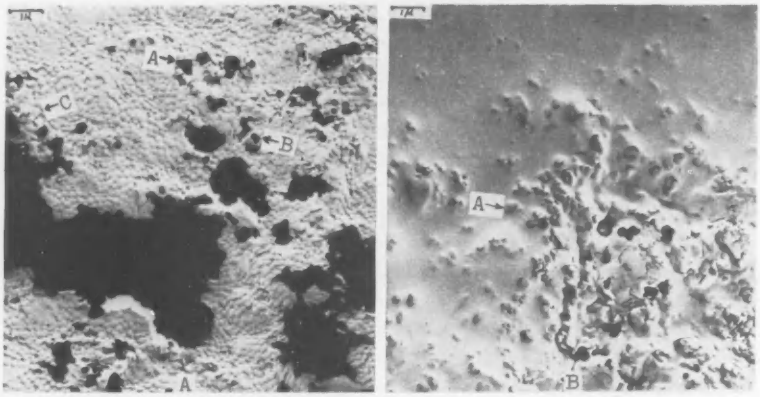

Fig. 19. Surface replicas of latex paint films: (*A*) 67–33 styrene–butadiene copolymer; (*B*) experimental 60–40 styrene–butadiene copolymer.

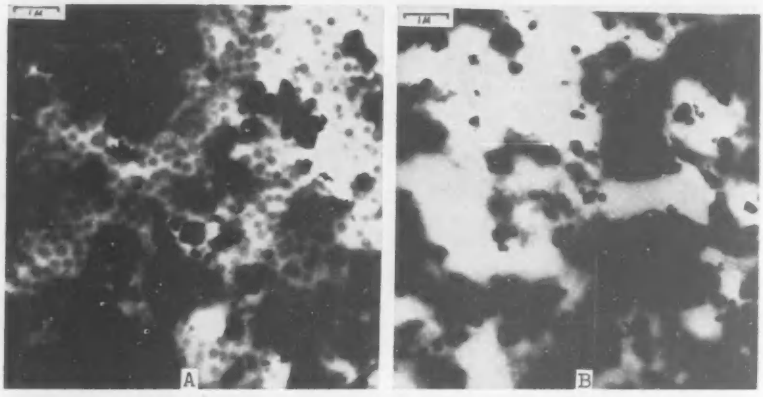

Fig. 20. Microtomed sections of paint films: (*A*) 67–33 styrene–butadiene copolymer; (*B*) experimental 60–40 styrene–butadiene copolymer.

shows a surface replica of a paint film prepared from an experimental 60–40 styrene–butadiene copolymer latex; this latex, when formulated and evaluated under identical conditions, gives films of greater hiding power, or opacity. Compared to Figure 19*A*, this micrograph shows that fewer pigment particles were extracted from the film during the replication process, more individually-dispersed pigment particles (arrow A) are observed in the film surface, and the latex particles are coalesced to such an extent that their surface contours are not visible.

Microtomed cross sections of films cast from these same latex paints were compared; the latex paint films were embedded in a 50-50 *n*-butyl methacrylate–methyl methacrylate mixture which was then polymerized at 45°C. with 1% benzoyl peroxide initiator; these specimens were then

microtomed to a thickness of ~1700 A. Figures 20*A* and *B* show the film sections for the 67–33 and the experimental 60–40 styrene–butadiene copolymers. The dispersion of pigment particles is similar in both figures; both agglomerates and individually-dispersed pigment particles can be seen. As was observed in the surface replicas, the contours of the individual 67–33 styrene–butadiene copolymer particles are plainly visible, while those of the experimental 60–40 styrene–butadiene copolymer particles are not discernible.

Dispersions of these same two paints were also compared; Figures 21*A* and *B* show the dispersions for the 67–33 and the experimental 60–40 styrene–butadiene copolymers. In Figure 21*A*, many individually-dispersed latex particles are seen; their average particle diameter is ~2000 A., and their particle size distribution is relatively narrow. In Figure 21*B*,

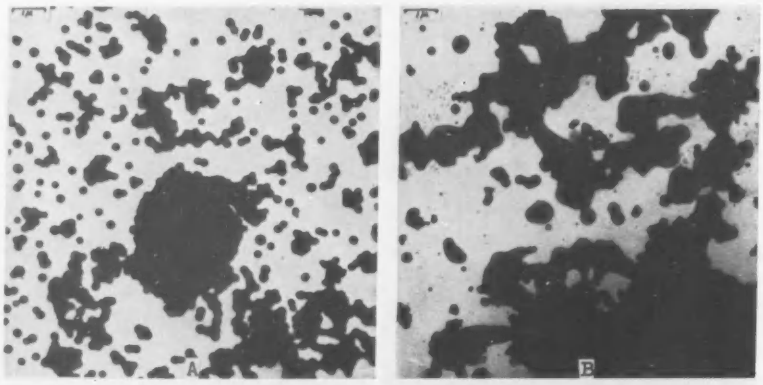

Fig. 21. Latex paint dispersions: (*A*) 67–33 styrene–butadiene copolymer; (*B*) experimental 60–40 styrene–butadiene copolymer.

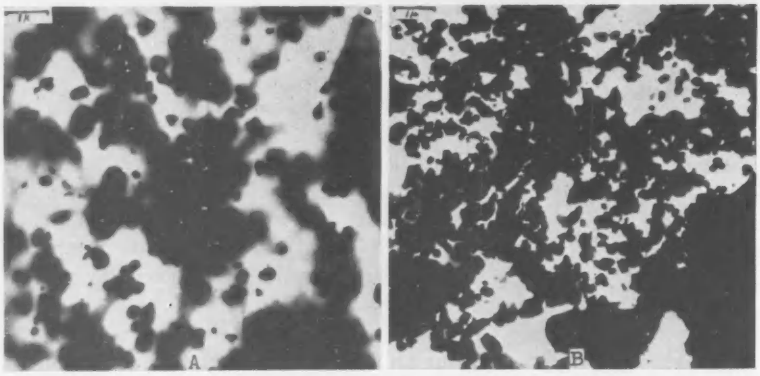

Fig. 22. Microtomed sections of a latex paint film embedded in: (*A*) 50–50 *n*-butyl methacrylate–methyl methacrylate copolymer; (*B*) epoxy casting resin.

few individually-dispersed latex particles are seen; most of them are agglomerated with the pigment particles; these latex particles have a larger average diameter and a broader particle size distribution.

These experiments show morphological differences in film structure and colloidal dispersion between two paints which display different hiding power; however, the significance of these morphological differences has not been proven.

The embedding mixture described previously has been observed to swell paint films, but this imparts coherence to the paint film so that thin microtome sections can be obtained; epoxy casting resins swell these paint films only negligibly, but the thin microtome sections tear and crumble during sectioning. Figures 22*A* and *B* show the effect of these methacrylate and epoxy embedding systems on the film structure of a paint prepared from a 65–35 isobutyl acrylate–methyl methacrylate copolymer latex. The expansion of the film structure can be seen plainly when Figure 22*A* is compared with Figure 22*B*. This expansion must be considered when conclusions are drawn concerning the morphology of the film.

B. Morphology of Latex Paper Coating Films

Latex paper coating systems differ from latex paints in that the volume fraction of pigment is greater than the CPVC. The volume fraction of polymer is ~0.6 in a typical paint and ~0.2 in a typical paper coating. The use of latexes in paper coatings is relatively new; the usual adhesives have been casein or starch. It has been hypothesized[16] that these soluble polymers function as adhesives by forming discrete rings of polymer around the points of contact between pigment particles. The colloidal latex particles probably function in an analogous manner by forming adhesive bridges between adjacent pigment particles. In practical applications, the latexes are substituted for all or part of the casein binder; the formulations containing latex are used, despite their higher cost, because they im-

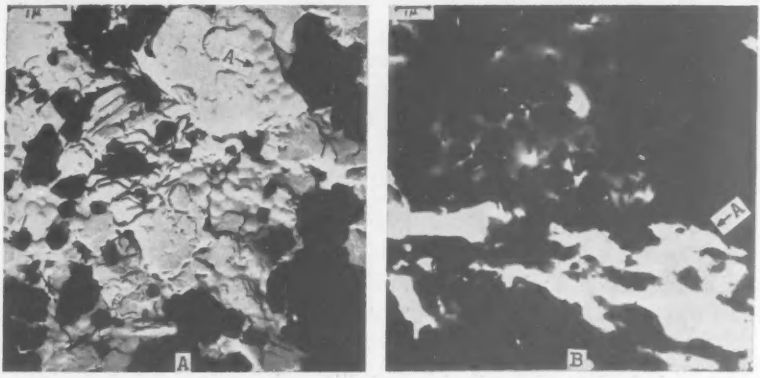

Fig. 23. Latex paper coating film: (*A*) surface replica; (*B*) microtomed cross section.

part desirable properties not obtained with the coating systems containing casein or starch.

The morphology of these latex paper coatings can be studied by electron microscopy in the same manner as the paint films. Figure 23*A* shows a surface replica of a paper coating which contains 15% by weight of a 60–40 styrene–butadiene copolymer. As expected from the small volume fraction of latex polymer, the clay pigment particles comprise most of the sur-

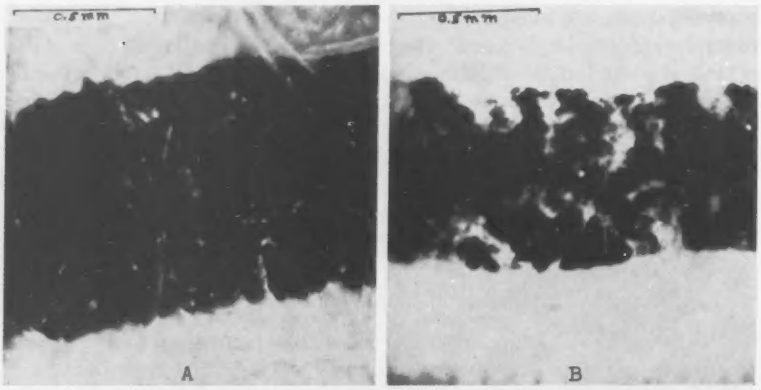

Fig. 24. Ink lines on coated paper: (*A*) good ink receptivity; (*B*) poor ink receptivity.

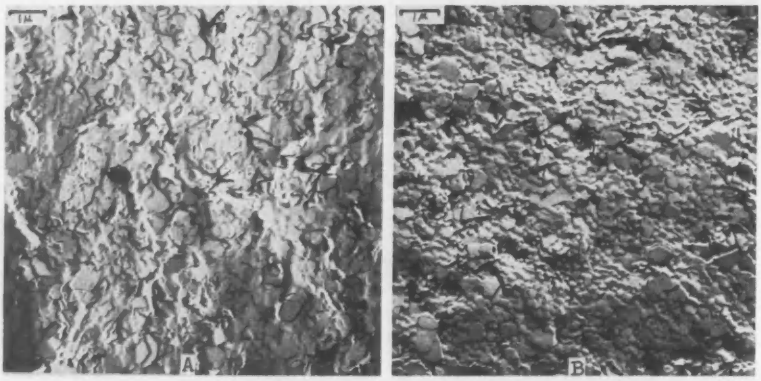

Fig. 25. Surface replicas of paper coatings: (*A*) good ink receptivity; (*B*) poor ink receptivity.

face; however, a few coalesced latex particles (arrow A) can be seen. Figure 23*B* shows a microtomed cross section of a similar film; this specimen was embedded in the methacrylate mixture described previously. At this magnification, the boundary between the paper substrate and the coating film is diffuse; however, the light area (arrow A) is interpreted as a paper fiber in contact with the coating. The coating film appears contin-

uous, and the distance separating the pigment particles is greater than expected from the original coating composition; this expansion of the film structure was demonstrated by optical microscopy to be the result of swelling by the embedding mixture. As long as this expansion is borne in mind, however, the film morphology can still be visualized.

The primary purpose of the clay coating on paper is to provide a printable surface. In practice, when the coatings are applied and dried very rapidly, a variation in the uniformity of ink absorption is frequently observed. Figure 24 shows optical micrographs of ink lines drawn across two coated papers; the binder, a mixture of casein and styrene–butadiene copolymer latex, was the same in both cases, but the formulation and application conditions were varied to give differences in ink receptivity. The ink has wetted the coated surface more uniformly in Figure 24*A* than in Figure 24*B*; in the former case, the ink has penetrated uniformly into the substrate, and the boundaries of the inked line are relatively straight; in the latter case, the ink has penetrated into the substrate less uniformly, and islands are observed where the ink has not wetted the substrate at all. Surface replicas of these same coated papers are shown in Figure 25. In the sample of uniform ink receptivity (Fig. 25*A*), the surface is comprised predominantly of clay particles, with few coalesced latex particles visible. In the sample of poorer ink receptivity (Fig. 25*B*), the proportion of coalesced latex particles in the surface is much greater; indeed, the coalesced latex particles appear to form a matrix containing the dispersed pigment particles. The proportion of latex particles in this film surface is significantly greater than in the original coating composition. The greater preponderance of the hydrophobic styrene–butadiene copolymer particles in the film surface reduces the surface porosity of the coating to the extent that the ink is not absorbed uniformly. These differences in the film surface structure depend so strongly upon the many intricacies of the coating process that a discussion of the many variables involved is beyond the scope of this paper; however, these examples demonstrate the dependence of the properties of the coated surface on the film morphology.

The authors acknowledge gratefully the assistance of W. D. Keiser and L. E. Morford in the preparation of many of the micrographs.

References

1. Protzman, T. F., and G. L. Brown, *J. Appl. Polymer Sci.*, **4**, 81 (1960).
2. Vanderhoff, J. W., and E. B. Bradford, *Tappi*, **39**, 650 (1956).
3. Vanderhoff, J. W., and E. B. Bradford, abstracts, p. 20-I, 131st Meeting of the American Chemical Society, Miami, Fla., April, 1957.
4. Rinehart, R. E., H. P. Smith, H. S. Witt, and H. Romeyn, Jr., *J. Am. Chem. Soc.*, **83**, 4864 (1961); A. J. Canale, W. A. Hewett, T. M. Shryne, and E. A. Youngman, *Chem. Ind.*, **1962**, 1054.
5. Bradford, E. B., and J. W. Vanderhoff, *J. Colloid Sci.*, **17**, 668 (1962).
6. Bradford, E. B., and J. W. Vanderhoff, *J. Appl. Phys.*, **26**, 864 (1955).
7. Bradford, E. B., J. W. Vanderhoff, and T. Alfrey, Jr., *J. Colloid Sci.*, **11**, 135 (1956).

8. Brown, W. E., *J. Appl. Phys.*, **18,** 273 (1947); E. A. Willson, J. R. Miller, and E. H. Rowe, *J. Phys. Colloid Chem.*, **53,** 357 (1949); E. B. Bradford, and J. W. Vanderhoff, *J. Colloid Sci.*, **14,** 543 (1959).

9. Bradford, E. B., and J. W. Vanderhoff, *J. Colloid Sci.*, **14,** 543 (1959).

10. Dillon, R. E., L. A. Matheson, and E. B. Bradford, *J. Colloid Sci.*, **6,** 108 (1951); W. A. Henson, D. A. Taber, and E. B. Bradford, *Ind. Eng. Chem.*, **45,** 735 (1953); G. L. Brown, *J. Polymer Sci.*, **22,** 423 (1956); S. S. Voyutskiĭ, *J. Polymer Sci.*, **32,** 528 (1958); L. Ivan, *Bor Cipotech.*, **11,** 161 (1961); J. C. H. Hwa, abstracts, p. 1-R, 142nd Meeting of the American Chemical Society, Atlantic City, N. J., Sept., 1962; J. G. Brodnyan, and T. Konen, abstracts, p. 2-R, 142nd meeting of the American Chemical Society, Atlantic City, N. J., Sept., 1962; R. R. Myers, and R. K. Schultz, abstracts, p. 2-R, 142nd Meeting of the American Chemical Society, Atlantic City, N. J., Sept., 1962.

11. Bradford, E. B., *J. Appl. Phys.*, **23,** 609 (1952).

12. Alfrey, T., Jr., E. B. Bradford, J. W. Vanderhoff, and G. Oster, *J. Opt. Soc. Am.*, **44,** 603 (1954).

13. Henson, W. A., D. A. Taber, and E. B. Bradford, *Ind. Eng. Chem.*, **45,** 735 (1953).

14. Dillon, R. E., E. B. Bradford, and R. D. Andrews, Jr., *Ind. Eng. Chem.*, **45,** 728 (1953).

15. Asbeck, W. K., D. D. Laiderman, and M. Van Loo, *Offic. Dig. Federation Paint Varnish Prod. Clubs*, **326,** 156 (1952).

16. Cobb, R. M. K., *Tappi*, **41,** 581 (1958).

JOURNAL OF POLYMER SCIENCE: PART C NO. 3, PP. 65–76

Colloidal Particles in the Thermosetting Resins

EDWARD H. ERATH, *Hughes Aircraft Company, Culver City, California,*
and MORTON ROBINSON, *Hughes Research Laboratories,*
Malibu, California

INTRODUCTION

Almost sixty years have passed since the first entirely synthetic thermosetting resins were developed for commercial use, and over twenty years since the epoxies that are used so widely in industry were introduced. But, due to the complexity of the reactions involved in the synthesis of these materials, and the infusibility of the products formed at gelation, their chemistry—and especially the fine structure of molded resins—still escapes complete elucidation.

Over the years, since the discovery of synthetic resins, considerable effort has been devoted to studies of resin synthesis and to the structure of both fusible and structurally insoluble condensation products, and the peculiar properties of these materials have evoked many theories pertaining to their fine structure, all of which rely to one extent or another, on the existence of extremely large molecules. For example, Carothers[1] proposed that molecular units of high functionality could polymerize into infinitely large, three-dimensional molecules—the size of which was limited only by the volume of the reaction vessel—and Flory[2] was able to specify the statistical conditions that must obtain in a multifunctional system to give rise to the formation of infinitely large molecules.

On the basis of his calculations, and in agreement with Carothers, Flory proposed: that an insoluble gel consists of a giant three-dimensional network that extends throughout the material; that the formation of this molecule is responsible for the abrupt change of physical properties at gelation, and that low molecular weight material that does not take part in the formation of the network yields comparatively small molecules that are interspersed throughout the larger matrix. However, calculations of the physical properties of molded resins, based upon a similar model lead to results that grossly disagree with actual measurements.

de Boer[3] calculated the tensile strength of phenolformaldehyde resin in the C— stage assuming that, as hypothesized, only primary bonds exist throughout a macromolecule formed at gelation and obtained a value that is at least 550× the actual tensile strength of the molded material. Even when he assumed that steric conditions prohibit the formation of a macromolecule, and that the only cohesive forces between structural units are

secondary bonds (van der Waals' forces), the calculated tensile strength was five times greater than the value determined by experiment. Houwink[4] suggested that, in general, this discrepancy could be explained by realizing that, due to the irregular shape of resin molecules, not all of the van der Waals' bonds that occur can reach their maximum binding energy, and furthermore, that opportunities for such bonding are minimized, and Megson[5] and Pritchett[6] have developed these ideas arguing that extensive primary bonding is extremely improbable. For example, Megson[7] has demonstrated with the use of molecular models that crosslinking on a large scale in resins like phenolic is extremely unlikely, and Pritchett suggests further that insoluble gels are formed by multifunctional chain molecules as they branch and become entangled with their neighbors, and that this entanglement, which finally leads to the immobility of the molecules, is responsible for the abrupt change of physical characteristics in a resin at gelation.

In spite of this later work, which obviously has had a great influence on our contemporary models of resinous material structure, the idea that the formation of macromolecules by extensive branching and crosslinking is the mechanism responsible for gelation still persists. The only real discrepancy that exists between the two models is the hypothesis of extensive primary bonding throughout molded thermosetting resins. Most of these ideas are simply speculation however, since neither the infinitely large skeletal networks nor the large, irregularly shaped, branched-chain molecules have been isolated and identified, and little or no physical evidence of their occurrence exists.

Parallel to these theoretical studies, a considerable amount of controlled synthesis, isolation and identification of intermediates, and fractionation of molded resin has been performed, with the result that our knowledge of the reactions leading up to condensation, and of the low molecular weight material contained in molded resins has constantly improved. Freeman,[8] for example, isolated and identified no less than eighteen methylol phenol related compounds by chromatographical methods during the condensation of a base catalyzed phenolformaldehyde reaction and at the beginning of the last decade all seven of the theoretically possible tri-nuclear compounds of phenol had been synthesized. Subsequently, in more recent years, multinuclear compounds of higher order have been synthesized but few have been extracted from molded materials, and it is unlikely that many will because of their low thermal stability. Madorsky[9] at the National Bureau of Standards, has performed extensive fractionation experiments over wide temperature ranges on many resinous materials and has not been able to isolate anything as complex as the cyclic, octanuclear Novalak or its crosslinked decanuclear derivative that Hunter and Turner[10] have synthesized, and these are far from the infinitely large molecules that have been proposed, or even the large branched chain molecules that have been hypothesized.

Thus, for the present at least, our models of molded thermosetting

resins will have to be the result of predictions, such as those of Megson, Flory, Houwink, de Boer, Pritchett, and others which are based upon a composite of whatever knowledge can be obtained about the structure from fractionation of molded material, controlled synthesis and isolation of reaction intermediates, radial distribution calculations based upon x-ray and electron diffraction experiments, direct observation of the fine structure with the electron microscope, statistical considerations, molecular models, and paramagnetic resonance and spectroscopic measurements. Electron microscopy provides an especially powerful tool with which resin structure may be observed directly, and it is the purpose of this paper to describe some recent microscopical studies of several molded, thermosetting, resins that revealed a particulate structure which appears to be common to many of these materials.

EXPERIMENTAL

Four thermosetting resins—phenolic, diallyl phthalate, epoxy, and silicone—were molded and cured, and their fine structures examined with electron microscopical techniques.[11] Each material exhibited, to various degrees, a micellular structure similar to that proposed by Houwink, Megson and others, giving some support to the idea that resin molecules are relatively small, irregular, three dimensional networks, the ultimate size of which is limited by a steric hindrance that minimizes the occurrence of intermolecular reactions. Although it was not possible with this technique to tell whether intermolecular chemical reactions occur, no evidence of the infinitely large molecules hypothesized by Carothers, Flory, and others, was observed in any of the samples. The most predominate structural feature of these resins as seen in the electron microscope, with the exception of silicone, is an agglomerate of irregularly shaped particles ranging in diameter from 800–900 A. (Table I), and no indication of large skeletal frameworks existing throughout the materials was observed.

Samples that were to be examined in the electron microscope were prepared for observation by various methods. Thin sections of resin were cleaved with an ultramicrotome and examined directly with transmitted electrons, and newly fractured resin surfaces were replicated with

TABLE I
Micelle Size for Various Thermosetting Resins

Resin	Exposed micelles, A.	Standard deviation, %
Phenolic	809	7.2
Diallyl phthalate	929	9.6
Epoxy	856	4.9
Leached epoxy	822	10.8
Silicone		

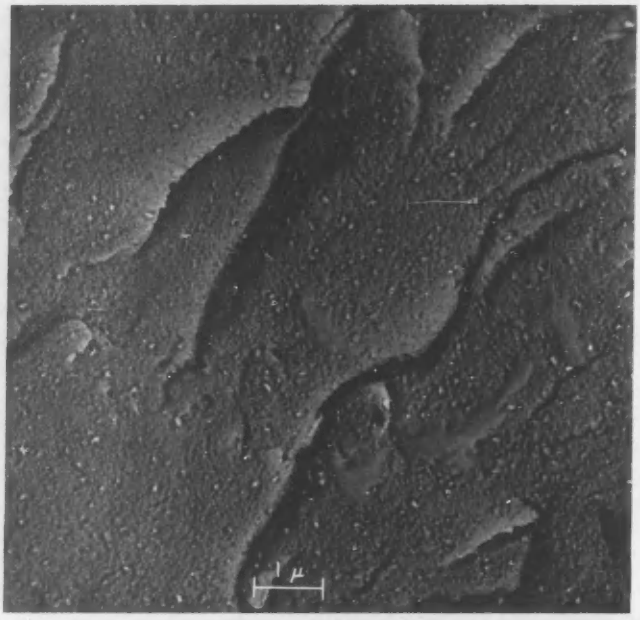

Fig. 1. Epoxy resin.

the usual preshadowed carbon replica techniques. Occasionally, during the replication process, thin resin strips adhered to a replica and it was possible to observe the resin's structure along the edge of these strips, while in rare cases, when working with material that had been leached in acetone, individual micelles were stripped from the sample and adhered to the replica. With the exception of silicone resin, all of the samples showed the micellular structure referred to above.

Figure 1 is an electron micrograph made from a preshadowed carbon replica of a newly fractured surface of epoxy resin that had received an optimum amount of ovencure after it was molded. The particulate matter that is visible on the entire surface is typical for the epoxy that was studied. The particles appear to be randomly distributed and discrete, and there is no apparent spacial relationship between neighboring particles that could be invoked to support the idea that a large skeletal network exists throughout the material. On micrographs of this kind, that are positive prints made from the negatives that are exposed in the microscope, depressions in the original sample appear lighter than their surroundings and protuberances are darker, while material that is stripped from the sample and adheres to the replica is black because it is usually opaque to the electron beam.

In Figure 1, strips of material from the sample have adhered to the replica along several of the fracture ridges and the particulate nature of

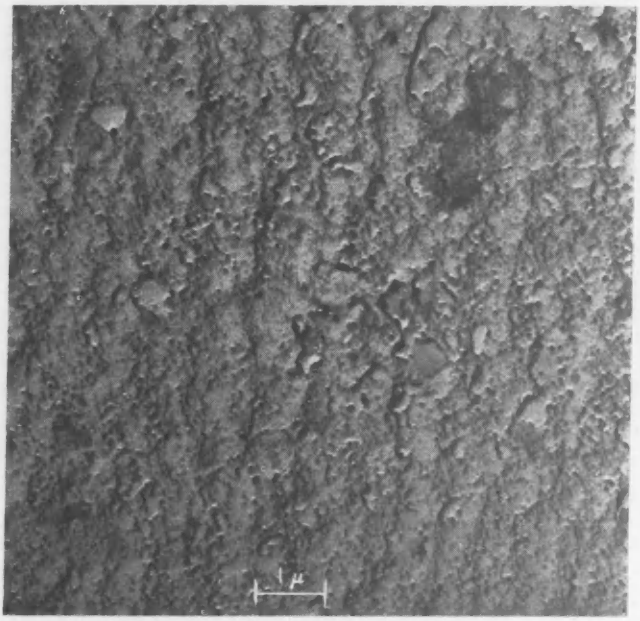

Fig. 2. Epoxy resin leached with acetone.

the sample can be seen in outline along the edge of these strips. The strip in the center of the upper left quadrant of the micrograph, is an excellent example. The strips provide an excellent opportunity to measure the diameters of particles which average about 850 A. for epoxy. The light spots that are distributed randomly about the micrograph represent large cavities that were left in the surface by particles that adhered to the mating surface, and those areas that appear to be completely featureless are due to gas bubbles that were trapped between the replica and the resin. There are some approximately linear arrays of micelles on the surface of the sample that are not associated with fracture ridges or adhering resin strips but these are few in number, of very short length (4–10 particles), and appear to be coincidental.

When molded epoxy resin is leached with acetone, surfaces such as the one exhibited in Figure 2 result. Large quantities of material have been removed resulting in the cavities that are visible on the surface and many individual particles, which have not decreased in size in spite of the solvent action, have adhered to the replica. Obviously bonding within these particles is much stronger than it is in the substrate material in which they were imbedded and it is difficult to imagine that they are linked to one another through epoxide and hydroxyl groups since they apparently separate from the body of the material as individuals. There is some evidence of long particle chains, such as those to the right of center

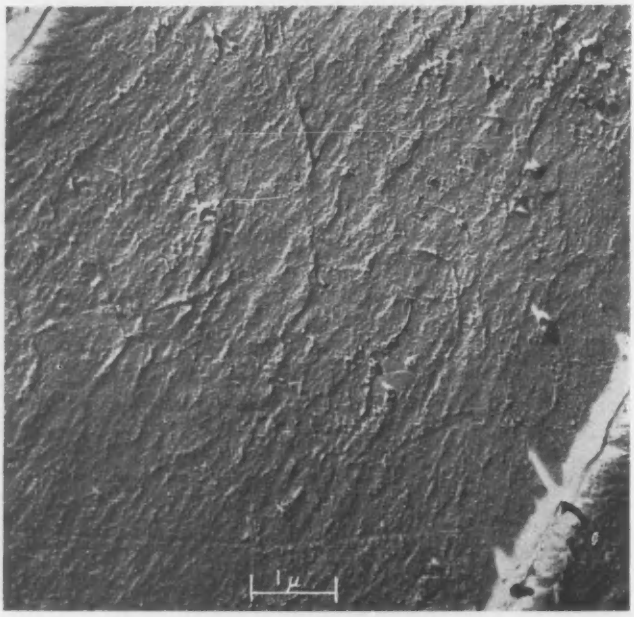

Fig. 3. Phenolic resin.

and at the top of the micrograph, but they do not appear to be a predominate feature of the material.

Figure 3 is an electron micrograph made of a preshadowed replica of a fracture surface of phenolic resin. The molded material was prepared from a sodium hydroxide catalyzed mixture of phenol and formaldehyde. The particulate matter that covers the surface supports the ideas of Megson and Pritchett that crosslinking does not occur to any great degree in these resins because of the irregular shape of methylol phenol chains which causes the interchain distances between active nuclear positions to be variable, and that a lack of rotational and translational freedom occurs after the molecules reach a certain critical size, reducing the occurrence of primary bonds between the molecules still further; all of which results in a structure that consists of relatively small, irregularly shaped, branched chain molecules inbedded in a substrate of low molecular weight material. Of course, whether or not primary bonds exist between the observed particles cannot be determined with this experimental technique, and no additional information regarding the structure was obtained by studying leached surfaces since acetone has little or no detectable affect on this material, even when viewed submicroscopically. The character of the structure observed does agree, however, at least on a large scale—500 to 1000 A.—with models that have been developed on a theoretical basis. No evidence was seen that would support the idea that voids exist in the

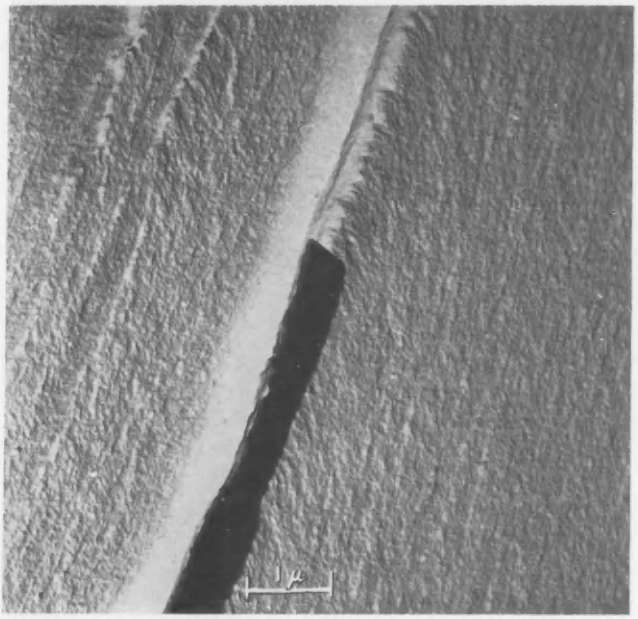

Fig. 4. Silicone resin.

molded material and are responsible for its high water and ion absorptivity as proposed by Megson, but voids could be smaller than the resolution capability of the sample preparation technique that was used and thereby escape detection. Again, as with the epoxies, no linear or parallel arrays of particles of any significance were observed that would support an argument for the occurrence of extensive crosslinking or the existence of a large skeletal network.

An interesting difference between Figure 1 and 3 is that the particles in epoxy appear at first glance to be much larger than those in phenolic, and if diameters are measured without concern for the fact that some are buried deeper in the substrate than others, the results support this impression. On the other hand, if only those particles are measured which are completely exposed, the difference reduces to about 50 A.; but, comparatively few phenolic particles are exposed. There appears to be a smoother transition from the substrate material to particulate material than in epoxy resin where the particles appear to be discrete.

In stark contrast with the first three micrographs which illustrate the particulate nature of epoxy and phenolic resins, Figure 4 exhibits a fracture surface of a silicone resin and the lack of any identifiable structure is remarkable. The material appears homogeneous and no structural units large or small can be seen. It is possible that particulate matter exists but that the micelles are too small to be resolved. Rochow and

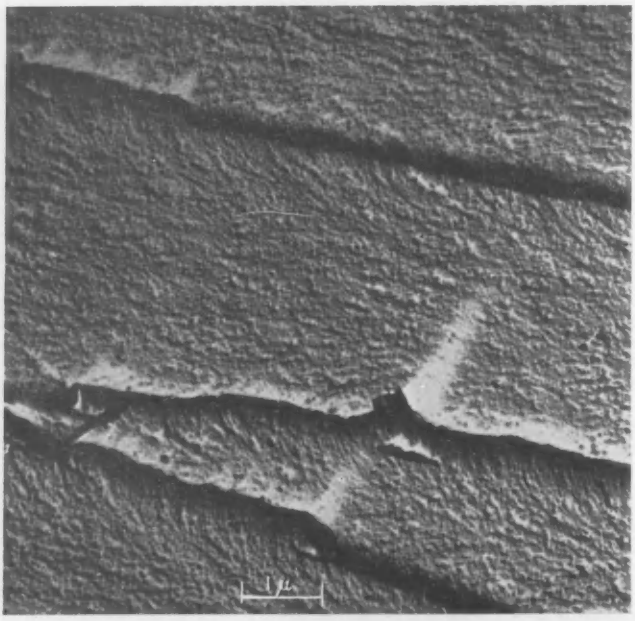

Fig. 5. Diallyl phthalate resin.

Rochow[12] observed a micellar structure in silicone rubber the average particle diameter of which was about 100 A. with some particles as large as 800 A., but only a few such particles were observed in this resin.

A rough calculation of the molecular weight for this material utilizing the typically observed diameters obtained with the electron microscope, assuming each spherical micelle is a macromolecule, gives values several orders of magnitude higher than those obtained indirectly. This is not generally the case for silicones[13] where molecular weight values determined by osmotic pressure techniques and those obtained through calculations on particulate matter[14] observed in electron micrographs lie in the same range.

Figure 5 is a micrograph made from a preshadowed replica of a fracture surface of diallyl phthalate. It is immediately apparent that the structure is distinguishable from each of the others, but it is extremely difficult to specify precisely what that difference is. Particulate matter covers the surface, there are only a few linear arrays of micelles, no underlying matrix is visible and the colloidal particles are only about 11% larger on the average than those observed in epoxy and phenolic resin.

All of the resins scatter x-rays in a manner typical of amorphous materials and no effects of crystallinity were observed for any of them, regardless of the extent of ovencuring they received. Scattered x-ray intensity was plotted as a function of the Bragg angle 2θ, and the typical halo pattern

produced by amorphous materials was observed. A scanning goniometer with a Geiger tube detector was used to plot the spectrum and this gave better resolution and sensitivity than the usual photographic technique. With this equipment it was possible to detect and follow the shift in position of the principal maxima of these halo patterns to smaller Bragg angles that occurs for phenolic and silicone resins.[15,16] This measurement was not performed on epoxy and diallyl phthalate for reasons described below.

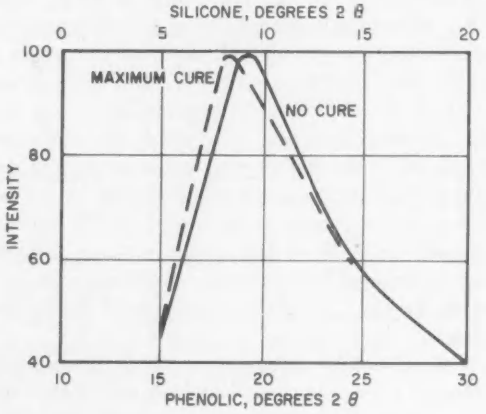

Fig. 6. X-ray diffraction spectrum for phenolic and silicone resins.

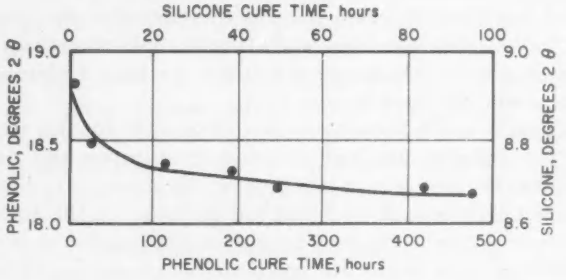

Fig. 7. Position of maximum intensity in the x-ray diffraction spectrum for phenolic and silicone resins.

Megson[17,18] and Hunter[19] suspected that such a shift occurred, but could not demonstrate its existence because of the difficulties inherent in determining the position of the maxima from photographic negatives with a densitometer. Figure 6 represents the x-ray diffraction spectrum for phenolic and silicone resins and illustrates the shift that takes place for both, while Figure 7 is a plot of the position of the principal maximum vs ovencuring time for the two resins.

When the value of θ for the position of the scattering maximum is substituted in the Bragg equation for first order reflections

$$\lambda = 2d \sin \theta$$

where λ is the wave length of the x-rays used, it is possible to solve the equation for the periodicity d for resins, which is approximately 4.8 A. for phenolic and 10 A. for silicone resin when copper K_α radiation is used. The change of periodicity for optimum cure is 0.148 A. and 0.283 A. respectively; the percentage change being approximately the same for both materials. Since the change of physical properties during postgelation curing has been attributed to the advancement of the polymerization reaction, which should decrease the periodicity, it is interesting that the periodicity actually increases. Probably, the shift results because of the predominance of the loss of low molecular weight material which has low average periodicity, over the advancement of the polymerization reaction. As the curing process is advanced to the optimum point the tensile and impact strengths of the resins increase implying that polymerization is advancing and low molecular weight material is being evolved. Both of these processes are thought to contribute to the observed shrinkage of the material.

The shape of the intensity versus angle curve can be used to calculate a radial distribution curve for these materials and Klug[20] claims that the position of the most predominant maximum in this function corresponds to the interchain distance in the resin, and further that $1.22d$ corresponds to the most prevalent interatomic distance. For phenolic these values, as determined from the diffraction pattern, are reasonable since the distance between the two benzene rings in dihydroxy diphenylmethane is about 4.5 A., but in silicone they appear to be much too large if siloxane bonding is the mechanism of polymerization.

Only phenolic and silicone resins were examined by this method, because of the difficulty involved in sample preparation and the lack of understanding of what preparation does to the structure of the material. Solid samples, large enough to fill the sample holder on the diffractometer used in this work, cannot be used because of inhomogeneities in the material, and surface irregularities that create spurious scattering effects making it difficult to locate maxima reproducibly. Therefore, it was necessary to grind the resin samples to a rouge-like powder so that all sample orientation effects were eliminated. When this was done the average deviation was about $0.05° 2\theta$.

DISCUSSION

While the experimental evidence presented here is entirely qualitative in nature, it does provide support for some aspects of various hypothesized models of resin structure and suggests how some fruitful work might be performed on these materials in the future. It is apparent from this work,

at least in phenolic, epoxy, and diallyl phthalate that no large skeletal networks extend throughout the materials and that instead they consist of agglomerates of colloidal particles, which are probably immersed in a substrate of low molecular weight intermediates of the polymerization reaction. Certainly the experimental work of Madorsky and Freeman, and the theoretical work of Megson and Houwink are in agreement with these experimental observations. However, the existence of the observed colloidal particles should be verified by some independent experimental technique such as very small angle x-ray diffraction measurements. If the particles actually exist and constitute regions of high density relative to their surroundings, then they also constitute abrupt periodic changes of electron density relative to their surroundings and should scatter x-rays at angles that are characteristic of their size. Since they are large compared to the usual interplanar separations in crystals, the scattered radiation intensity maximum would occur at very small Bragg angles—approximately $0.1°2\theta$—but with special laboratory techniques it is possible to make accurate measurements at such small angles. If the particles exist in the form observed, their average size could be measured and any size change that occurs with advancing cure could be followed and correlated with electron microscopical observations which indicate that particle size decreases with advancing post-gel cure,[21] and also correlated with measurements of physical parameters that change with increasing cure.

Particle size is important since the rate of decrease of secondary valence strength is proportional to the $^1/_6$ power of the distance between molecules. This may be a contributing factor giving rise to the large discrepancy between theoretical and experimental tensile strengths for polymers where a high degree of secondary bonding may be assumed and for which colloidal particles have been observed. The regions between particles may be defect sites in the polymer and, since indications are that van der Waal forces are only effective when molecules are within 5 A. of each other, the number and size of micelles may be important criteria for the correlation of experimental and theoretical properties such as the tensile and impact strength. Numerous particles, several orders of magnitude larger than 5 A. presumably drastically weaken the high cohesivity of structural entities that is observed in their absence.

No attempt was made in our work to carefully calculate the molecular weight of particles, as Rochow and Rochow[12] did for silicone rubber, since we have not verified that they are individual molecules. In addition, our sample preparation technique limited resolution to about 100 A. making it impossible to observe the fine structure of the particles. It is not inconceivable that they are skeletal networks themselves or possibly agglomerates of smaller particles that occur because of the high polarity of the polynuclear resin constituents. Certainly this would be the case if the model proposed by Megson is accurate, in which the largest units may be only octa, deca, or dodeca nuclear.

Unfortunately, the colloidal particles are so small that it is difficult to perform chemical and physical experiments directly on them. If they are actually macromolecules their molecular weight would run as high as 5×10^8 atomic mass units. Better etching experiments, performed with solvents that have polarities that closely match those of the fractions that are to be leached, could be used to improve our ability to observe the structures of the resins and thus increase our knowledge of the fine structure of these materials. For example, if unreacted phenol is contained in a matrix of larger molecules, it may be possible to selectively remove it from a newly fractured surface with an appropriate solvent and to test for it as a solute. Another fraction to extract would be cresol, and so on, observing the structure of the surface at each step. If skeletal networks actually exist, they should be visible, or at least concrete evidence of their existence should be detectable, in the electron microscope during such a process, and any change of the observed colloidal particles could be followed.

References

1. Carothers, W. H., *Chem. Rev.*, **8**, 402 (1931).
2. Flory, P. J., *J. Am. Chem. Soc.*, **63**, 3083 (1941).
3. de Boer, J. H., *Trans. Faraday Soc.*, **32**, 10 (1936).
4. Houwink, R., *Trans. Faraday Soc.*, **32**, 122 (1936).
5. Megson, N. J. L., *J. Soc. Chem. Ind.* (*London*), **67**, 155 (1948).
6. Pritchett, E. G. K., *Chem. Ind.* (*London*), **1949**, 295.
7. Megson, N. J. L., *Phenolic Resin Chemistry*, Academic Press, New York, 1958, ch. 8.
8. Freeman, J. H., *Anal. Chem.*, **24**, 955 (1952).
9. Madorsky, S. L., and S. Straus, WADC Tech. Rept., 59-64 Part II (1960).
10. Hunter, R. F., and O. Turner, *Chem. Ind.* (*London*), **1957**, 72.
11. Erath, E. H., and R. A. Spurr, *J. Polymer Sci.*, **35**, 391 (1959).
12. Rochow, T. G., and E. G. Rochow, *Science*, **111**, 275 (1950).
13. Scott, D. W., *J. Am. Chem. Soc.*, **68**, 1877 (1946).
14. Roth, W. C., and D. Harker, *J. Am. Chem. Soc.*, **69**, 474 (1947).
15. Spurr, R. A., E. H. Erath, and H. Myers, *Ind. Eng. Chem.*, **49**, 1838 (1957).
16. Erath, E. H., and R. A. Spurr, *J. Polymer Sci.*, **28**, 233 (1958).
17. Finn, S. R., N. J. L. Megson, and E. J. W. Whittaker, *Chem. Ind.*, **69**, 5849 (1950).
18. Megson, N. J. L., and W. A. Wood, *Nature*, **140**, 642 (1937).
19. Hunter, R. F., and V. Vand, *J. Applied Chem.* (*London*), **1**, 298 (1951).
20. Klug, H. P., and L. E. Alexander, *X-ray Diffraction Procedures*, Wiley, New York, 1954.
21. Spurr, R. A., E. H. Erath, H. Myers, and D. C. Pease, *Ind. Eng. Chem.*, **49**, 1839 (1957).

JOURNAL OF POLYMER SCIENCE: PART C NO. 3, PP. 77-89

Morphology of Molded Melamine-Formaldehyde

H. P. WOHNSIEDLER, *Stamford Research Laboratories, American Cyanamid Company, Stamford, Connecticut*

INTRODUCTION

The organization of the physical and chemical structure of a thermoset resin on a macromolecular level is a challenging question. Inherent in the physical structure are factors which may have an important bearing on strength as well as other properties of the resin or plastic derived from it. The polymer chemical structure of a thermoset resin is generalized as a crosslinked one and in one concept as being a continuous polymer network. Yet the thermoset resins, as a rule, do not exceed in ultimate strength the strength of other resins in which secondary valence forces alone exist between polymer chains. This raises questions as to whether a crosslinked structure or lattice operates effectively and over what range of dimensions within the overall structure to influence various properties. Features of surface morphology may be particularly important for durability to atmospheric exposure or factors involved in normal use of the plastic. The need for new information has stimulated the present interest in the subject.

In 1949 Rochow and Rowe published the first electron micrographs of surfaces of molded melamine-formaldehyde resin, molded polyacrylonitrile[10] and (1950) phenolformaldehyde.[14] The surfaces were exposed by brittle fracture of the plastics and replicated by a gelatin silica technique. A particulate structure was characteristic in each case with particle sizes for the three types in much the same range. The particles were considered to be near if not equal to the macromolecular sizes.

Shortly thereafter Siegel, Johnson, and Mark[15] published electron micrographs of polystyrene deposited from solution by an atomizing technique on glass and shadowed with metal. They estimated the molecular weights of the individual particles, purportedly the macromolecules.

Since the early work, the electron micrograph has come into increasing use to reveal the fine structure of polymeric materials on a macromolecular level. With such diverse materials as silicone elastomers, naturally occurring polymers and polystyrene, molecular weights have been estimated from the particle volumes seen collectively or individually in electron micrographs. It has been found that these values are in reasonable agreement with molecular weights estimated by physical chemical techniques. The thermosetting polymer field is devoid of these confirmatory methods. The purpose of this paper is to review the chemical evidence which bears on

melamine-formaldehyde polymer structure and polymer size in conjunction with the visible structural evidence of the electron micrograph to see whether a clearer view and interpretation of the structure of the molded resin can emerge.

The Electron Micrographical Structure and Polymer Size

The typical features of this structure have been revealed in previously published micrographs.[10,11] One of these is reproduced at a higher magnification in Figure 1. For the original micrographs the plastic surface was replicated by the gelatin silica technique without shadowing. Gelatin

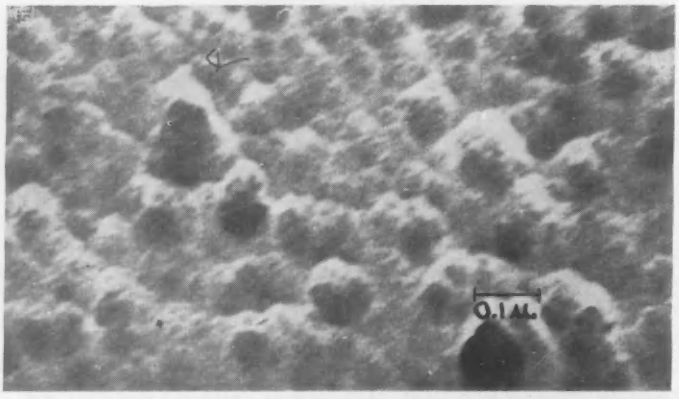

Fig. 1. Electron micrograph of replica of fracture surface of molded melamine-formaldehyde.[11]

itself is polymeric and while it does not appear to have added any discernible structure to a variety of polymeric materials in electron micrographs, confirmation of the melamine-formaldehyde molded structure was sought by a different replicating technique. In this case a molded disc of the same material represented in Figure 1 was brittle fractured and replicated with silica alone. Prior to deposition of the silica a film of liquid Joy* detergent was formed from aqueous solution over the fractured surface as a parting agent. A glass slide similarly coated was used as control. Fragments of the replicating silica were recovered by water flotation. Figure 2 shows a coarse granular texture similar to that previously associated with samples of this type. The silica separated from the glass control was structureless.†

At a magnification of $\sim$100,000$\times$ an area of the micrograph shown in Figure 1 and considered particularly distinctive and characteristic was redrawn to bring out essential details of size and organization. The simplified version appears as Figure 3. Three dimensional structure is emphasized in the drawing in conformity with both the three dimensional

* Registered trademark of Proctor and Gamble.

† M. C. Botty, American Cyanamid Company.

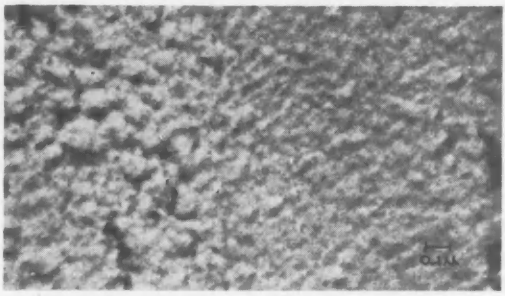

Fig. 2. Replica of fracture surface by JOY detergent-silica technique.

structure of the fracture surface as seen with the unaided eye and with an interpretation of normal shadowing in the electron micrograph.

The electron micrographs show a number of fairly distinctive features which can be attributed to the melamine-formaldehyde resin. The structure is seen to be a particulate one composed of what may be primary particles 150–200 A. in diameter and what are seen to be aggregates 700–800 A. in diameter. Contours are invariably rounded and in three dimensions all particles appear to approximate spheres. While particles and aggregates of these size ranges are quite prominent close inspection shows the presence also of intermediate and larger sizes.

Before proceeding with the discussion of these particles the work of other investigators concerned with the interpretation of electron micrographs of polymer particles should be mentioned. Rochow and Rochow[12] in a study of the size of silicone rubber molecules cited the high molecular weights of dimethylsiloxane elastomer as determined by osmometry and showed close agreement between the values estimated in this way and values of molecular weights estimated for the same type polymer from electron micro-

Fig. 3. Simplified rendition of melamine-formaldehyde structure.

graphs. Hall and Doty[5] compared the average sizes of isolated macromolecules determined by electron microscopy and physical chemical methods also finding close agreement. More recently Richardson,[9] working with polystyrene, and by careful choice of solvent, has isolated by spraying, individual macromolecules as well-defined spheres.

In the case of melamine-formaldehyde polymers physical chemical methods for molecular weight estimation are available only for relatively low molecular polymer. Previous estimates of polymer size, where crosslinking is known to have occurred have of necessity been based on conjecture. Kohler[7] showed that melamine-formaldehyde condensates up to the point where they lost solubility in pyridine attained molecular weights of 3000. This indicates that certain soluble polymers can be prepared having an average degree of polymerization of about 20. Polymers are formed in this system by condensation and the linking of melamine units through methylene groups. As the degree of reaction increases, the number of linkages in relation to number of triazine rings, i.e., the ratio (—CH_2—/ melamine) moles, increases. This ratio, designated L_m, is significant in that it is essentially a linking index.[16] It does not differentiate however between intermolecular and intramolecular linkages. Relationships between L_m and DP for polymer models are useful in discussion and interpretation of experimental L_m values in terms of possible polymer sizes and crosslinking densities.

In Figure 7 as a preliminary to discussion of polymer models, certain features which are to be expected in a melamine-formaldehyde polymer are set forth in a conventional two dimensional structure. Features include the methylene linkage, the randomness of functional group distribution, chain branching, and crosslinking and it suggests spatial requirements. Not represented are the many arrangements in three dimensions which an individual polymer can assume under favorable conditions due to normal rotations about bonds. In a Stuart model of the methylenedimelamine structure, rotation about the bonds between methylene carbon and amino nitrogen permits the two triazine rings to be aligned with the one behind and parallel to the second. While there seems to be no reason for this to be a preferential orientation in polymer having such units, this normal freedom of movement makes possible the twisting and coiling of polymer chains and their interlocking with other chains under certain conditions.

The N—H- - -N, N—H- - -O, and O—H- - -O bonds represent secondary, low energy bonds which may have an influence on a number of properties of the melamine resin.[17] In the crystal structure of melamine, Hughes[6] has shown that unit cell packing of the molecules is dominated by the NH- -N bonds between ring nitrogen and extra-nitrogen hydrogen forming chelate rings and in such a way that the planar triazine rings occur both parallel and near normal to each other. In the lowest DP polymer there are opportunities for more diverse hydrogen bonding than in melamine and their bonding force is undoubtedly a factor for crystallinity which, ordinarily latent, can be observed after exposure to a suitable environment. In

TABLE 1
Polymer Series Models

Polymer series model		Relationship of L_m and DP	Maximum value of L_m, (DP = ∞)
Model	Number		
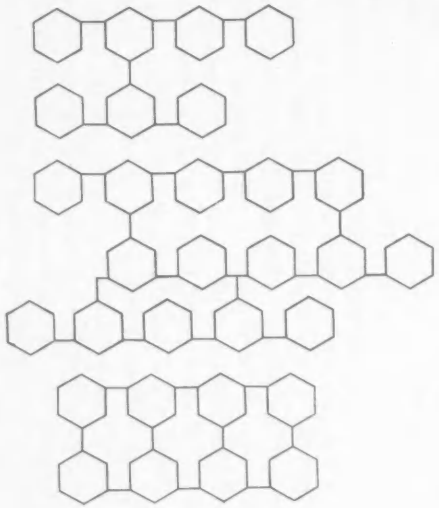	M_1	$L_m = \frac{DP - 1}{DP}$	1.0
	M_2	$L_m = \frac{4 + \frac{DP - 5}{5} \times 6}{DP}$	1.2
	M_3	$L_m = 1.5 - \frac{2}{DP}$	1.5

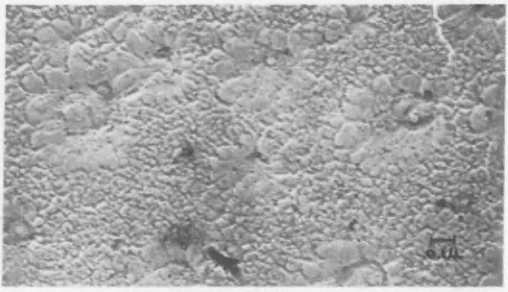

Fig. 4. Replica of melamine-formaldehyde condensate, DP = 1.3.

Figure 4, for example, the spherulites observed for a sample of average DP 1.3[8] were probably produced by partial solution and crystallization during an attempted replication with gelatin in solution. With increase in polymer size and heterogeneity of the chain manifestation of crystallinity becomes nil. Random orientation apparently is forced on the chains by other factors than hydrogen bonding. For this reason, the role of this bond in polymer orientation as seen for example in the crystalline linear polyamides[1] and crystalline polypeptides[2] has no analogy in the melamine-formaldehyde system. Until a detailed examination of bonding possibilities and crystallinity in the system is carried out it must be assumed that hydrogen bonds are distributed randomly in higher polymer.

All of the compositions discussed in this paper are based on a formaldehyde melamine mole ratio (F/M) of 2.0, as a typical ratio. A molding resin formulated with F/M = 2.0 and $L_m = 0.78$ and then cured by molding for various intervals showed a progressive increase in L_m value to 1.30.[17] At this point recourse to polymer models[16] is helpful in further discussion.

In Table I a number of these are given, each representing a polymer series in which the polymer is enlarged by the regular addition of one unit to a like one. At the L_m value of 0.78 noted for the molding composition one is dealing with an average DP of 4–5 and a linear or branched polymer. At $L_m = 1.30$ for the advanced molded state it is apparent that the average state of the polymer corresponds with, in the one extreme, an infinitely large polymer with a degree of crosslinking somewhat greater than that represented by polymer series model M_2 and in another extreme with polymer represented by model M_3 and an average DP of only 10.

Model M_2 appears to be a truer average representation than M_3. The kinetics of polymer growth in a fluid medium under ideal conditions favor the extension of the chain much more than crosslinking. In early stages of growth the individual polymer is surrounded by many others as well as monomer in close proximity and the chances for reaction of two molecules is much greater than for combination of groups on the same molecule. This is particularly true for the polymer as an extended chain. When confined in space, by coiling and interlocking with other molecular species, growth

of the chain by the same preferential process, although less obvious, is still probable. Ultimately, when the material in a confined region becomes a single large polymer molecule or a small number of large branched chains, further reaction must of necessity form intramolecular linkages with the crosslinking density progressively increasing.

Granting for the moment that the melamine-formaldehyde polymer in its most advanced degree of reaction as measured bears in its average condition an analogy with either of the two extremes discussed but more likely with that of model M_2, what significance does this have in connection with the electron micrographic morphology?

Representative of the weight and size of the average monomeric unit of model M_2 is the following:

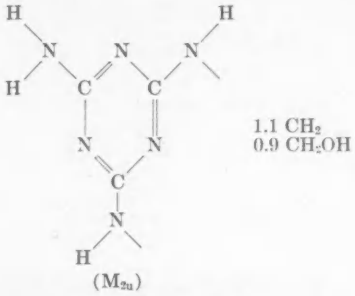

(M_{2u})

Actually from DP 10 to DP ∞ the only change in this unit will be from $\begin{bmatrix}1.0\ CH_2\\1.0\ CH_2OH\end{bmatrix}$ to $\begin{bmatrix}1.2\ CH_2\\0.8\ CH_2OH\end{bmatrix}$. On a molar basis the weight of this unit is 167.3 g. By assuming the resin to consist only of polymer the volume of the molar unit (density of molded resin 1.50) would be 111.6 cc. and from this the volume occupied by the unit as part of a molecule calculates to $(111.6 \times 10^{24})/(6.02 \times 10^{23})$ or 185 A.^{3}. The volume of a primary particle seen in the electron micrograph having a diameter of 150 A. and calculated as a sphere is (1.767×10^6) A.^{3}. Thus a single such particle would be equivalent in volume to $(1.767 \times 10^6)/(1.85 \times 10^2)$, or 9550$\times$ that of the M_{2u} unit.

In actuality the resin consists of not only polymer but a small amount of condensation water in addition, this being dispersed throughout the polymer. In cured resin having L_m value 1.3 the free moisture is on the order of 6.0%. To obtain a corrected value for the volume of the M_{2u} unit, allowance for the volume occupied by the free water must be made. Associating a mole of unit, 167.3 g., with 10.7 g. water, the total weight, 178.0 g., will occupy 178.0/1.50 or 118.7 cc. The volume occupied by the M_{2u} unit then becomes $(118.7 \times 10^{24})/(6.02 \times 10^{23})$ or 197 A.^{3} and the number of such units equivalent to the volume of the primary particle of 150 A. diameter, $(1.767 \times 10^6)/(1.97 \times 10^2)$ or 8960. The sizes of the corresponding M_{1u} and M_{2u} units were calculated in the same way but uncorrected for free water volume in the plastic. All unit sizes are listed in

TABLE II
Number of Structural Units per Micrograph Particle for Different Polymer Models

Number	Polymer series unit		Volume of unit, A.[3]	Number of units per micrograph particle	
				150–200 A. particles	700–800 A. particles
M_{1u}		0.99 CH_2 1.01 CH_2OH	188	$(9.6–22)10^3$	$(9.6–14.2)10^5$
M_{2u}	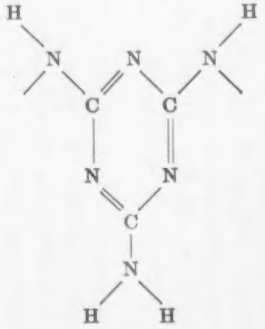	1.1 CH_2 0.9 CH_2OH	185	$(9.6–23)10^3$	$(9.7–14.5)10^5$
			197[a]	$(9.0–21)10^3$	$(9.1–13.6)10^5$
M_{3u}		1.25 CH_2 0.75 CH_2OH	182	$(9.7–23)10^3$	$(9.9–14.7)10^5$

[a] Corrected unit volume for 6% water in the plastic.

Table II together with the calculated number of such units per micrographic particle.

The values listed in this table show very little change in the calculated number of polymer structural units per micrographic particle for the molecule visualized as an infinitely long chain, a large crosslinked chain with low crosslinking density or a highly crosslinked relatively small molecule. Model M_3 can be eliminated from serious consideration since it represents a highly improbable one. It requires the association of high crosslinking density with small molecules. Model M_2 represents a more rational average degree of crosslinking coupled with very large molecules.

Assuming as one possibility that the particles seen in the micrograph represent individual macromolecules of M_2 type their sizes in terms of DP and $\bar{M}_w$ are as follows:

Particle diameter, A.	DP	$\bar{M}_w$
150–200	9,000–21,000	1,500,000–3,500,000
700–800	910,000–1,360,000 (using corrected unit size)	150,000,000–230,000,000

Units as small as 110 A. and a range of particle sizes of 110–600 A. were reported in the earliest work of Rochow, Botty, and Rowe.[13] From these sizes they calculated $\bar{M}_w$ to be 630,000–100,000,000.

DISCUSSION

Confronted with the physical features of the molded melamine resin as revealed in the electron micrograph a concept must be developed regarding the form and distribution in space of the macromolecular network which is in harmony with these features.

The micrographical structure which appears after a brittle fracture seems reasonably to be the result of the distribution of strengths between its various units. The smallest detected unit or primary particle, 110 A. in size, was well within the resolving power of the early type instrument.[10] Based on frequently seen sizes the primary particle is therefore equivalent to a macromolecule of about 0.6–3.5 million molecular weight or to intercoiled macromolecules having a total number of chain units equal to that of the single macromolecule. The primary particle is the strongest unit of the structure, a fact which strengthens the chance that it is a macromolecule with covalent bonds or macromolecules so highly interlocked as to be for practical significance a single molecule.

The brittle fracture of the molded resin exposes the perimeters of the primary particles and their aggregates and therefore the bond strength between the primary particles and aggregates is lower than within the pri-

mary particle. It would seem that this is largely due to a much lower density of covalent bonds at the particle interfaces than within the particles. This viewpoint is strengthened by the type of failure illustrated in Figure 6. The crack appears to follow the contours of the aggregates unopposed.

The type of disperse structure revealed in the resin is in harmony with a view presented of the reaction kinetics and the degree of reaction found for the resin. The kinetics must be considered with other factors in order to

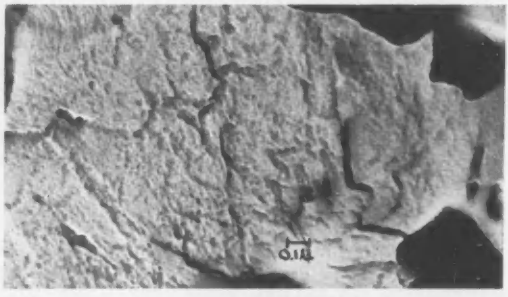

Fig. 5. Replica of molding composition by polystyrene tape-silica technique (M. C. Botty).

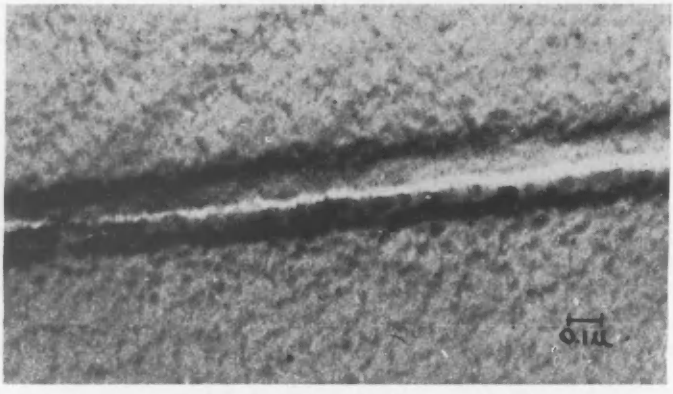

Fig. 6. Replica of molded sample cracked at −78°C. (gelatin-silica).

suggest the origin and development of a macromolecular network consistent with the observed structure. This network is one of tightly packed spheres with the principal macromolecular structure within the spheres and a lower density system of normal bonds or principally secondary force bonds connecting them. This physical structure is to be explained more in terms of colloidal phenomenon, steric requirements and habit of the growing macromolecule and the special conditions which apply in the preparation and final cure of the resin through various stages.

Beginning with the crystalline monomers or methylol melamines, as condensation takes place some crystallinity is retained in the lowest polymer. As polymerization progresses and the chain becomes more diversified chemically, crystalline order disappears and a lower degree of order, that of the aggregate, a result of random hydrogen bonding, must take over. The micrograph for the molding composition, Figure 5, shows an overall structure quite different from that of the molded resin shown in Figure 2 at the same magnification. While some rounded particles do appear they correspond in size with the smallest particles noted for molded resin. Therefore this structure is best interpreted as due to aggregates of low molecular material.

Early views regarding the aggregated and colloidal form of phenolic resins have been reviewed by Barkhoff and Carswell.[3] Electron micrographs of cured, unfilled phenolic resins by Rochow[14] and more recently Erath and Spurr[4] have depicted globules varying in diameter from 300 to 600 A. which are considered by the recent authors to be micelles. In the early stages of preparation of phenolic and melamine molding resins during which the DP rarely exceeds 10 and 5, respectively, their properties are characteristically colloidal. Solubility features, sol→gel transformations and syneresis of gels all point to a colloidal organization. During the molding operation, rapid polymerization and physical transformation occur and the advanced macromolecular state is reached. The morphological features attributable to the macromolecule then become of paramount interest.

Previous studies of a melamine-formaldehyde molding resin have shown that during the first 30 sec. of application of heat and pressure in the molding operation, the polymerizing composition flows throughout the die cavity and becomes rigid with the degree of reaction corresponding with L_m 0.95. In terms of a branched chain polymer this is equivalent to an average DP of about 20. Visualizing the average polymer molecule at this stage as being coiled and twisted after its formation period from the original aggregate, this being a more random orientation (higher entropy) than the extended chain, further polymer growth, due to packing and restraint upon molecular movement, must take place within a restricted volume of material enclosed by the chains and immediately surrounding them. In this way the formation of long chains irregularly coiled and twisted but assuming a physical state approximating the sphere becomes a reasonable possibility in conformity with the electron micrographic structure. Acting as a nearly independent dynamic unit, the material within the sphere, through being in contact longer, can ultimately become a single, large, branched chain macromolecule and then a crosslinked one according to the reaction order expressed earlier. While this view favors the building of the largest, coupled with the more highly crosslinked, polymer within the primary particle, linking can also proceed simultaneously across the boundaries of the primary particles to link the particles within the aggregated structure of the micrograph. Many of the outwardly appearing aggregates

may in themselves be single macromolecules having molecular weights of 150–250 million. While no limit to the extension of the polymer molecule throughout the mass of material can be envisioned theoretically, it can be inferred from the micrographical structure that fracture probably follows the path of lowest bond density and that linking discontinuities in the secondary structure exist. The distribution of condensation water throughout the physical structure is an uncertain feature. Its concentration at the particle interfaces due to a syneresis effect, as a strong possibility, could serve to retard linking in this area.

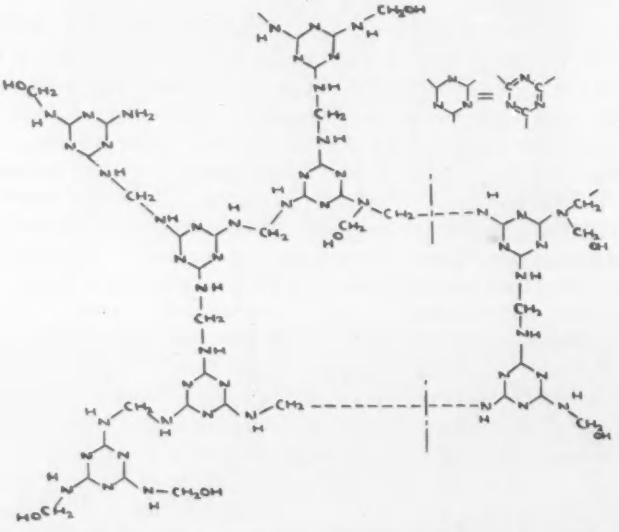

Fig. 7. Melamine-formaldehyde polymer showing chemical structure features.

In conclusion, the electron micrograph has provided what may ultimately be the most reliable insight into the macromolecular structure of the thermosetting type plastic exemplified by the melamine-formaldehyde system. Provided here is a tentative interpretation of how the macromolecule, having sizes previously reported, can appear as a seemingly discrete entity through the manner of its formation. The special nature of the macromolecular network with primary units of indicated sizes and having higher linking density than the secondary structure appears to be the morphological feature against which an interpretation of properties should be sought. It is hoped that experimental results can be presented in the future to provide a firmer basis for such interpretation.

The writer wishes to acknowledge the stimulating and helpful discussions held with T. G. Rochow and I. H. Updegraff and the skillful contribution of M. C. Botty.

References

1. Baker, W. O., and C. S. Fuller, *J. Am. Chem. Soc.*, **64**, 2399 (1942).
2. Bamford, C. H., and A. Elliott, W. E. Hanby, *Synthetic Polypeptides*, Academic Press, New York, 1956.
3. Barkhoff, R. A., and T. S. Carswell, *Ind. Eng. Chem.*, **36**, 461 (1944); also T. S. Carswell, *Phenoplasts*, Chapter V, Interscience, New York, 1947.
4. Erath, E. H., and R. A. Spurr, *J. Polymer Sci.*, **35**, 391 (1959).
5. Hall, C. E., and P. Doty, *J. Am. Chem. Soc.*, **80**, 1269 (1958).
6. Hughes, E. W., *J. Am. Chem. Soc.*, **63**, 1737 (1941).
7. Kohler, R., *Kolloid-Z.*, **103**, No. 2, 138 (1943).
8. Ledden, H. P., and I. H. Updegraff, *Tappi*, **42**, No. 2, 165 (1959).
9. Richardson, M. J., *Fifth International Congress for Electron Microscopy*, **1**, BB 12, Academic Press, New York, 1962.
10. Rochow, T. G., and F. G. Rowe, *Anal. Chem.*, **21**, 261 (1949).
11. Rochow, T. G., *Anal. Chem.*, **33**, 1810 (1961).
12. Rochow, T. G., and E. G. Rochow, *Science*, **111**, 271 (1950).
13. Rochow, T. G., M. C. Botty, and F. G. Rowe, Private report, 1949.
14. Rochow, T. G., Photographic Exhibit, ASTM, Atlantic City, N. J., June 26, 1950; also *Encyclopedia of Microscopy*, G. L. Clark, ed., Reinhold, New York, 1961, Figure 6, p. 529.
15. Siegel, B. M., D. H. Johnson, and H. Mark, *J. Polymer Sci.*, **5**, 111 (1950).
16. Wohnsiedler, H. P., *Ind. Eng. Chem.*, **45**, 2307 (1953).
17. Wohnsiedler, H. P., I. H. Updegraff, and R. H. Hunt, Jr., *Ind. Eng. Chem.*, **48** 82 (1956).

JOURNAL OF POLYMER SCIENCE: PART C NO. 3, PP. 91–101

The Morphology of Polymer Fracture Surfaces

J. P. BERRY,* *General Electric Research Laboratory, Schenectady, New York*

To an increasing extent polymers are replacing metals in applications as structural materials. For such purposes their mechanical, and particularly ultimate, properties are of primary importance. Even so, there has been surprisingly little research conducted in this field compared with that on the properties of the older established materials.

Much of the understanding of the fundamental atomic or molecular processes which underly failure in metals has been gained from the study of fracture surfaces, and it is therefore pertinent to consider what information can be obtained from similar studies on polymers. It should be realized at the outset, however, that the level of interpretation will depend on the nature of the molecular organization of the material under consideration.

Metals are normally polycrystalline aggregates, the crystalline phase having a relatively simple geometrical atomic structure. It is also possible to produce single crystals of metals of sufficient size for fracture experiments to be performed on them. Because of the simplicity of structure and physical homogeneity of such samples, and the elegance of the investigational techniques that are available, it is possible to explain the observed behavior in terms of the responses of the atomic lattice itself. The scale of the entities involved, and the structural regularity are such that electron microscopy and x-ray diffraction have played a major role in the interpretation of the observed behavior.

The structure of crystalline polymers is a subject of considerable complexity and the center of much current controversy. Though it is known that the bulk material is a polycrystalline aggregate, the details of the organization of the crystallites is much more complicated than in metals. The individual crystallites are much smaller than are normally found in metals, and though polymer single crystals have been prepared, and their structure established with a considerable degree of certainty, they are presently too small to be used for conventional strength and fracture experiments. Furthermore, it is probably the larger associative entity, the spherulite, that determines the fracture behavior, and hence the morphology of the fracture surfaces of the bulk material. For this reason, experiments on polymer single crystals are not likely to be as useful in providing infor-

* Present address: Rubber and Plastics Research Association, Shawbury, Shrewsbury, Shropshire, England.

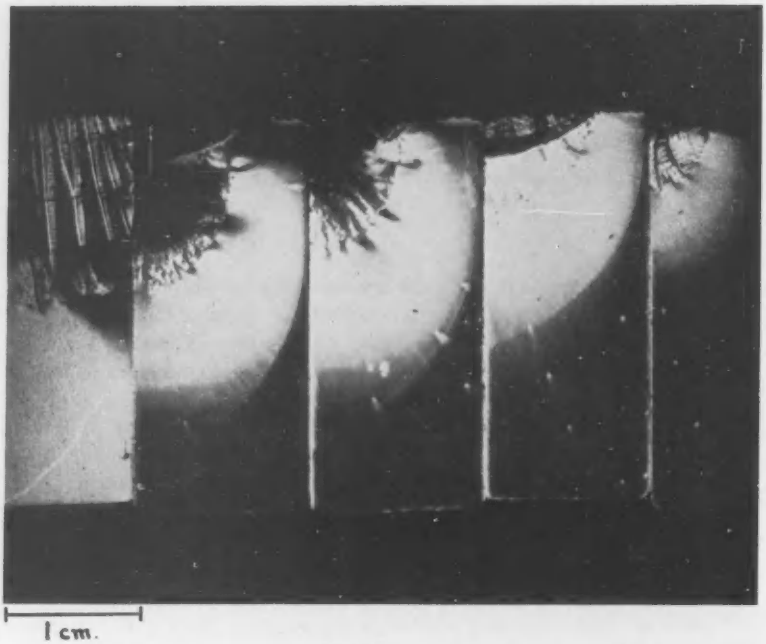

Fig. 1. The dependence of fracture surface character on the size of the initial crack in samples of poly(methyl methacrylate).

mation on the properties of the bulk material as have been the corresponding experiments on metals. Most of the fracture studies on single crystal and bulk crystalline polymers have been designed to provide information on the structure of the materials, rather than a knowledge of the structure being invoked to interpret the details of the fracture behavior. Clearly the second type of study can only proceed when the structural details have been established with reasonable certainty.

From an organizational point of view, glassy polymers have much in common with the inorganic glasses. There is a similar lack of structural order, and the body responses in both cases can be adequately represented as those of an isotropic elastic continuum down to essentially molecular dimensions. Consequently, the characteristics of the fracture surfaces are due to mechanical, rather than molecular, responses. By the same token, they are of a different order of size than those observed in metals, and optical rather than electron microscopical techniques are appropriate for their study. Moreover, the lack of structural order precludes the use of diffraction techniques for the determination of changes in the structure. Studies of fracture surfaces of glassy polymers have been concerned with the superficial features as revealed by optical and electron microscopy,[1,2] and the surface topography determined by interference microscopy or profilometry.[3]

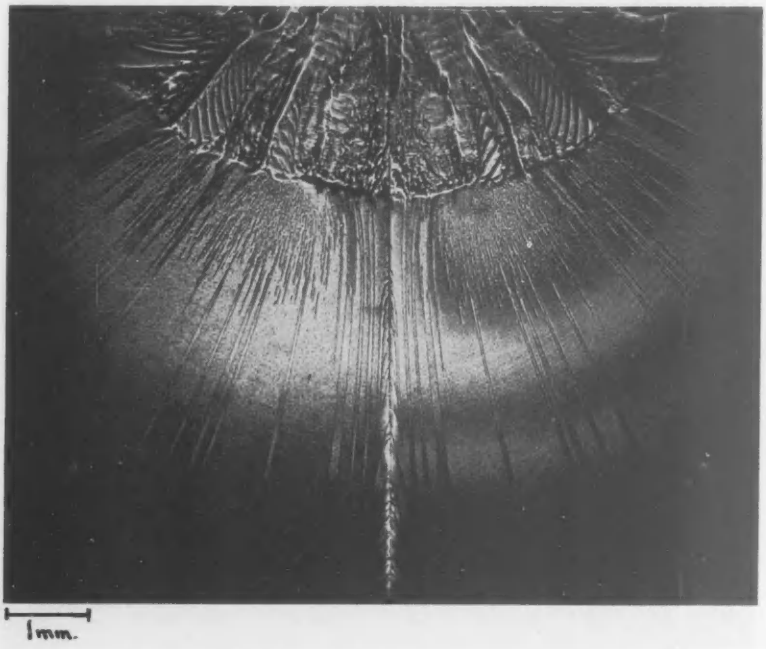

Fig. 2. The effect of the transition from low to high crack propagation velocity on the fracture surface of poly(methyl methacrylate).

Although the importance of the mechanical responses in determining the character of fracture surfaces of glassy materials is recognized, it has not yet been possible to define those responses sufficiently to relate them to the nature of the surface. The propagation of fracturing cracks has been studied,[4] but little attempt has been made to determine how far the characteristics of the fracture surface produced depend on those of crack growth.

The glassy polymer that has received the most attention in this respect is poly(methyl methacrylate), and it has been demonstrated that the nature of the fracture surface depends on the rate of load application,[5] the molecular weight of the material,[6] and the temperature of the experiment,[7] presumably since these factors influence the mechanical properties of the material.

In experiments to assess the validity of the Griffith tensile strength theory as applied to glassy polymers,[8] it was found that the nature of the fracture surface of poly(methyl methacrylate) depended on the size of the flaw (crack) that had been introduced into the sample (Fig. 1). In a conventional sample, the site of initiation of failure can usually be distinguished as a bright reflecting spot, frequently at the original outer surface of the sample. Immediately surrounding this area the surface is granular

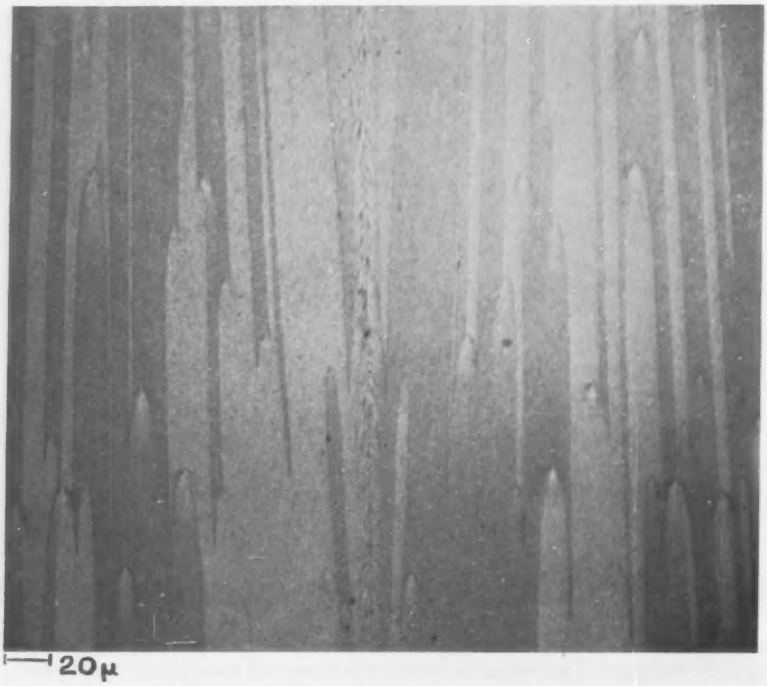

Fig. 3. Matching fracture surfaces of poly(methyl methacrylate) in the region of rapid crack growth.

and nonreflecting, the degree of roughness increasing with increasing distance from the initiation site. In this region parabolic surface markings are frequently observed. Eventually the crack becomes multiplanar, the fracture plane having bifurcated, and frequently a wedge of material is split off the further edge of the sample.

When the sample contains a crack, the same general characteristics are found, but the point on the surface at which they occur depends on the size of the initial crack. The larger this crack, the greater is the distance travelled in the direction of propagation before a particular kind of feature is detected. This fact makes possible the increase in area of surface occupied by the individual features, so that they can be examined in detail. For example, with large initial cracks, the reflecting mirror area can be made to occupy most of the fracture surface.

Observation of the sample as it fractures indicates that the primary flaw begins to increase in size relatively slowly. There is then a discontinuity in the propagation rate, which increases to a much higher value.[9] The transition in velocity corresponds to a change in the character of the surface, and it is the region of rapid crack propagation that is normally smooth and highly reflecting. Since the acceleration of the crack would be expected

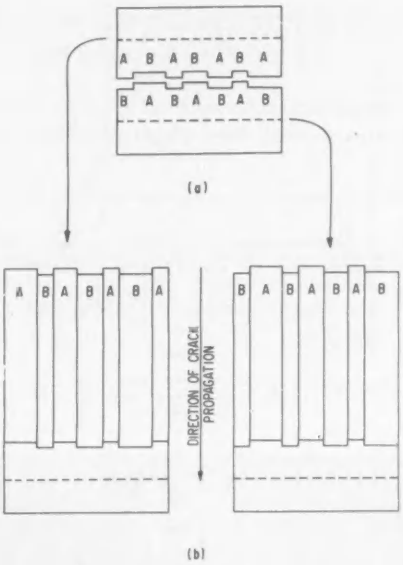

Fig. 4. Model of the fracture surfaces of poly(methyl methacrylate). In the (*a*) and (*b*) regions the surface layer is of different thicknesses and hence displays different interference colors.

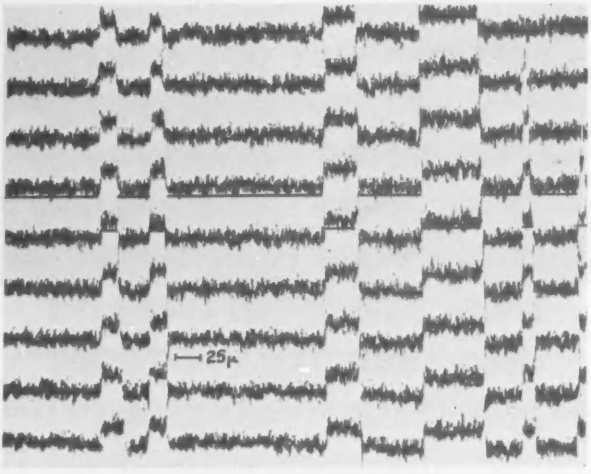

Fig. 5. Interference micrograph of a fracture surface. The reference line indicates the shift in a single fringe as it crosses the boundary of the color areas.

to depend on its initial size,[10] it is possible that the characteristics of the surface at any point are determined by the instantaneous velocity at that point.

One of the most striking characteristics of the slow growth region and the succeeding mirror area is that they display brilliant surface colors.[7,9,11]

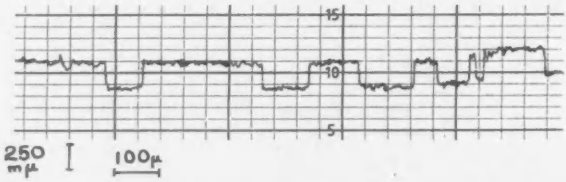

Fig. 6. Profilometer trace of a fracture surface in a region similar to that illustrated in Figure 5.

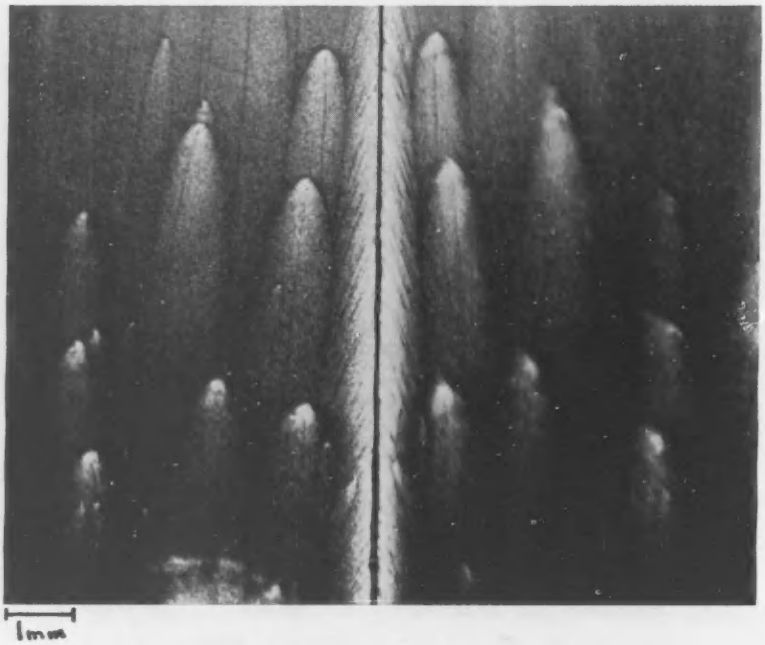

Fig. 7. Granular fracture surface of poly(methyl methacrylate).

Such colors are also present in the mirror area of a conventional sample, but because of the much smaller size of the area in this case they are not readily observable. The colors are believed due to optical interference in a thin film at the fracture plane where the structure of the material has been altered by the stresses associated with the travelling crack tip.[8,11]

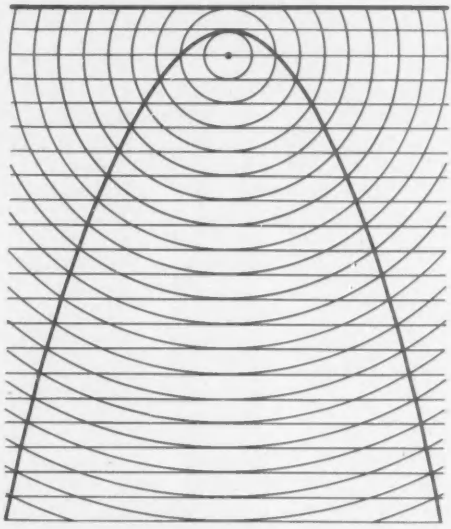

Fig. 8. Development of a parabolic surface figure by the intersection of linear and circular crack fronts.

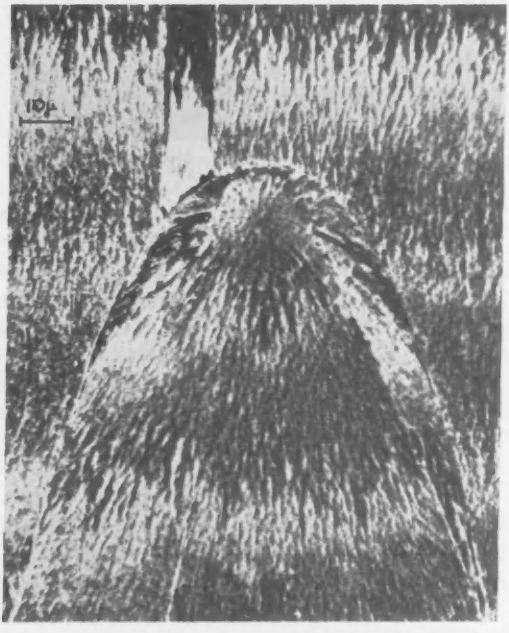

Fig. 9. Interference micrograph of a parabolic surface feature, showing evidence of the secondary fracture front.

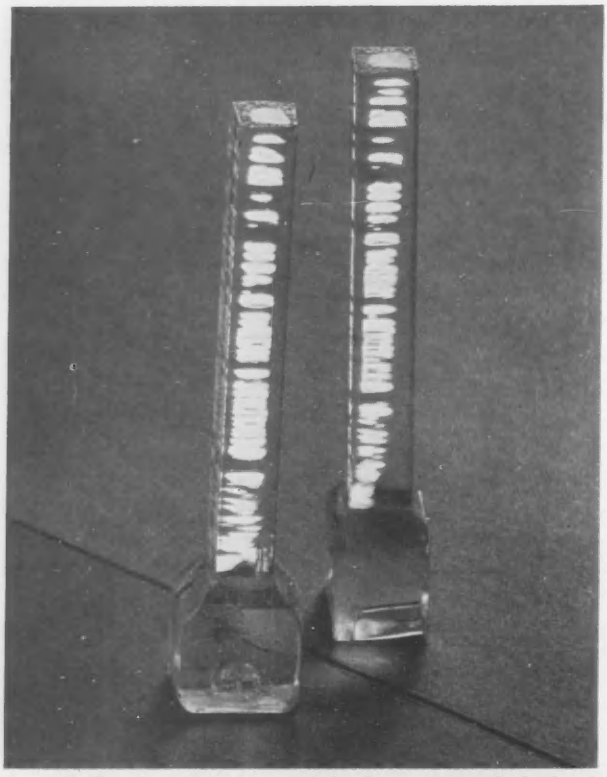

Fig. 10. Internal failure in an injection molded polystyrene sample, broken in tension.

The fracture surface of poly(methyl methacrylate) thus consists of a series of fairly well defined regions, though there is a true discontinuity in passing from one to the next only in the case of the first (slow growth) region to the second (mirror) region. The transition from the mirror area to the nonreflecting, granular region is not a sharp discontinuity even though it may appear to be so on casual examination of the fracture surfaces of conventional samples. It is convenient, therefore, to discuss in turn the features of these regions as they are produced successively by the passage of the fracturing crack.

The slow growth region has received little attention, presumably since it is usually not detectable in conventional samples. However, a similar effect is observed in metals,[12] where it has been attributed to the local ductile response of the material.[13] The fracture surface of a polymer is here quite irregular, with relatively deep furrows running roughly in the direction of crack propagation (Fig. 2).

In the mirror zone the surface features are remarkably simple, consisting essentially of fine lines running in the direction of crack propagation.

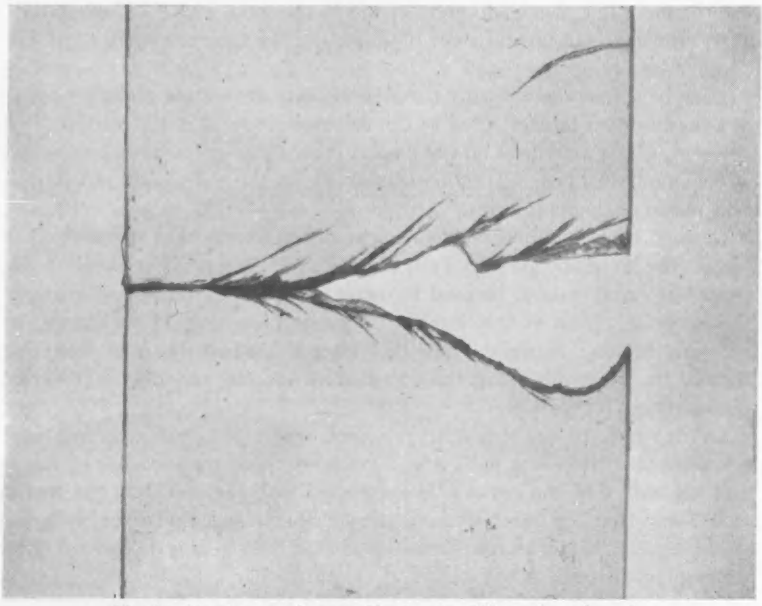

Fig. 11. Fracture surface profile showing bifurcation of crack.

There is a close relationship between the surface lines and the colors in the areas which they define. This relationship persists in the matching fracture surface, and is illustrated in Figure 3 and diagrammatically in Figure 4.[3] On the assumption that the colors are, in fact, due to thin film interference, the particular arrangement of the colors is consistent with a biplanar fracture surface topography. Interference microscopy and profilometry reveals that in this region the surface does display biplanar characteristics[3] (Figs. 5 and 6).

Parabolic surface features are frequently found in the mirror region, though they are more common in the granular region formed later (Fig. 7). They probably arise from the interaction of the primary crack with a secondary fracture that is initiated some distance ahead of the primary front.[14,15] Assuming that the primary front is linear, and the secondary fracture propagates uniformly from a point, a simple geometrical construction reveals that the intersection of the two fractures defines a parabola (Fig. 8). This hypothesis for the formation of the parabolas is supported by the observation of circular markings centered about the focus of the parabolas, which are occasionally detected by interference microscopy (Fig. 9).[3]

The occurrence of parabolas is therefore predicated on the possibility of the initiation of fracture at internal flaws in the material. The susceptibility of glassy polymers to this type of failure is also indicated by experiments in shock loading of rod samples, and such experiments reveal

that the inorganic glasses do not respond in the same way.[16] Correspondingly, parabolic features are not observed on the fracture surfaces of inorganic glasses.

It can be shown theoretically that the velocity of fracture crack propagation has an upper limit, related to the velocity of sound in the medium.[10,18] However, glassy polymers do not display such a well-defined limit since the moving crack can propagate discontinuously by the activation of internal flaws ahead of the main front.[4]

An important consequence of this type of response is that the method of toughening inorganic glass by inducing a residual compressive stress in the surface probably cannot be used to increase the strength of organic glassy polymers. A stress of this kind is frequently produced, fortuitously, in injection molded samples, but the sample frequently fails from an internal fracture initiated in the region that is under an effective residual tension (Fig. 10).[17]

As the crack passes through the region where the parabolas are most prevalent it is travelling with a high velocity. One consequence of this is that the nature of the stress field associated with the crack tip changes in such a way that the point of maximum tensile stress is no longer along the crack axis.[19] The maximum broadens so that the stress is uniform over an arc symmetrical about the axis, and at still higher velocities two maxima are found, also symmetrically disposed about the axis. Since the direction of propagation is determined by the locus of the maximum tensile stress, the shift in the position of the maximum induces a shift in the direction of propagation. At these high velocities the crack has a tendency to fork, therefore, each branch following a maximum stress locus. When the far side of the sample is reached a wedge of material is frequently detached (Fig. 11).

The fractography of polymers is in its infancy, but a degree of understanding has been gained of some of the features that are displayed, in terms of the mechanical, and in some cases, molecular responses of the material. A detailed understanding of the influence of a wide range of external (rate of testing, temperature) and internal (molecular weight and distribution, chemical constitution) experimental variables is still lacking. Since these features are produced under dynamic conditions, it would appear reasonable that they should depend in some way on those conditions (e.g., the crack velocity). However, little has been done to establish this relation. In most cases the fracture surfaces have not been examined in detail, nor is it known how the experimental variables affect the dynamic mechanical conditions under which the surfaces are formed. Such studies would do much to place the interpretation of fracture markings on a firm foundation, and would provide greater insight into those factors which govern the strength of polymeric materials.

References

1. Rochow, T. G., and F. G. Rowe, *Anal. Chem.*, **21**, 461 (1949).
2. Kies, J. A., A. M. Sullivan, and G. R. Irwin, *J. Appl. Phys.*, **21**, 716 (1950).
3. Berry, J. P., *J. Appl. Phys.*, **33**, 1741 (1962).
4. Schardin, H., *Fracture*, B. L. Averbach, D. K. Feldbeck, G. T. Hahn, and D. A. Thomas, Eds., Chap. 16, Technology Press and Wiley, New York, 1959.
5. Zandman, F., *Etude de la Deformation et de la Rupture des Matieres Plastiques*, Publications Scientifiques et Techniques du Ministere de l'Air, Paris, France, 1954.
6. Newman, S. B., and I. Wolock, *J. Appl. Phys.*, **29**, 49 (1958).
7. Wolock, I., J. Kies, and S. B. Newman, *Fracture*, B. L. Averbach, D. K. Feldbeck, G. T. Hahn, and D. A. Thomas, Eds., Chap. 13, Technology Press and Wiley, New York, 1959.
8. Berry, J. P., *J. Polymer Sci.*, **50**, 107 (1961).
9. Berry, J. P., *Nature*, **185**, 91 (1960).
10. Berry, J. P., *J. Mech. Phys. Solids*, **8**, 194 (1960).
11. Higuchi, M., *Repts. Res. Inst. Appl. Mech. (Japan)*, **6**, 173 (1958).
12. Felbeck, D. K., and E. Orowan, *Welding J. Research Suppl.*, **34**, 570-s (1955).
13. Stroh, A. N., *J. Mech. Phys. Solids*, **8**, 119 (1960).
14. Schwarzl, F., and A. J. Staverman, *Die Physik der Hochpolymeren*, Vol. 4, H. A. Stuart, ed., Chap. 3, Springer-Verlag, Berlin, 1956.
15. Smith, G. S., *Metallurgia*, **33**, 55 (1945).
16. Kolsky, H., *Fracture*, B. L. Averbach, D. K. Feldbeck, G. T. Hahn, and D. A. Thomas, Eds., Chap. 15, Technology Press and Wiley, 1959.
17. Schmitt, J. A., and H. Keskkula, *J. Appl. Polymer Sci.*, **3**, 132 (1960).
18. Roberts, D. K., and A. A. Wells, *Eng. Mining J.*, **178**, 820 (1954); *J. Mech. Phys. Solids*, **8**, 194 (1960), reference 6.
19. Yoffe, E. H., *Phil. Mag.*, **42**, 739 (1951).

THE CRYSTALLINE PHASE

JOURNAL OF POLYMER SCIENCE: PART C NO. 3, PP. 105–107

Morphological Aspects of Polymerization in the Solid State

DONALD G. GRABAR and CATHERINE S. HSIA CHEN,
American Cyanamid Company, Stamford, Connecticut

Morphology in the broad sense being considered here can be taken to include a wide range of characteristics, extending in size from the external shape of large objects to dimensions of the crystal lattice. Many examples can be found which demonstrate the effects of this spectrum of morphological features on a material's physical properties. As examples of the extremes just cited, one can alter the flexural characteristics of formed polymeric objects by altering their shape. Flexural characteristics of some polymers can also be modified by altering their degree of crystallinity. Morphological considerations on the crystal lattice scale relating to effects on physical properties of polymers have received increasing attention in recent years, particularly with the advent of stereoregular polymers. Less is known of the influence of this submicroscopic morphology on chemical reactions. This discussion will deal with some aspects of submicroscopic morphology on a particular type of chemical reaction; namely, polymerization in the solid state. Following a few general considerations, data will be presented to illustrate some specific influences of the crystal lattice on polymerization in the solid state.

In considering polymerization in the solid state it is apparent that two general factors are involved: (*1*) the chemical constitution of the monomer, and (*2*) its crystal lattice. Although the minimum chemical requirement for polymerization to occur is easy to specify (the monomer must have an appropriate functional group), even the minimum crystallographic criteria are not clear in absolute terms. However, some of the morphological factors which can be expected to exert an influence on solid state polymerization behavior are the following.

(*1*) The spatial arrangement of active groups of the monomer in the crystal lattice—their distance apart, and their relative orientation.

Molecular mobility is vastly more restricted in the solid state compared to that in the melt or solution, and so for at least the initiation of polymerization, the molecules must be "within reach" of each other. Once polymerization is initiated, the same factors may then influence the reaction rates, and conceivably also the structure (morphology) of the resulting polymer.

(*2*) "Texture" of the monomer, as related to the size of the crystals, number and type of lattice defects, and the presence of impurities.

These factors may all exert their influence through related mechanisms or arise from common causes. For example, crystal edges and defects may in some cases inhibit the propagation of polymerization through physical separation of the polymerizing units, while in other cases they may act as "active centers" for initiation. Impurities may act by creating lattice defects which subsequently affect polymerization, may act as a physical diluent to impede polymerization, or may serve to increase molecular mobility and aid in polymerization.

These and other factors relating morphology of the monomer to its behavior in solid state polymerizations have been noted by various investigators in this field, but generally an insufficient amount and detail of information in this area have been accumulated to define exactly the roles which these factors play. Pertinent data are often experimentally difficult to obtain—for example, crystal structures—and such data must be accumulated on a large number of systems before generalizations are possible.

A promising experimental approach to the isolation of crystallographic effects from chemical effects in solid state reactions lies in the study of polymorphs. When a compound can be obtained in two or more polymorphic modifications, the chemical identity of the compound remains a constant, and observed differences in behavior must be ascribed to differences in crystallographic properties. A study of the solid state polymerization behavior of two polymorphs of tributylvinylphosphonium bromide has been made by the authors, and was reported in detail at the International Symposium on Macromolecular Chemistry in Paris, July 1963.[1] Although one of the crystallographic modifications of this compound is thermodynamically unstable, it can be obtained in a metastable condition over a wide temperature range without its transforming to the more stable modification. The polymerization of both modifications, initiated by x-radiation, was studied by microscopical techniques in which the extent of polymerization of the crystalline monomer to amorphous polymer was assessed by measuring with a Berek compensator the loss of optical retardation accompanying polymerization.[2] Both polymorphs were found to yield amorphous polymers. Both behaved similarly kinetically with regard to the shape of their conversion-time curves, their values of dose-rate dependence, and the nature of inhibition and acceleration by oxygen. However, under all experimental conditions investigated the unstable modification exhibited a faster polymerization rate than the stable modification. Arrhenius-type plots of reciprocal half-times versus reciprocal temperatures show that the slopes of the lines are essentially the same. The similarities in their polymerization behavior can be ascribed to the fact that the two polymorphic modifications are chemically identical. The differences in their behavior—their polymerization rates—are reflected in the differences in the pre-exponential factors in the Arrhenius equation, which are governed in this situation by the crystal structures.

One can conclude from this study that morphology can exert an influence on the production of polymers as well as on their properties when polymerization is carried out in the solid state. Furthermore, in this case, it is the morphology of the starting materials which must be considered.

References

1. Hsia Chen, C. S., and D. G. Grabar, *J. Polymer Sci., Part C, Number 4*, to be published.

2. Grabar, D. G., and C. S. Hsia Chen, contribution to the ASTM Symposium on Resinographic Methods, Atlantic City, June 27–28, 1963; to be published as a Special Technical Publication of the American Society for Testing and Materials, Philadelphia, Penna.

JOURNAL OF POLYMER SCIENCE: PART C NO. 3, PP. 109–116

The Morphology of Crystalline Polymers, with Especial Reference to Single Crystals Grown from the Molten State

N. K. J. SYMONS,* *Plastics Department, E. I. du Pont de Nemours & Co., Wilmington, Delaware*

INTRODUCTION—THE "FRINGED MICELLE" CONCEPT

At an early stage in the study of natural and synthetic high polymers it was found that they showed crystalline properties in many cases, notably in giving definite although broad Bragg x-ray reflections. In the early thirties, a theory known as the "fringed micelle" concept was proposed[1,2] to explain the observed diffraction behavior. A solid polymer was regarded as a tangled mass of molecular chains, through which the individual chains wandered in a random manner; certain regions were visualized where a number of chain segments happen to be sufficiently precisely aligned to constitute small crystallites, these being interspersed with amorphous regions where the chain disorder was too great to permit crystallization. The relative amounts of the total crystalline and amorphous regions thus decided the degree of crystallinity of the polymer. As the latter was found to vary with such factors as chain branching in a manner predictable by the theory, for a number of years the fringed micelle concept was generally accepted for describing polymer morphology.

In more recent years, an increasing amount of experimental evidence has been found which does not find an explanation in the fringed micelle theory. By 1947, Bunn and co-workers had already studied spherulites in polyethylene[3] and nylon[4] and showed that these contained the molecular chains arranged in a regular manner, tangentially to radial growth elements of the spherulite. Some years later, electron microscopical evidence was obtained[5,6] showing polyethylene spherulites to have a complex lamellar surface structure. It was not easy to see how these experimentally established structures were formed on the basis of the micelle model. Further important evidence, requiring broader concepts of crystalline polymer morphology was soon forthcoming as a result of the polymer single crystal studies described below. Thus, while the fringed micelle may remain a suitable model to describe the morphology of polymers of quite low crystallinity, recent views regard the more crystalline polymers as made up

* Present address: Wilkinson Sword (International) Ltd., Colnbrook, Slough, Bucks., England.

of discrete lamellar elements, in which the molecular chains are accommodated in a rather regular folded configuration. On this basis, the x-ray diffraction amorphous halo is ascribed to lattice imperfections associated with the folds, and with terminal groups and branch points, rather than to disorder of the type envisaged in the earlier theory.

A. Polymer Crystallization from Dilute Solution

During 1957 the growth from dilute solution of single crystals of linear polyethylene was reported by three independent sources.[7-9] Electron diffraction showed that in these single crystal platelets the molecular chains were oriented in a direction normal to the flat surface of the crystal; this, taken with the fact that the approximately 100 A. crystal thickness is much less than the extended length of the constituent polymer chains, led Keller to suggest[8] that the chains must be accommodated in a folded configuration within the crystal thickness.

Since that time, solution growth of single crystals has been reported for a number of other polymers, including polyoxymethylene,[10] poly-4-methylpentene-1,[11] nylon 6,[12] nylons 7 and 8,[13] and polyacrylonitrile.[10] In the case of each of the polymers mentioned, the single crystals grew in the form of thin plates in which electron diffraction showed the chains oriented perpendicularly to the flat surface; thus it has become fairly well established that the chain folding mechanism proposed by Keller is a general phenomenon in the growth of polymer single crystals, at least from dilute solution.

In the case of linear polyethylene, careful studies[15-17] using electron diffraction and crystallographic darkfield techniques have shown that the lozenge-shaped single crystals observed actually grow most frequently as hollow pyramids composed of four structurally distinct sectors, or fold domains. Although these customarily collapse on drying, to form pleated platelets, under favorable conditions they have been observed by optical microscopy in their original pyramidal shape while still floating in the solution.[18] The different sectors are believed to be a consequence of chain folding occurring along each of the four (110) planes corresponding to the growing prism faces of the crystal. Evidence that the folding occurs in these planes has been found in the fracture behavior of the crystals, clean fracture, involving only weak van der Waals forces, being observed in directions parallel with the growth face, whereas on fracture normal to the growth face small fibrils of the polymer are pulled out across the break.[8,19]

Considerable attention has been given also to providing a theoretical explanation of why chain folding should occur during polymer crystallization from solution, and perhaps also from the molten state, and of the observed[20] dependence of the fold length on the crystallization temperature. These studies have led to theories based on both kinetic[21-25] and equilibrium[26,27] considerations.

B. Crystallization from More Concentrated Solutions

Although little data have been published for polymers other than linear polyethylene, the formation of well-defined single crystals appears restricted to quite dilute solutions. With polyethylene, these are typically under about 0.05% concentration, although the actual limit depends on the polymer molecular weight, the crystallization temperature, and the solvent used; in the case of polyoxymethylene, single crystals have been obtained from phenol solutions at the 0.2–2% level.[10]

When polyethylene is crystallized from solution at concentrations slightly above that leading to single crystal formation, the growth tends to be in dendritic forms,[7] and it appears that these also grow by chain folding.[28] With still further increase in concentration, the growth forms become progressively more complex. The composite structures also become too thick to permit penetration by an electron beam, which means they can be studied in the electron microscope only in the form of surface replicas, and electron diffraction is no longer applicable. Despite these obstacles, progress in the study of such complex structures has recently been made by Keller,[18] using the optical microscope together with a "detachment replica" technique[29] which allows the top layer of the composite growth to be removed for study by electron diffraction. These studies show the growth forms to consist of complicated splaying aggregates of monolayers which become more intimately connected and more resembling spherulites with increasing concentration of the solution. It appeared that chain folding remains an important factor in the growth of these structures, but with increasing numbers of the chains leaving any given layer to form tie molecules connecting it with its neighbors as the solution concentration becomes greater.

C. Crystallization from the Molten State

The crystallization of molten polymers normally results in the formation of spherulites. These are most readily observed and studied when the polymer is crystallized as thin films in which the spherulite growth is constrained to two dimensions, but the presence of three dimensional spherulites in the interior of the bulk material is shown on examining microtomed sections.

Electron microscopical examination shows the surface of spherulitic films is composed of a number of overlapping thin plates or lamellae, and the banded appearance of certain spherulites seen with the polarizing microscope has been attributed[9] to periodic variations in the orientations of these lamellar growth elements. A detailed analysis of the optical properties of two-dimensional spherulites on the basis of this model has been made by Keith and Padden.[30] Electron microscopical examination of fracture surfaces has shown that similar lamellae also exist in the interior regions of bulk specimens of many crystalline polymers, notably polytetrafluoroethylene,[31] polyoxymethylene,[32] and polyethylene.[33]

It is evidently very tempting to regard these lamellar structures in the melt crystallized bulk polymer as analogous to the solution grown single crystals, and so containing the constituent molecular chains in the same regular folded configuration, and there is some x-ray diffraction evidence to support this view. This evidence rests on the similarity of the observations made in the measurement of long period spacings in bulk specimens and in compacted aggregates of polyethylene single crystals. Such long spacings in the compacted crystal aggregates have been shown to agree well with the thickness of the constituent crystal platelets as measured in the electron microscope;[34] moreover, changes in the single crystal thickness produced by annealing, and apparently involving chain refolding to a longer fold length, are accompanied by a corresponding increase in the observed long period spacing.[35] As such long spacings, also dependent on the annealing treatment, have been found in melt crystallized bulk specimens of both polyethylene[36] and polyoxymethylene,[32] it appears likely that these spacings arise from a similar cause, namely, the presence of extensive chain folding in the polymer.

While there is thus both optical and x-ray evidence to indicate chain folding of crystalline polymers also occurs in the bulk state, this evidence is inferential rather than direct. The disadvantage of such bulk specimens is that they can so far (see, however, reference 29) be studied in the electron microscope in the form of surface replicas only, and are not suitable for examination by electron diffraction. This is also the case with the so-called "hedrites" observed in the melt crystallization of polyoxymethylene[32] and some other polymers.

However, direct evidence based on electron diffraction and showing chain folding in polymers crystallized from the molten state has recently been obtained. This evidence is contained in the work of Geil[37] with polypropylene, Magill and Harris[38] with nylons, and Symons[39] with polytetrafluoroethylene, described in the following section.

D. The Growth of Single Crystals from the Melt

1. Polypropylene[37]

Polypropylene can crystallize in either monoclinic or hexagonal crystalline modifications. Working with the polymer in the form of slowly cooled thin films, areas crystallizing in both modifications were observed in different regions of the film. Figure 1 represents an area crystallizing in the hexagonal modification, as is apparent from the outlines of the lamellar growth elements, and also shown by the electron diffraction pattern from a similar region of the film. As the diffraction pattern shows the molecular chains to be oriented perpendicularly within the thickness of the lamellae, and this thickness was seen from the micrographs to be only about 100 A., which is considerably less than the extended chain length, it is evident that the polymer molecules must be folded within these lamellae.

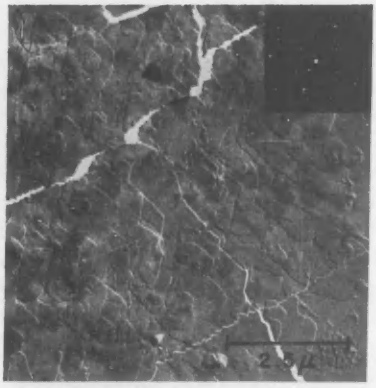

Fig. 1. Electron micrograph of lamellae in a thin film of polypropylene crystallized from the melt.[37] Inset: electron diffraction pattern.

2. *Nylons*[38]

By crystallizing the polymers in the form of very thin films compressed between glass cover slides, preparations containing apparently single crystal regions were obtained with a number of nylons. Figure 2 shows such regions in a thin film of nylon 5,7 as seen between crossed polarizers in the optical microscope; in this figure the inset electron diffraction pattern was obtained from an approximately 40 μ^2 region of film. A similar electron diffraction pattern was obtained with a film of nylon 5,6. The symmetry of these electron diffraction patterns indicated that the molecular chain direction was again essentially normal to the plane of the film; as the film thickness was only about 0.1 μ (1000 A.), here again it appears that chain folding probably has taken place.

Fig. 2. Optical micrograph of a thin film of nylon 5,7 crystallized from the melt;[38] viewed between crossed polarizers. Inset: electron diffraction pattern.

3. Polytetrafluoroethylene[39]

In this work, very small and physically isolated deposits of polymer were obtained by spraying droplets of dilute aqueous dispersions onto glass slides. These were heated at 350°C. and allowed to crystallize during cooling to below the polymer melting point (327°C.). The resulting discrete crystal formations were studied by electron microscopy, electron diffraction and optical microscopy.

The observed morphology depended on the amount of polymer involved in the crystallization. With quite scanty deposits, thin plates, such as those shown in Figure 3, were found. The electron diffraction pattern shows that, as suggested by their hexagonal outlines, such plates consist of

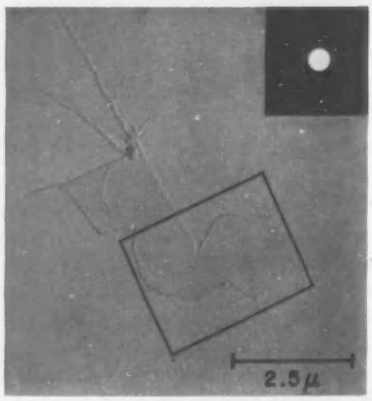

Fig. 3. Electron micrograph of single crystal of polytetrafluoroethylene grown from the melt. The framed region shows the area giving the inset electron diffraction pattern.[39]

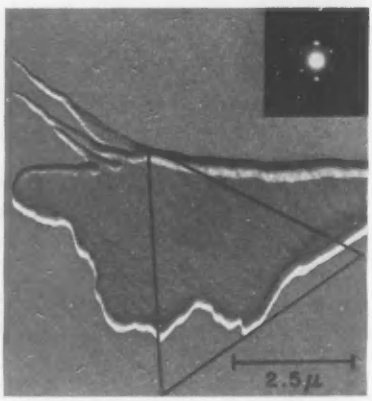

Fig. 4. Electron micrograph of polytetrafluoroethylene single crystal plate (~900 A. thick) grown from the melt. The framed region shows the area giving the inset electron diffraction pattern.[39]

single crystals, and also that the polytetrafluoroethylene (PTFE) molecular chains are oriented normal to the base of the crystal. Measurement showed the crystal thickness to be about 150 A.; as this corresponds to a PTFE chain segment of molecular weight only about 5750, and as the molecular weight of the dispersion polymer is known to be several million, the long chain molecules must be folded within the crystal thickness.

Somewhat heavier polymer deposits gave larger and thicker plates. Although these lacked the regular outlines of the thin hexagonal plates, if annealed for a period above 327°C., they, also, gave single crystal diffraction patterns, as shown in Figure 4. The thickness of the crystal in this picture is about 900 A.; this corresponds to a PTFE chain segment of molecular weight about 34,500, which still implies the necessity for chain folding. Many of these thicker plates were large enough for study with the polarizing microscope, and were found to present an isotropic view when seen in their normal position lying flat on the stage; this optical evidence supports the electron diffraction evidence that they are single crystals with perpendicular chain alignment.

In addition to the single crystal plates, both the scanty and heavier polymer deposits were seen to contain a number of broad bladelike crystal growths. As described in detail,[39] the optical and electron microscopical evidence indicated these to consist of stacks of overlapping inclined lamellae, so relating them to similar structures seen on the surface of annealed films and in the interior of bulk specimens[31] of this polymer.

References

1. Gerngross, O., K. Herrmann, and W. Abitz, *Z. Physik Chem.*, **B10**, 371 (1930).
2. Herrmann, K., and O. Gerngross, *Kautschuk Gummi*, **8**, 181 (1932).
3. Bunn, C. W., and T. C. Alcock, *Trans. Faraday Soc.*, **41**, 317 (1945).
4. Bunn, C. W., and E. V. Garner, *Proc. Roy. Soc., (London)*, **A189**, 39 (1947).
5. Peck, V., and W. Kaye, paper presented at the 12th Annual Meeting of the Electron Microscopical Society of America, Highland Park, Ill., 1954.
6. Claver, G. C., R. Buchdahl, and R. L. Miller, *J. Polymer Sci.*, **20**, 202 (1956).
7. Till, P. H., *J. Polymer Sci.*, **24**, 301 (1957).
8. Keller, A., *Phil. Mag.*, **2**, 1171 (1957).
9. Fischer, E. W., *Z. Naturforsch.*, **12a**, 753 (1957).
10. Geil, P. H., N. K. J. Symons, and R. G. Scott, *J. Appl. Phys.*, **30**, 1516 (1959).
11. Frank, F. C., A. Keller, and A. O'Connor, *Phil. Mag.*, **4**, 200 (1959).
12. Geil, P. H., *J. Polymer Sci.*, **44**, 449 (1960).
13. Holland, V. F., paper presented at the 18th Annual Meeting of the Electron Microscopical Society of America, Milwaukee, Wis., 1960.
14. Holland, V. F., S. B. Mitchell, W. L. Hunter, and P. H. Lindenmeyer, *J. Polymer Sci.*, **62**, 145 (1962).
15. Bassett, D. C., and A. Keller, *Phil. Mag.*, **6**, 345 (1961).
16. Neigisch, W. D., and P. R. Swan, *J. Appl. Phys.*, **31**, 1906 (1960).
17. Reneker, D. H., and P. H. Geil, *J. Appl. Phys.*, **31**, 1916 (1960).
18. Keller, A., *Polymer*, **3**, 393 (1962).
19. Holland, V. F., paper presented at the 143rd Annual Meeting of the American Chemical Society, Atlantic City, N. J., Sept., 1962.
20. Bassett, D. C., and A. Keller, *Phil. Mag.*, **7**, 1553 (1962).
21. Lauritzen, J. I., and J. D. Hoffman, *J. Res. Natl. Bur. Std., A*, **64**, 73 (1960).

22. Hoffman, J. D., and J. I. Lauritzen, *J. Res. Natl. Bur. Std., A*, **65**, 297 (1961).
23. Hoffman, J. D., and J. J. Weeks, *J. Chem. Phys.*, **37**, 1723 (1962).
24. Frank, F. C., and M. P. Tosi, *Proc. Roy. Soc. (London)*, **A263**, 323 (1961).
25. Price, F. J., *J. Polymer Sci.*, **42**, 49 (1960); *J. Chem. Phys.*, **35**, 1884 (1961).
26. Peterlin, A., and E. W. Fischer, *Z. Phys.*, **159**, 272 (1960).
27. Peterlin, A., E. W. Fischer, and C. Reinhold, *J. Chem. Phys.*, **37**, 1403 (1962).
28. Geil, P. H., and D. H. Reneker, *J. Polymer Sci.*, **51**, 569 (1961).
29. Bassett, D. C., *Phil. Mag.*, **6**, 1053 (1961).
30. Keith, H. D., and F. J. Padden, *J. Polymer Sci.*, **39**, 101, 123 (1959).
31. Bunn, C. W., A. J. Cobbold, and R. P. Palmer, *J. Polymer Sci.*, **28**, 365 (1958).
32. Geil, P. H., *J. Polymer Sci.*, **47**, 65 (1960).
33. Fischer, E. W., *Ann. N. Y. Acad. Sci.*, **89**, 620 (1960).
34. Keller, A., and A. O'Connor, *Nature*, **180**, 1289 (1957).
35. Statton, W. O., and P. H. Geil, *J. Appl. Polymer Sci.* **3**, 357 (1960).
36. Mandelkern, L., A. S. Posner, A. F. Diorio, and D. E. Roberts, *J. Appl. Phys.*, **32**, 1509 (1961).
37. Geil, P. H., *J. Appl. Phys.*, **33**, 642 (1961).
38. Magill, J. H., and P. H, Harris, *Polymer*, **3**, 252 (1962).
39. Symons, N. K. J., proceedings of the Fifth International Congress for Electron Microscopy, Academic Press, New York, 1962, p. GG 16; *J. Polymer Sci.*, **A1**, 2843 (1963).

JOURNAL OF POLYMER SCIENCE: PART C NO. 3, PP. 117–119

Kinetics of Spherulite Formation

FRASER P. PRICE, *General Electric Research Laboratory, Schenectady, New York*

A discussion of the kinetics of spherulite formation is pertinent to the description of the morphology of plastics because it is possible through a comprehension of the processes of transformation of liquid into crystals to obtain a more detailed understanding of the final state of the system—its morphology. Further if rational control over the resultant morphology is to be exercised, intimate knowledge of the kinetics of the transformation is imperative.

In the present case we are concerned with the kinetics of the liquid to crystal phase transformation when the crystals are aggregated into spherulites. Spherulite formation can be divided into two processes, nucleation (birth), and growth.

We will first consider the nucleation of the spherulite. This process can be either homogeneous or heterogeneous. In the former case, the first crystals in the spherulites start as a result of random fluctuations of order in the melt of the supercooled polymer. Theories, developed to describe this process,[1] usually lead to expressions for the nucleation rate I of the type

$$I = I_0 e^{-E^{\pm}/kT} e^{-\Delta F_n^*/kT} \tag{1}$$

where I_0 is a constant dependent on molecular parameters of the crystallizing molecule, $E^{\pm}$ is the activation energy for transport across the crystal–liquid interface, ΔF^* is the work required to form a critical sized nucleus, and k and T have their usual significance. The quantity ΔF^* depends on the bulk free energy of transformation as well as the various crystal–liquid interfacial energies. In particular, if the nucleus is assumed to be a right prism of square cross section

$$\Delta F_n^* = \frac{32\ \sigma^2 \sigma_e}{(\Delta S)^2\ (\Delta T)^2}, \tag{2}$$

where ΔS is the entropy of fusion per unit volume, ΔT is the supercooling, σ is the interfacial energy of the four equal sides, and σ_e is that of the other two sides. Now $E^{\pm}$ is usually taken to be the activation energy for viscous flow (of the order of 3–6 kcal.). Thus since ΔF^* is such a strong function of temperature, nearly the entire temperature dependence of I resides in the last exponential. Hence measurements of nucleation rate versus tem-

perature, when obtainable, can be used to calculate the quantity $\sigma^2\sigma_e$. Alternatively, since the product $I_0 e^{-E^*/kT}$ usually turns out to be about 10^{30}, I must be about 10^8 (cc. sec.)$^{-1}$ to be observable and is such a very strong function of ΔT, determination of the supercooling at which homogeneous nucleation sets in can be used to obtain an estimate of $\sigma^2\sigma_e$. The importance of this energy product will be discussed below. For reasons outlined subsequently, it is very difficult in polymeric systems to obtain homogeneous nucleation. In fact the only systems for which reasonable estimates of the homogeneous nucleation temperature are available are linear polyethylene[2] ($\Delta T_n \geqslant 65°$), poly(ethyleneoxide)[3] ($\Delta T_n \geqslant 70°$), and poly(chlorotrifluoroethylene)[1] ($\Delta T_n \geqslant 70°$). Only in the case of the linear polyethylene was a determination of the temperature coefficient of the rate obtained. It was about a factor of ten for two degrees change in temperature.

Unfortunately, for the determination of the $\sigma^2\sigma_e$, product, attainment of conditions of homogeneous nucleation is very difficult. This is due to the fact that nucleation of spherulites is facilitated by the presence of surfaces in contact with the melt—surfaces that are wetted by the crystalline phase. These result in formation of spherulites at temperatures that are so high that homogeneous processes are nonexistent. In the three polymers, whose homogeneous temperature range we know, spherulites appear at significant rates at supercoolings of only about 20°C. In these, as in many other polymers, the spherulites appear time after time at the same points in the polymer, and generally do not increase in number with time. Further the number of spherulites frequently depends on the melting temperature. These observations are consistent with the conclusion that under usual conditions of crystallization spherulites are heterogeneously nucleated. It should further be noted that nucleation that is sporadic in time and space is not unambiguously homogeneous in nature. Weakly wetted heterogeneities will exhibit this behavior. An excellent example of this behavior is that reported[4] for polydecamethylsebecate, where the number of spherulites increase with both time and supercooling, but at each supercooling at sufficiently long times, the number becomes constant. This shows unambiguously that here there are a fixed number of weakly wetted heterogeneities.

We will now consider the growth of spherulites. It has been shown for a wide variety of polymers that the radial growth rate is constant at a fixed temperature and for a given polymer system depends only on the temperature. Further the growth rate has an exceedingly high temperature coefficient. Both these observations imply that the growth is nucleation controlled. By this is meant that the formation of new crystalline regions, either extensions of existing crystals or totally new crystals, is controlled not by diffusion of material to or heat away from the crystal–liquid interface, but rather by the work required to form a small new crystalline region in contact with the old. This small new crystalline region will be called a growth nucleus and the rate of formation of such nuclei is expressed by an

equation similar to eq. 1. Thus the spherulite radial growth rate G can be expressed by

$$G = G_0 e^{-E^*/kT} e^{-\Delta F_g^*/kT} \tag{3}$$

where G_0 is a constant and

$$\Delta F_g^* = \frac{4\sigma\sigma_e b_0}{(\Delta S)(\Delta T)} \tag{4}$$

Here σ and σ_e are those defined for eq. 2, and b_0 is the height of the nucleus.

It should be noted that the products $\sigma^2\sigma_e$ and $\sigma\sigma_e$ are the only quantities in eqs. 2 and 4, respectively, that are not accessible to independent experimental determination. Thus knowledge of the homogeneous nucleation behavior combined with the temperature coefficient of the growth rate is sufficient to permit calculation of σ and σ_e.

These quantities in their most general sense may be regarded merely as adjustable parameters which permit correlations to be made between nucleation and growth phenomena. However if desired they may be interpreted as *bona fide* interfacial tensions and speculations can be made regarding their origins and magnitudes. In particular σ_e has been interpreted as the surface energy of the surface of folds of polymer molecules and from theoretical considerations is expected to be relatively large. These predictions have been borne out by studies on two polymers, polyethylene and poly(chlorotrifluoroethylene). However several more crystallizable polymers must be investigated before the general validity of these concepts can be considered to be established.

References

1. Hoffman, J. D., and J. J. Weeks, *J. Chem. Phys.*, **37**, 1723 (1962).
2. Cormia, R. L., F. P. Price, and D. Turnbull, *J. Chem. Phys.*, **37**, 1333 (1962).
3. Price, F. P., paper presented at IUPAC Symposium on Macromolecules, Wiesbaden, Germany, 1959.
4. Sharples, A., *Polymer*, **3**, 250 (1962).

JOURNAL OF POLYMER SCIENCE: PART C NO. 3, PP. 121–122

Mechanisms and Kinetics of Spherulitic Crystallization in High Polymers

H. D. KEITH, *Bell Telephone Laboratories, Murray Hill, New Jersey*

Abstract

A paper recently presented to the American Chemical Society dealt in a general way with mechanisms of spherulitic crystallization.[1] Attention was drawn to the fact that spherulites of remarkably similar morphology are found in polymeric and nonpolymeric materials, and to the implication that growth mechanisms of widespread validity are involved. It was shown that the grosser details of this morphology can be explained on a sufficiently broad basis by appealing to the observation that spherulitic crystallization is almost always found in multicomponent systems. The crucial point is that some of these components—which we call crystallization-rejected species or, simply "impurities"—are rejected preferentially by growing crystals and have a drastic influence on crystal habit. Our subsequent purpose was to describe in greater detail how this interpretation would apply to the specific case of high polymers.[2]

In the crystallization of a polymer melt there are principally two types of crystallization-rejected species to be considered. On one hand, stereoirregular molecules of various kinds—atactic, stereoblock or heavily branched molecules—may be present, and these will tend to be rejected on the grounds that their structures are less compatible with crystalline ordering than those of their stereoregular isomers. On the other hand, crystallization is accompanied by fractionation and molecules of low molecular weight will also tend to be rejected. In the melt, the concentration of these "impurities" will be greatest at growing crystal faces and the crystals will be surrounded by impurity-rich layers. In general, molecules which crystallize readily must first diffuse through these layers in order to reach growth sites, and the crystals are unlikely to grow indefinitely without developing a fibrous habit. As shown previously,[1] a fuller analysis of crystal growth under these conditions in melts of appreciable viscosity yields a rational explanation for most of the observed features of spherulitic morphology.

For present purposes, we may summarize the results as follows. As the surface of a growing spherulite advances into the melt, most of the readily crystallizable molecules are built into the advancing tips of radial crystalline fibers. Rejected impurities, on the other hand, diffuse away from the tips and are left behind to accumulate in the interstices between the fibers.

The widths of the fibers should be about D/G, where D is the self-diffusion coefficient of the melt and G is the radial growth rate of the spherulite. On this view, one may easily deduce the likely dependence of crystalline texture upon such variables as temperature of crystallization, average molecular weight, molecular weight distribution, and stereoregularity. Experimental studies confirm our expectations, and the results of these investigations will be outlined.[1,2]

Measurements have been made of the influence of impurity concentration upon the radial growth rates of spherulites. These assist us in analyzing the kinetics of bulk crystallization, by allowing estimates to be made of rates of crystallization in the "impure" melt left behind after the radial fibers have grown. Regardless of whether the impurities are stereoirregular molecules or molecules of low molecular weight, these rates will be shown to be relatively slow in almost all cases, corresponding to commonly observed departures from Avrami isotherms at large values of t, the time of crystallization. The data can also be analyzed to demonstrate the role of self-diffusion in the melt in determining rates of crystallization, thus providing a basis for understanding variations in crystallization kinetics with molecular weight.

References

1. Keith, H. D., paper presented to the 143rd American Chemical Society Meeting, Atlantic City, September, 1962; *J. Polymer Sci., Part A*, to be published.

2. Keith, H. D., paper presented to the 144th American Chemical Society Meeting, Atlantic City, April, 1963; to be published in conjunction with above.

JOURNAL OF POLYMER SCIENCE: PART C NO. 3, PP. 123–134

Fracture Studies of Isothermally Bulk-Crystallized, Linear Polyethylene

FRANKLIN R. ANDERSON, *Chemstrand Research Center, Inc., Durham, North Carolina*

INTRODUCTION

The fracture properties of thermoplastics have been studied quite extensively.[1–3] In addition, Speerschneider and Li[4] studied the fracture surfaces of deformed specimens of polytetrafluoroethylene and thereby elucidated the deformation modes. Studies of deformation have also been conducted on polyethylene films by Frank et al.,[5] on polyethylene spherulites by Keith and Padden,[6] and on solution-grown single crystals of polyethylene by Geil and Reneker,[7] Holland,[8] Kobayashi,[9] and Hirai et al.[10] These studies established that the folded molecules in polyethylene spherulites and solution-grown single crystals were pulled out and, to a large extent, unfolded during deformation. A schematic model for this process was developed by Hirai et al.[10]

The purpose of this paper is to describe the fracture conditions for bulk-polyethylene necessary to produce surfaces suitable for electron microscopical examination and where possible to define the deformation processes which produce unsuitable surfaces.

EXPERIMENTAL

For this study, whole polymer and fractions of Marlex 50 polyethylene were isothermally crystallized from the melt at various temperatures and for different times. The low molecular weight samples were fractured at room temperature and other samples were cooled in liquid nitrogen prior to fracture.

RESULTS AND DISCUSSION

By carrying out the fracturing process with sufficient care at these very low temperatures, the resulting fracture surfaces were shown to contain a lamellar structure such as that in Figure 1. This figure shows clearly two distinct types of lamellae. The lamellae in the upper left of Figure 1 are similar to those previously observed by Fischer[11] and we shall designate them as "regular" or Type I lamellae. This is to distinguish them from the "narrow" or Type II lamellae, which were previously described[12]

and are shown in the lower right of Figure 1. As reported earlier[12] these narrow lamellae are not simply regular lamellae seen edge on but have about the same thickness or step-height as the regular lamellae.

These two types of lamellae occur with about equal frequency, not only on the fracture faces but also on the free surfaces (Fig. 2) of all fractions with molecular weights above approximately 12,000. When lamella similar to Type I occur in melt-crystallized thin films, we have established

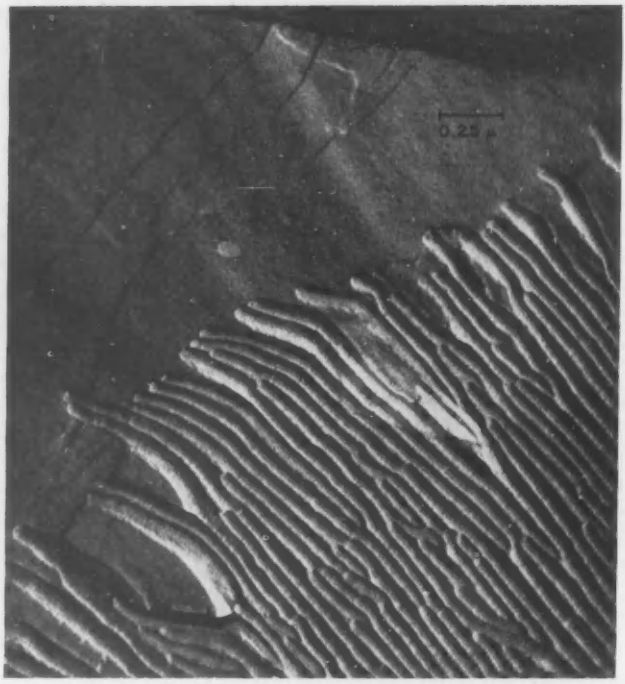

Fig. 1. Fracture surface of 50,200 M_η polyethylene.

by electron diffraction that the polymer chain axes are essentially perpendicular to the platelet or lamella thickness. Thus it would appear that the polymer molecules must be folded in order to fit into lamellae of both the "regular" and the "narrow" types.

The thickness or step-height of both Type I and II lamellae was observed to vary from about 150 to 350 A. depending upon the temperature of crystallization—the larger thickness corresponding to the higher crystallization temperatures. The widths of the Type II lamellae also vary with crystallization temperature, from about 350 to 800 A. Thus the widths of the Type II lamellae are always a little more than twice their thickness, and that of the Type I lamellae, although this is only a very rough approximation.

Fig. 2. Free surface of 64,600 M_η polyethylene.

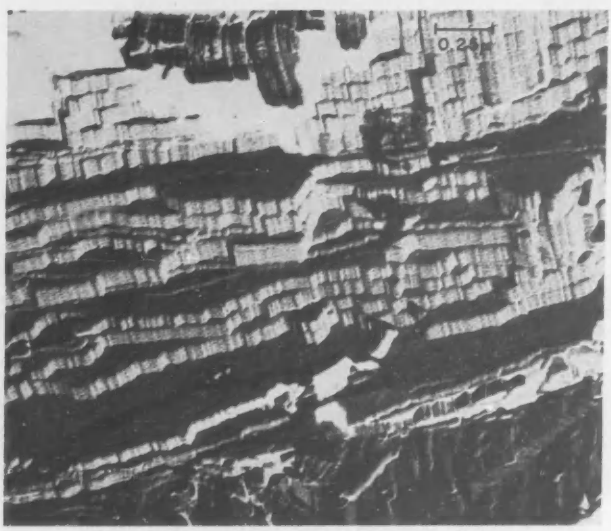

Fig. 3. Fracture surface of 5,890 M_η polyethylene.

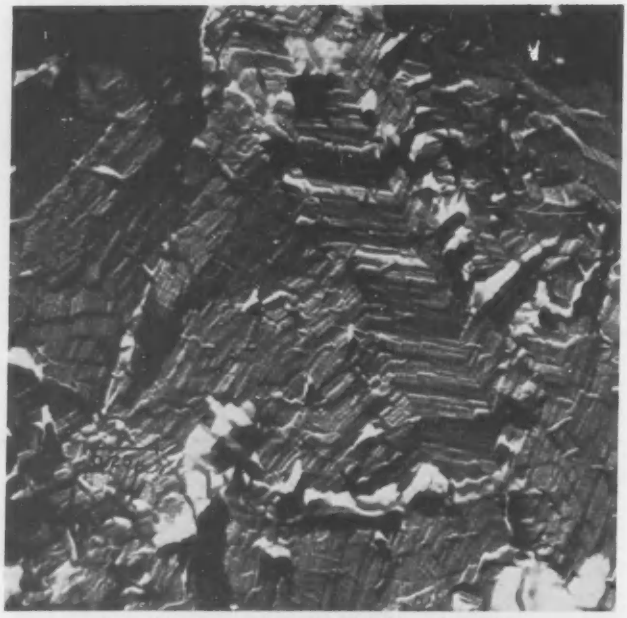

Fig. 4. Fracture surface of 10,000 $M\eta$ polyethylene.

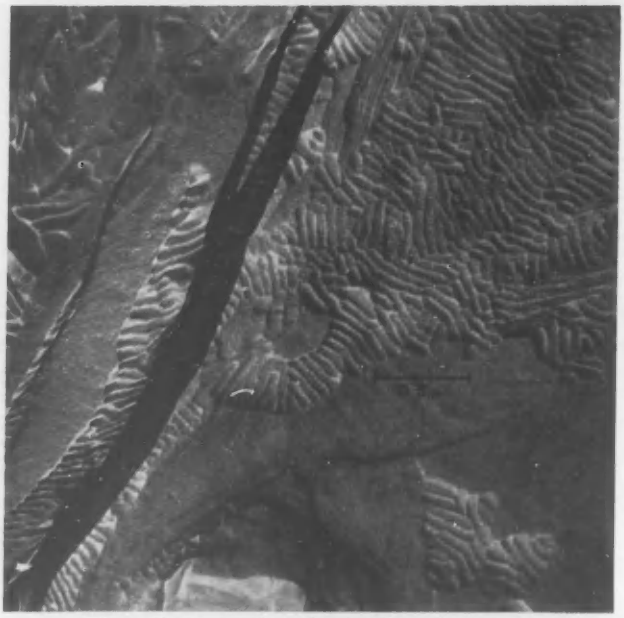

Fig. 5. Fracture surface of 11,900 $M\eta$ polyethylene.

Fig. 6. Fracture surface of 11,900 $M\eta$ polyethylene.

Fig. 7. Fracture surface of 10,000 $M\eta$ polyethylene.

Fig. 8. Fracture surface of 2,890 $M\eta$ polyethylene.

With fractions having a molecular weight of less than about 12,000, still a third type of lamella was observed, as shown in Figure 3. These lamellae (designated Type III) are similar in appearance to the "bands" observed in polytetrafluoroethylene by Bunn et al.[13] and by Speerschneider and Li.[4] These Type III lamellae tend to fracture perpendicularly to their widths, in a very irregular manner, leaving striations on the broken edges. These striations are of the order of 150–300 A. in width. In some cases the striations appear to be more prominent than the lamellae and they are tilted or inclined with respect to the lamella thickness, as shown in the center portion of Figure 4.

In a fraction with a viscosity-average molecular weight of 11,900 which had been isothermally crystallized for ten days at 128°C., it was possible to observe all three types of lamellae on different portions of the fracture faces. From a single fracture face, we obtained Figure 5, in which Type I and II lamellae are seen, and Figure 6, in which Type III lamellae are seen. In samples prepared from fractions with lower molecular weights, only Type III lamellae were normally observed. This is shown in Figures 6–8 and in Figure 3. Although it is not so apparent in these figures, the

Fig. 9. Fracture surface of 5,890 M_η polyethylene quenched into ice water.

step-heights of the Type III lamellae vary directly with M_η. The observed thicknesses of these Type III lamellae and the crystallization conditions used for the low molecular weight samples are summarized in the first four columns of Table I. In the last column of this table, the step-heights calculated from the viscosity-average molecular weights (with the assumption of fully extended chains) are given for each molecular weight.

From the data in this table, it can be seen that the measured thicknesses

TABLE I
Step-Heights of Low Molecular Weight Samples

M_η	Crystallization conditions	Measured range, A.	Step-heights, average, A.	Theoretical step-height, A.
2,960	4 hr. at 120°C.	150–475	315	268
5,890	8 days at 128°C.	250–900	585	533
10,000	3 days at 128°C.	450–900	700	906
11,900	10 days at 128°C.	500–1050	700	1080

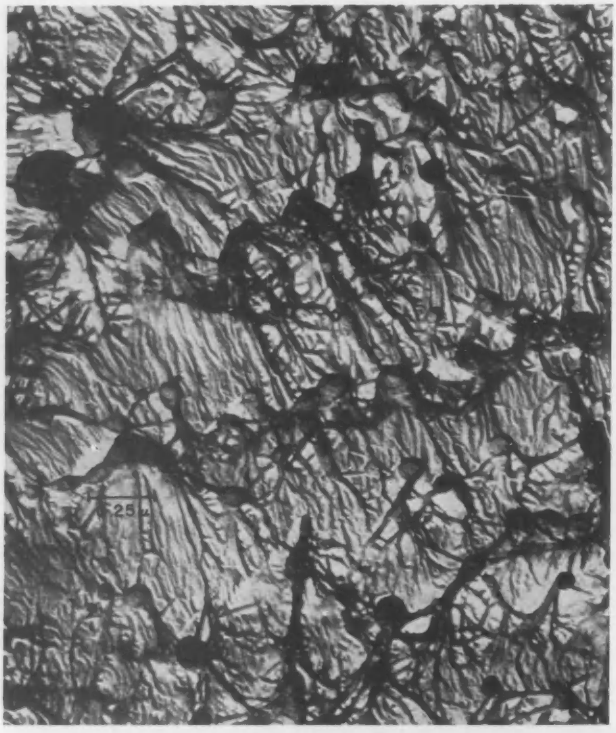

Fig. 10. Fracture surface of 64,600 M_η polyethylene.

or step-heights agree very well with the "calculated" step-heights. If one allows for a distribution of molecular weights, the uncertainties involved in a viscosity-average molecular weight relationship, and the possibility that at least in some cases the chains may be slightly tilted from perpendicularity, there appears to be good reason to believe that these Type III lamellae contain fully extended-chains.

Thus, under the conditions used here, molecular weights greater than 12,000 crystallized into a folded-chain conformation and below 12,000 they crystallized into an extended-chain conformation. However, it appeared that there should be nothing particularly sacrosanct about a molecular weight of 12,000. Whether one gets folded-chains or extended-chains during crystallization should be a function of the total crystallization conditions: molecular weight is just one factor. To test this conclusion, a 5,890 molecular weight sample was quenched from the melt into ice water and was subsequently fractured. The resulting fracture surfaces, illustrated in Figure 9, reveal lamellae with a thickness of about 150 A., which is much less than the estimated chain length of 533 A. and the previously measured thickness of 585 A. (Table I). These lamellae are

Fig. 11. Fracture surface of 64,600 $M\eta$ polyethylene.

undoubtedly of Type I. This was also confirmed by quenching a 2,890 molecular weight sample, in which case steps of 90–150 A. were observed in comparison with an estimated chain length of 268 A. From this, we can safely conclude that polyethylene can be crystallized from the melt either in the extended-chain conformation common to paraffins, or into a folded-chain conformation, analogous to the crystalline platelets grown from dilute solution. The conformation actually obtained depends upon the crystallization conditions, of which the degree of supercooling is the most important factor. Thus far, Type III lamellae have been obtained from molecular weights as high as 11,900 (crystallized for 10 days at 128°C.). Presumably, by waiting for longer periods of time at still higher temperatures it should be possible to obtain extended-chain crystallization of much higher molecular weights. This has recently been achieved using high pressures and temperatures during crystallization.[14]

As one might expect, samples containing chains in the extended conformation were extremely brittle and could be fractured easily at room temperature. On the other hand, the fracture surfaces obtained from the higher molecular weight samples were not always clean and sharp (Figure

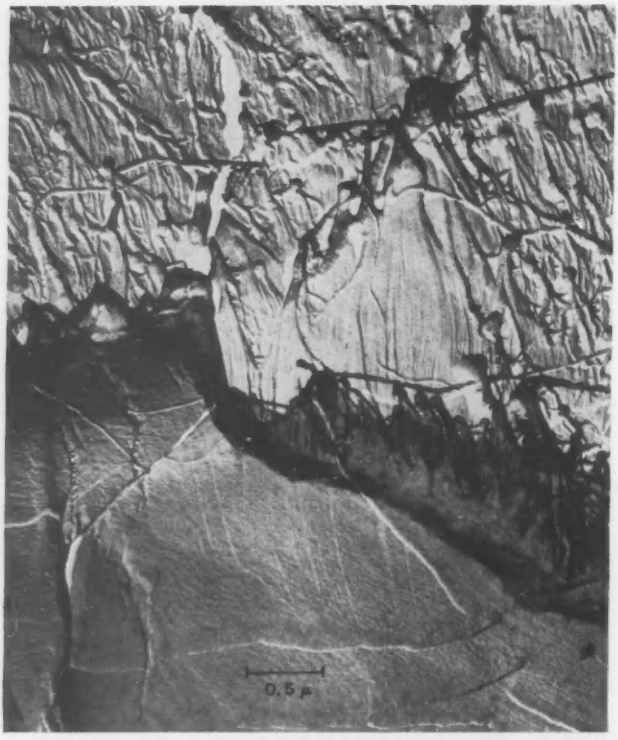

Fig. 12. Fracture surface of 64,600 M_η polyethylene.

10). Whether one obtains clean, sharp fracture surfaces or surfaces unsuitable for examination is dependent on the conditions of fracture to a much greater extent than with the lower molecular weight samples. In fact, it was necessary to cool the higher molecular weight samples prior to fracture, and also the temperature at fracture appeared to be critical. For instance, if the sample was cooled to the temperature of liquid nitrogen (≈ -195°C.) and fractured at this temperature, the type surface shown in Figure 10 was obtained. Adjusting the temperature at fracture to the range between ≈ -150 and -80°C. produced fracture surfaces like that shown in Figure 1. At temperatures above about -80°C. drawing occurred and an oriented structure was produced.

Thus, the temperature range in which fracture surfaces of higher molecular weight polyethylene suitable for examination in the electron microscope are obtained is in the same range as the gamma transition for polyethylene. This approximate temperature range has also been given as the tough-brittle transition range in polyethylene.[1] However, the reason for a relationship between the fracture surfaces obtained and these transitions is not yet clear.

The fracture surfaces which were examined and found to be unsuitable for observation of the inherent morphology can be explained through fairly well known deformation processes. When folded-chain lamellae are broken, the chains are pulled out and fibrils are formed. This is shown in Figure 11. If the pulling-out or orientation process is carried to the extreme, the fibrils which are formed begin to break and the energy thus produced is dissipated as heat. This heating causes the fibrils to melt at the broken ends and ball up in the manner shown in Figures 10 and 12. Therefore, to produce fracture surfaces in higher molecular weight polyethylene which reveal inherent morphology, it is necessary to adjust the temperature of fracture to the critical range between approximately −80 and −150°C. In this temperature range, inter-lamellae fracture (i.e., cleavage between the lamellae) occurs, thus producing clean, sharp fracture surfaces.

In conclusion, it has been shown in this investigation that polyethylene can be crystallized from the melt into either folded-chain (Types I and II) or extended-chain (Type III) lamellae, depending upon crystallization conditions. Type III lamellae fracture readily in a brittle mode whereas the Type I and II lamellae generally fracture in a ductile manner, in which chains are pulled out into fibrils. In order to obtain fracture between rather than within the folded-chain lamellae, it is necessary to control carefully the temperature at which the fracture occurs.

In general, Type III lamellae were obtained from the lower molecular weight fractions, while the higher molecular weight fractions crystallized into Type I and II lamellae. When the whole polymer was isothermally crystallized at relatively high temperatures, there was a tendency for fractionation to occur, with the higher molecular weights crystallizing in the form of folded-chain lamellae and the lower molecular weights crystallizing in the form of extended-chain lamellae.

Thus, the observation of these different types of lamellae now provides a morphological explanation for the effects which the different molecular weight fractions in polyethylene have on the mechanical properties of the polymer.

The author is indebted to Drs. P. H. Lindenmeyer and R. L. Miller for their helpful comments and discussions.

References

1. Vincent, P. J., *Polymer*, **1**, 425 (1960).
2. Hoff, E. A. W., and S. Turner, *ASTM Bull.*, **225**, TP208 (1957).
3. Maxwell, B., J. P. Harrington, and R. E. Monica, Princeton University Plastics Laboratory, Technical Report **24A** (1952).
4. Speerschneider, C. J., and C. H. Li, *J. Appl. Phys.*, **33**, 1871 (1962).
5. Frank, F. C., A. Keller, and A. O'Connor, *Phil. Mag.*, **3**, 64 (1958).
6. Keith, H. D., and F. J. Padden, *J. Polymer Sci.*, **41**, 528 (1959).
7. Geil, P. H., and D. H. Reneker, *J. Polymer Sci.*, **51**, 569 (1961).
8. Holland, V. F., private communication.
9. Kobayashi, K., private communication.

10. Hirai, N., H. Kiso, and T. Yasui, *J. Polymer Sci.*, **61**, S1 (1962).

11. Fischer, E. W., *Z. Naturforsch.*, **12a**, 753 (1957).

12. Anderson, F. R., paper presented before American Physics Society Meeting, St. Louis, Mo., March, 1963; to be published in the Special Polymer Issue of *J. Appl. Phys.*

13. Bunn, C. W., A. J. Cobbold, and R. P. Palmer, *J. Polymer Sci.*, **38**, 365 (1958).

14. Geil, P. H., F. R., Anderson, B. Wunderlich, and T. Arakawa, *J. Polymer Sci.*, to be published.

JOURNAL OF POLYMER SCIENCE: PART C NO. 3, P. 135

Relationship between Morphology and Deformation Mechanisms of Polyolefins*

KIICHIRO SASAGURI and RICHARD S. STEIN, *Polymer Research Institute, University of Massachusetts, Amherst, Mass.*

Abstract

The birefringence changes produced by stretching, polyethylene, polypropylene and polybutene were examined. It was found that the strain optical coefficient at low elongation for polypropylene and polybutene depends upon storage time at room temperature for quenched samples, changing sign from an initial positive value to a negative value. The change is similar to that observed upon changing temperature with polypropylene. At high elongation, the strain optical coefficient becomes positive in all cases. The change for polypropylene cannot be due to increased crystallization and does not correlate with changes in infrared spectra, x-ray diffraction, NMR, or light scattering. X-ray diffraction does reveal a difference in the crystal orientation mechanism for the fresh and aged sample.

For the fresh sample, the *c*-crystal axis tends to orient in the stretching direction, while for the aged sample, the *b*-axis orients in this manner. With polybutene, the time dependence of the strain-optical coefficient correlates with the transition in crystal structure observable by x-ray diffraction and infrared spectra. It is proposed that the changes are related to the amount of recrystallization or crystal deformation accompanying spherulite deformation upon stretching. A simple theory of these effects is presented which contains a parameter expressing this degree of change in internal structure. It is proposed that this parameter varies with time and temperature.

* The complete paper will appear in the special issue of the *J. Appl. Phys.*, devoted to the Meeting of the American Physical Society, Division of High-Polymer Physics at St. Louis, Mo., March 26–28, 1963.

POLYPHASE SYSTEMS

JOURNAL OF POLYMER SCIENCE: PART C NO. 3, PP. 139–149

The Morphology of Pressure-Sensitive Adhesive Films

CHARLES W. HOCK, *Physical Chemistry Division, Research Center, Hercules Powder Co., Wilmington, Delaware*

Just what adhesion is is still elusive in many respects. To ensure the continued development of the technology of adhesive bonding, we must increase our knowledge of the basic nature of the phenomenon. Enriching our understanding of the fundamentals of adhesion requires a multipronged approach embracing a variety of disciplines. Such things as an adhesive's composition, its specific physical and chemical nature at the molecular level, the manner in which it is used, and reliable tests for measuring its effectiveness are among the important and appropriate aspects of the problem. Another important consideration, and one not so frequently pursued, concerns the morphology of the adhesive systems. Or, in other words, what is their architecture?

The present discussion concerns the morphology of pressure-sensitive, or permanently tacky, adhesives. Pressure-sensitive adhesives exhibit tack although no solvent is present. The adhesive mass itself must both wet the substrate and deform at the interface to contact the substrate intimately enough to allow those forces which are responsible for adhesion to come into play. Tack is that property of the adhesive which enables it to form a bond of measurable strength immediately on contact with another material. Briefly, this property may be described as "instantaneous adhesion" or "quick stick."

The pressure-sensitive adhesives whose morphology we want to consider consisted of rubbery mixtures of an elastomer, either natural or synthetic, and a variety of rosin-based tackifiers. The adhesive masses were solvent cast from toluene and allowed to dry until solvent free. The resulting films consisted only of resin and rubber. Additives such as stabilizers were avoided, to surmount complexities which might have been introduced by their presence. The films' tack was measured by a method described by Wetzel.[1] A brass probe was applied to the pressure-sensitive surface for exactly one second. Thereupon, the stress required to break the bond was recorded. The morphology of the films was studied by means of electron microscopy.

Knowledge of the specialized techniques of electron microscopy is necessary but not sufficient for the successful application of this technique to difficult problems. Some grasp of the overall problem and the ability to correlate electron microscopical data with significant information from other sources is also a requisite. The analysis of pressure-sensitive adhe-

sion has been in progress in our laboratory for a number of years.[2] Electron microscopy has been a part of this program.[3] Our initial reports concerned adhesives made from various resins and natural rubber. More recently we have studied modified rosin tackifiers in adhesives based on synthetic elastomers.

The electron microscope is too well known an instrument to need any description here. We should recall, however, that the penetration of electrons through matter is slight and, accordingly, only very thin specimens can be used. Because the pressure-sensitive films consisting of resin and rubber were too thick for direct use, they had to be replicated. The adhesive films were first coated with a warm 10% aqueous solution of gelatin which on drying formed a negative replica of the adhesive surface. The latter was then removed by dissolving it in toluene. The remaining negative replica of gelatin was replicated with carbon, and shadowed with chromium to increase contrast in the images. This procedure appears to reproduce faithfully the surface of the adhesive films. It should be pointed out, however, that regardless of the excellence of the replication, there remains the task of examining enough microscopical fields of view to permit an accurate judgment regarding what is representative of the surface as a whole.

FILMS CONSISTING OF NATURAL RUBBER AND RESIN

In films consisting of unvulcanized natural rubber and resin, Wetzel[2] found that tack increased with increasing concentration of the tackifier. This relationship is shown graphically in Figure 1 for films consisting of rubber and Pentalyn* H, a pentaerythritol ester of hydrogenated rosin. Up to a concentration of 40% resin the films' tack was virtually the same as that of a 100% rubber film. From concentrations of 40–65%, tack increased very rapidly to a maximum and then dropped off sharply as the concentration of resin increased still further. What changes in film structure went hand in hand with these changes in tack? A film consisting only of rubber is shown in Figure 2. It is smooth and gives every indication of being homogeneous. Figures 3 through 7 illustrate how the structure of the films changed as the concentration of the resin was increased. You will notice that increase in tack is coincident with the formation of a second phase. This second phase is shown especially clearly in Figure 5, where the concentration of resin is 60% and the measured tack value of the film is high. A film consisting of 83% resin is shown in Figure 6. There are indications of a two-phase structure here, also, even though the film had no tack. Apparently, in this film the small amount of rubber is dispersed in a continuous phase of resin. At still higher concentrations of resin, i.e., around 90% and higher, the films lost their two-phase character entirely (Fig. 7).

These observations show that composition, tack and film morphology go

* Registered trademark, Hercules Powder Company.

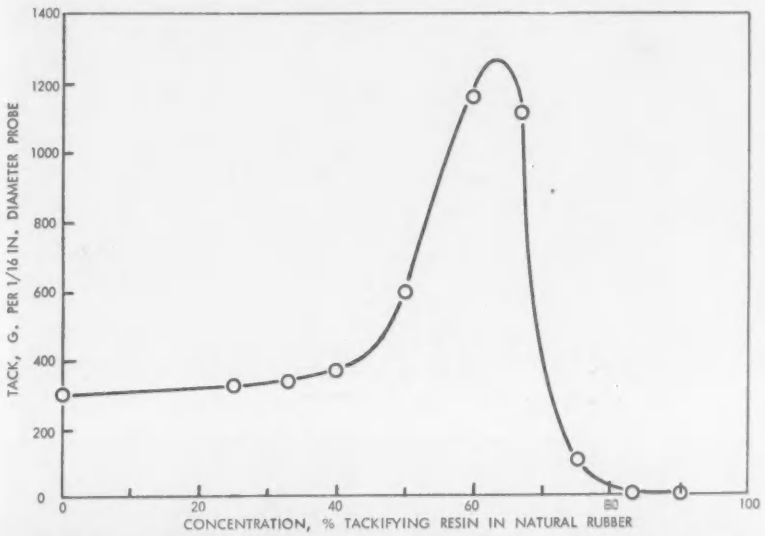

Fig. 1. Tack as a function of Pentalyn H (pentaerythritol ester of hydrogenated rosin) in natural rubber.

Fig. 2. Unaged film of natural rubber. Tack value 200–300, 7700×.

hand in hand. We find, for example, that in films having good tack, the tack is more dependent on the second phase which develops, and which probably consists of low molecular weight rubber molecules dissolved in resin, than on the continuous phase, which consists of rubber saturated with resin. Increasing the resin concentration evidently increases the amount of the second phase, and at the same time the films' tack. At maximum tack, presumably, the maximum amount of low ends of rubber has dissolved in the disperse resin phase. Further increases in resin concentration then result in phase inversion and a drop in tack.

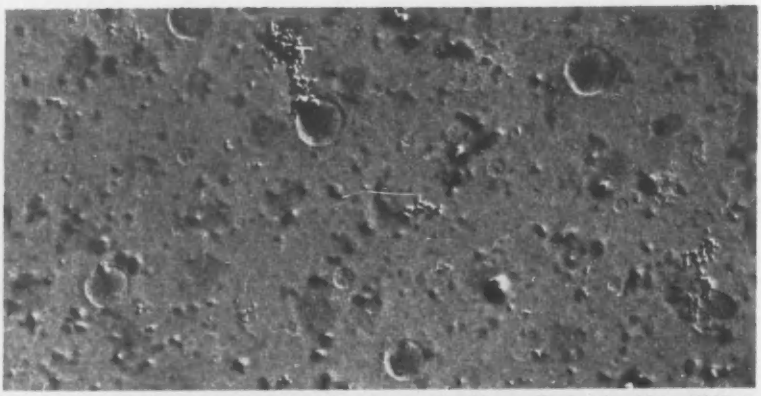

Fig. 3. Unaged film of 1:3 Pentalyn H and natural rubber. Tack value 320. 7700×.

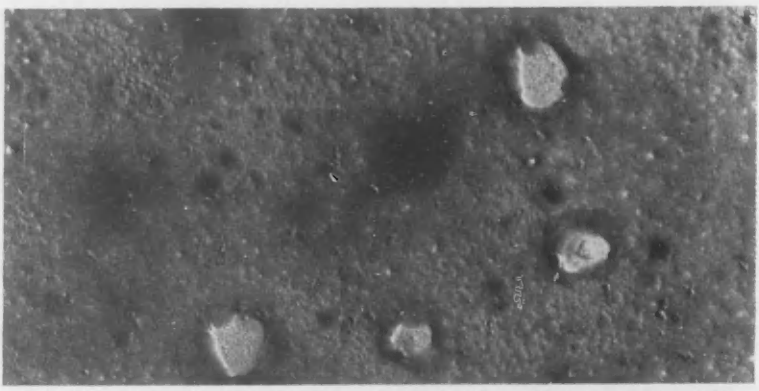

Fig. 4. Unaged film of 1:1 Pentalyn H and natural rubber. Tack value 930. 6300×.

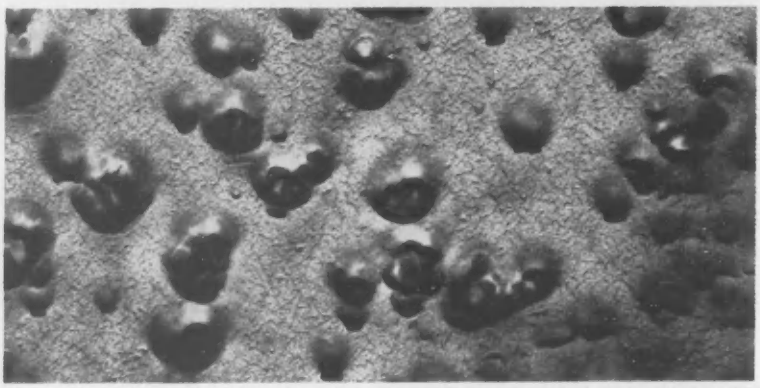

Fig. 5. Unaged film of 3:2 Pentalyn H and natural rubber. Tack value 1200–1300. 7700×.

These same general relationships prevailed when rosin-derived resins other than Pentalyn H were dispersed in rubber. However, the concentration at which the resin came out as a second phase, and at which tack increased over that of rubber alone, varied with each resin's softening point.

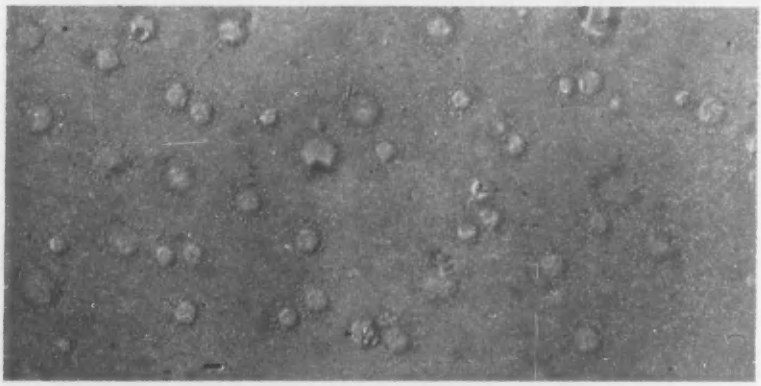

Fig. 6. Unaged film of 5:1 Pentalyn H and natural rubber. Tack value 0. 7700×.

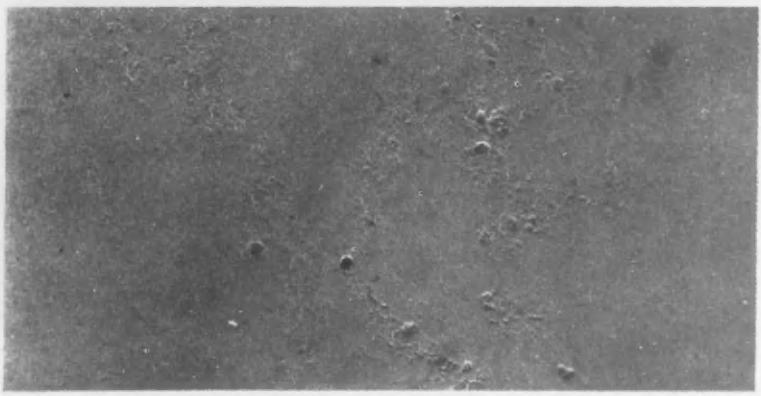

Fig. 7. Unaged film of 9:1 Pentalyn H and natural rubber. Tack value 0. 7700×.

Maximum tack, moreover, correlated inversely with the softening point of the resin. The higher the softening point, the lower the concentration of resin at which maximum tack was obtained.

FILMS CONSISTING OF SYNTHETIC RUBBER AND RESIN

The rubber-based adhesives industry was originally associated with natural rubber. More recently other elastomers—synthetic ones—have been used. We continued, therefore, studies of pressure-sensitive adhesive systems in which styrene–butadiene rubber (SBR), polyisoprene (synthetic

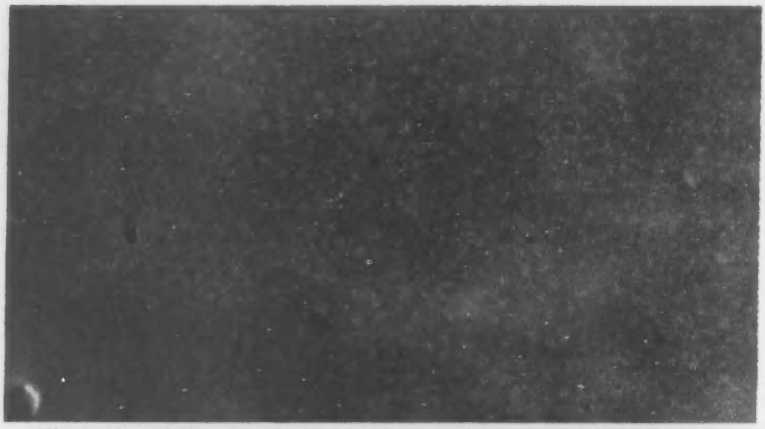

Fig. 8. Unaged film of synthetic polyisoprene. Tack value 250. 5600×.

Fig. 9. Unaged film of 2:1 Pentalyn H and synthetic polyisoprene. Tack value 1200. 5600×.

natural rubber), and polychloroprene (neoprene) replaced the natural elastomer.

First consider compositions of Pentalyn H and polyisoprene. Data obtained showed the same relationship between tack and composition as when natural rubber was used. What sort of structure do these films have? The all-polyisoprene parent film was very smooth and homogeneous (Fig. 8). A film containing 67% Pentalyn H—and having high tack—was distinctly two phase. Roundish disperse particles ranging in size from less than one up to several microns were distributed evenly throughout the continuous phase (Fig. 9). At lower concentrations of the resin, for example at 60% concentration, the two-phase character was readily evident

Fig. 10. Unaged film of SBR 1011. Tack value 200–250. 5600×.

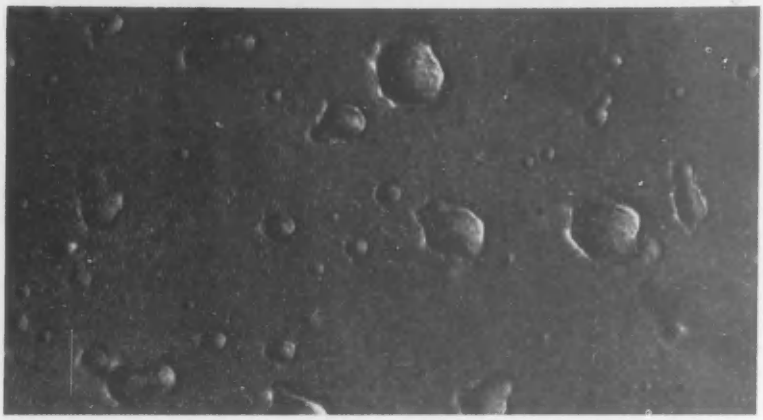

Fig. 11. Unaged film of 3:2 Pentalyn H and SBR 1011. Tack value 1000. 5600×.

also, but the dispersed particles were smaller and not so numerous. In short, the relationship between composition, tack, and structure was analogous to that of the corresponding system containing natural rubber.

The behavior of Pentalyn H resin in either of two types of styrene–butadiene rubber (one emulsion polymerized at 43°F., the other at 125°F.) approximated the behavior of that resin in both natural and synthetic polyisoprene. Films, made from elastomers only, had poor tack. They were fairly smooth and essentially homogeneous, but not as consistently so as the polyisoprene films (see Figs. 10 and 12). When Pentalyn H was added in amounts sufficient to affect the systems' tack, a second phase appeared in the films. When the concentration of the resin was at the level (60–65%) which gave maximum tack, the particles of the disperse phase were especially obvious, although different for the two types of SBR (Figs.

Fig. 12. Unaged film of SBR 1500. Tack value 200–250. 5600×.

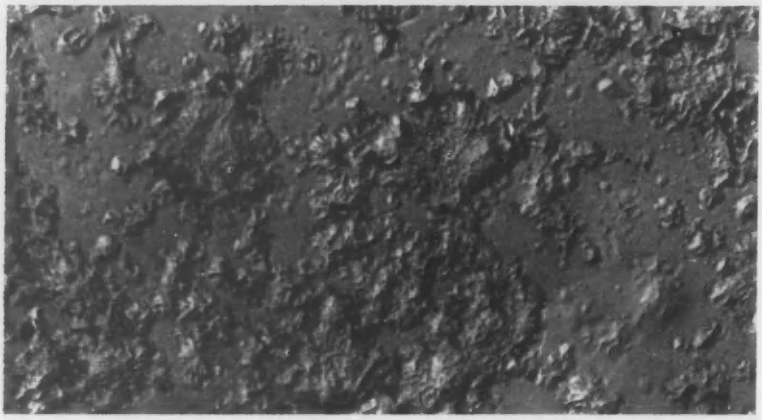

Fig. 13. Unaged film of 2:1 Pentalyn H and SBR 1500. Tack value 1000. 5600×.

11 and 13). In SBR 1011 the dispersed particles were roundish and ranged up to a few microns in diameter. In SBR 1500, on the the other hand, the roundish particles were wrinkled and had irregular margins.

The relationship between resin concentration and tack performance shown by Pentalyn H in polyisoprene and in SBR resembled the behavior of this same resin in natural rubber. However, the relationship did not hold when this resin, or different resins, were added to other elastomers. As discussed by Wetzel and Alexander in a forthcoming comprehensive paper on modified rosin tackifiers in adhesives based on synthetic elastomers,[4] the resins as a group did not behave as in the natural and synthetic polyisoprene systems. More specifically, the previously noted correlation between the resins' softening point and tack performance did not hold.

Fig. 14. Unaged film of 1:1 Pentalyn H and neoprene GRT. Tack value 1000. 5600×.

Fig. 15. Unaged film of 3:2 Staybelite ester 10 and neoprene WRT. Tack value 1000. 5600×.

Adhesives based on three different soft, crystallization-resistant neoprenes were examined. For Neoprene GRT the resin softening point—tack performance correlation applied, i.e., where maximum tack correlates inversely with the softening point of the resin. Such a correlation was less evident with Neoprene WRT and scarcely evident at all with Neoprene W. What did we find out about those neoprene–resin mixtures which had good adhesion? A one-to-one mixture of Pentalyn H and Neoprene GRT had good adhesion and an obvious two-phase character (Fig. 14). The resin phase was present as large irregular globules often several microns in diameter. At lower concentrations of resin, the dispersed particles were

smaller. In a film containing 60% Staybelite Ester* 10 (glycerol ester of hydrogenated rosin) and Neoprene WRT, a second phase showed up only as small pips (less than a micron) in the films (Fig. 15). The regions between those pips, although flat, were not as smooth as in the parent film consisting only of the Neoprene WRT. All the neoprene parents were smooth-surfaced. Finally, films which consisted of Cellolyn* 21 (phthalate ester of technical hydroabietyl alcohol) and Neoprene W were distinctive in their structure. Unlike any of the other films, those containing Cellolyn 21 had an overall pebbled or wrinkled character, as illustrated by Figure 16. The surface became coarser as the concentration of the resin increased. At 60% concentration, the size of the asperities was about 0.1 μ; at 67%

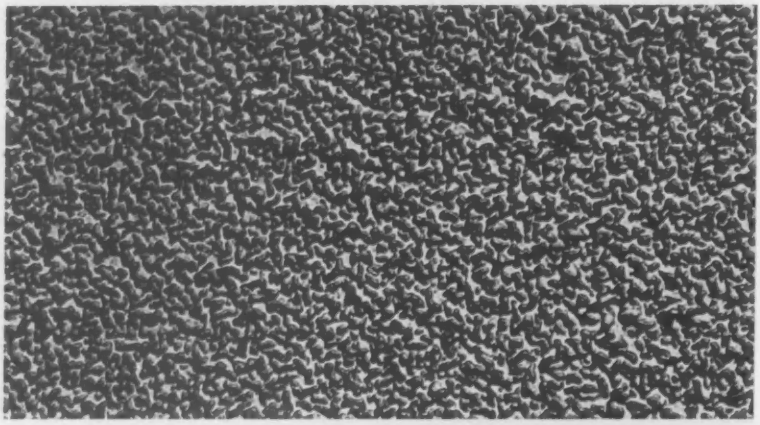

Fig. 16. Unaged film of 2:1 Cellolyn 21 and neoprene W. Tack value 1000. 5600×.

concentration, the size was several times as great. It is not entirely certain whether this structure should be interpreted as two-phase, such as we found in the other systems already discussed, or whether it represents simply a homogeneous material with a wrinkled surface.

When films which had high tack were aged to zero tack, by continued exposure to 200°F., they lost their two-phase character and became uniphase with smooth surfaces. This was true whether the elastomer was natural or synthetic. Furthermore, it was true regardless of the particular resin used in combination with the elastomer. What happens on aging may be this: The molecular weight of the rubber may change either by degrading or by crosslinking—or the composition may change by oxidation enough to alter the solubility relationships between resin and rubber. In any event, the resin and rubber become compatible, the readily-deformable dispersed phase is lost, contact with another surface is difficult, and adhesion is then no longer possible.

* Registered trademark, Hercules Powder Company.

SUMMARY AND CONCLUSIONS

What have we learned from these studies? More particularly, what have we learned about the morphology of pressure-sensitive films which help us to explain their behavior? Clearly, their most outstanding structural feature is their two-phase character. This is a structural circumstance common to adhesives based on both natural and synthetic elastomers. The pressure-sensitive masses appear to be homogeneous at low tackifier concentrations where the elastomer can completely dissolve the resin. At these low concentrations of resin the films have low tack. When more resin is added, a second phase forms and this is accompanied by an increase in tack. Adding still more resin increases the size and number of dispersed particles and also sharply increases the films' tack to a maximum, after which tack drops sharply. Tack appears to be more dependent on this second phase, evidently consisting of resin saturated with low molecular weight rubber molecules, than on the continuous phase, which consists of elastomer saturated with resin.

Recently, Dlugosz[5] described a somewhat similar situation in adhesives used to bond rayon or nylon tire cord to rubber. By immersing them in an aqueous dip, tire cords are coated with an adhesive whose principal components are resin and rubber. Examination of dried-down films of these adhesives revealed that the resin was present as a well-defined network enclosing the rubber globules. In short, the adhesive had a well-defined two-phase character.

In our pressure-sensitive adhesives what role does each phase play in bringing about good adhesion? Is their heterogeneous nature an advantage? We know, of course, that a good adhesive must both make and maintain good contact with the substrate. The modulus characteristics of unmodified elastomers are such that intimate contact with a surface can be made under pressure. However, once the pressure is removed, such systems recover elastically and withdraw from the surface. On the other hand, rosin-based tackifiers are hard, brittle glasses and cannot bring about short-time contact with any surface. When properly combined, however, the elastomer and resin form a two-phase system. The disperse phase is effectively a viscous fluid which can wet and flow to intimately contact a surface. But this viscous layer is so thin that failure cannot occur in it and ultimate adhesive properties are dependent on the predominantly elastomeric continuous phase. Thus, the dispersed phase contacts the three-dimensional microtopography of the substrate and the continuous phase carries the load.

References

1. Wetzel, F. H., *ASTM Bull.*, **221**, 64 (April, 1957).
2. Wetzel, F. H., *Rubber Age*, **82**, 291 (November, 1957).
3. Hock, C. W., and A. N. Abbott, *Rubber Age*, **82**, 471 (December, 1957).
4. Wetzel, F. H., and B. B. Alexander, to be published.
5. Dlugosz, J., *Electron Microscopy*, Vol. 1, Fifth International Congress for Electron Microscopy, Philadelphia, 1962.

JOURNAL OF POLYMER SCIENCE: PART C NO. 3, PP. 151–162

Morphology of Polyphase Solids

MARTIN C. BOTTY, *American Cyanamid Company, Stamford Research Laboratories, Research Service Department, Stamford, Connecticut*

INTRODUCTION

The blending of polymeric materials with other materials to impart desired physical properties has resulted in the appearance on the market of a variety of products ranging from ablating shields for space vehicles to zippers. In some cases, particulate or fibrillar units may be incorporated so as to impart greater toughness or tensile strength to the polymer. In other cases, viscous polymer syrups can be blended with glass rovings and then sprayed on hollow mandrels or forms; or the syrup may simply be allowed to flow into the interstices of sheets of glass cloth. Whatever the process and treatment may be, the demands for improvement and mass production of such products has been paralleled by an increasing interest among scientists to define the microstructures of these polyphase materials and to correlate morphology with inherent physical characteristics. By learning more about the means by which the desired physical attribute is produced, optimum conditions of synthesis can be achieved for consistent production of good quality products.

Many informative papers dealing with a wide range of materials, techniques, and instrumentation have been presented which enable us to learn more about polymeric materials. The application, accomplishment, and interdependence of microscopical methods are demonstrated by Claver and Merz[1] who used phase and electron microscopes to study heterogeneous polymer systems. Felton, Thomas, and Clark[2] in their investigation of complex fibrous systems employed the ultraviolet microscope. Another good example is Berry's[3,4] use of the light and interference microscopes for a better understanding of strength and fracture in plastics. New techniques and instrumentation will be forthcoming since the resinographer, like the metallographer, is constantly confronted with more complex materials and problems.

Sampling of molded polymers for microscopical study still presents certain difficulties because the characteristic region from the surface as well as from the subsurface has to be selected. Variations in texture in polyphase specimens could be induced by various reactions among the constituents, poor blending, or by turbulent or laminar flow during molding; therefore, it is important to be able to select differently located or oriented regions for critical evaluation. The molded surface can usually be examined directly

by reflected illumination in the light microscope; fine details of the surface texture can be duplicated by well established techniques of replication. The replica can then be examined electron microscopically.

Microtomy with the diamond knife has been used to expose internal detail, although the tendency for artifacts to develop at the sheared surface imposes limitations. The brittle-fracture technique is one way of minimizing the formation of artifacts. This method, which involves fracturing the specimen at Dry-Ice or liquid nitrogen temperatures, is not new. It was investigated initially in 1944 by Ladd[5] in his study of carbon-reinforced rubber systems and shortly thereafter in our laboratory to characterize the fine textures of polyphase systems of polymers.[9] Yet, during the past decade the electron microscopical study of brittle-fractures of such systems appears to have had only limited development and application. This is somewhat disappointing since it has been suggested by Evans[6] that fine-structured surface roughness over small areas of fracture sections might indicate the coexistence of separate phases. Others[7,8] have indicated that domain heterogeneity is a possible condition for increased strength. Since the brittle-fracture must be replicated for examination in the electron microscope, limited utilization of the method may be due in part to a lack of confidence in interpreting the electron micrographs. The purpose of this paper is to establish the validity of the brittle-fracture method by applying it to the examination of several polyphase systems to show that sublight-microscopic, particulate phases can be differentiated. These specimens consisted of a pigmented paint film, filled elastomers and commercially available impact resins.

SAMPLE DESCRIPTION

Paint Films and Elastomers

Several paint films were derived from experimental blends of vehicle and TiO_2 pigment formulated in our laboratory. The paint was applied to a metal surface and partially heat cured. Another metal strip was gently pressed in contact with the surface of the tacky paint film which was then baked until thoroughly dry. This arrangement made it possible to eventually brittle-fracture and expose the interior of the paint films.

A commercial grade of white, TiO_2-filled silicone elastomer and a carbon-reinforced "rubber" were brittle-fractured while in $^1/_8$ in. sheet form.

Impact Resins

The specimens used in this part of the study represent (*1*) a commercial grade of clear, thermoplastic polymer of relatively low impact strength and (*2*) a commercial polymer mixture used to fabricate high impact strength moldings. These materials, obtained in the form of pellets, were molded into small bars for tests and microscopical examination.

EXPERIMENTAL

The electron microscopist is always cognizant of the possibility of introducing artifacts which might lead to erroneous or limited interpretation of the micrographs. Consequently, he prudently will couple two or more techniques and use several methods of instrumentation to validate interpretation. The more complex the system, the greater the need to resort to complementary methods. The various methods used in the examination of the test specimens will be briefly described.

Brittle-Fracture Technique

The molded test bars, approximately $1/4 \times 1/2 \times 5$ in. in size, were notched, wrapped in aluminum foil and then cooled to about $-60°C.$ for two hours while in contact with solid CO_2. After removal from the Dry-Ice chamber, the aluminum wrapper was partially slipped off and the bars were fractured, in the vicinity of the notch, in a tensile tester whose specimen holder had been precooled with Dry-Ice. The bars were placed in a desiccator, allowed to dry and to attain room temperature.

It should be mentioned that it is not necessary for the specimen to be a bar. We have used the brittle-fracture technique on specimens which were in the form of sheets only about 1 mm. thick. These were scored with a needle, wrapped in foil and fractured, with a wedge-shaped edge while still in contact with granules of Dry-Ice. The aluminum foil prevented contamination and contained the fragments, most of which would have been lost when the specimen shattered. Before cooling and fracturing the thin sheets, the edges were abraded and marked with red ink so that the fractured surfaces could be readily identified.

The paint film, because of its extreme thinness, and the elastomers, because of their high extensibility, were brittle-fractured after cooling in the liquid nitrogen. Liquid nitrogen can be used for cooling the impact resin samples, although without careful precooling uncontrolled fracture frequently resulted in these relatively large bars due to thermal shock. Cooling to Dry Ice temperatures was generally found to be satisfactory for the impact resin samples.

GELATIN-SILICA REPLICA METHOD

This method of replication has been in use for almost twenty years. However, certain refinements used in this study should be mentioned. The concentration of gelatin in water solution, used for a first application, was maintained at 5% and was spread at a temperature of about 130°F. over the surface of the fractured specimen. The gelatin was dried at room temperature. Because of the rough, somewhat undercut surface of the fracture, a second layer of 10% gelatin-water solution was spread over the first one. The second layer, which was thoroughly dried in a desiccator, facilitated stripping of the gelatin from the rough specimen surface. Sufficient silica was vacuum-deposited to build up a silica layer about

150 A. thick on the side of the gelatin that had previously been in contact with the fracture-surface. Removal of the gelatin from a small square of the composite replica was accomplished in a one-liter water bath which was raised from room temperature to 150°F. over a one-hour period. The replica floating on the surface of the water had a tendency to fragment. By floating the gelatin-silica composite in a ring, having a one-inch inside-diameter, punched from a two-inch square of photographic paper or suitable material, the fragments could be conveniently contained and recovered. In the few instances where fragmentation was extreme, the silica side of the remaining portions of the composite replica was backed with a thin film derived from a 0.25% Formvar-ethylene dichloride solution. The gelatin was then removed from the water bath as just described, resulting in satisfactory silica replicas for examination in the electron microscope.

MICROTOMY WITH THE DIAMOND KNIFE

Microtomy with the diamond knife was a valuable aid in preparing cross sections of suitable thinness and quality for both ultraviolet and electron microscopical examinations of commercial impact resins. These resins had not been successfully sectioned by us with glass or steel knives and the liquid etching of flat surfaces frequently produced artifacts which confused interpretation. With the diamond knife and the Porter-Blum Ultramicrotome sufficiently thin, intact, plane-parallel sections, ranging from several tenths of a micron to below 800 A., were prepared directly from the tapered end of the polyphase test bars. The sections, which curled and were slightly wrinkled when cut, were made flat by floating them on warm water from which they were recovered on quartz slides for subsequent UV microscopical examination with 265 mμ emanation, or on 200 mesh screens for study in the electron microscope.

Some improvement in the quality of the cut sections was obtained when the specimen was cooled with a Dry-Ice collar. There was less distortion of the individual particles and the relatively low electron opacity of some of the larger particles indicated that they were actually being sectioned. This technique, currently being evaluated in our laboratory, can be considered an example of a brittle-fracture induced by the fine cutting edge of the diamond knife. The method is difficult to control. Fragmentation and a wide variation in the thickness of the cut samples, knife-chatter and condensation of ambient water vapor were some of the problems encountered. However, since only small areas of a cut section are required for electron microscopical examination, this method should not be overlooked, especially if modification of texture within and at the surface of a discontinuous phase is to be studied.

SMEAR TECHNIQUES

An important feature of this study was the development of the smear technique for validating the interpretation of the electron micrographs of

the silica replicas of the impact resins. The wet-smear method involved the partial solubilization or softening of a small fragment of the polymer chipped from the broken end of the test specimen. The fragment, which was swollen with a drop of chloroform for about 1 min., was then rapidly sheared between two glass slides. By applying sufficient pressure, electron microscopically thin films were formed which could be recovered by water flotation. In the dry-smear method, the fractured dry end of the test bar was streaked across the surface of the glass slide. The dry-smeared patches were thicker than the films formed by the wet-smear method. Both methods revealed enough detail to recognize the phases.

In a similar approach, an area selected from the fractured paint film was dissolved in solvent and centrifuged. The sediment was then smeared onto suitable substrates for examination in the electron microscope. With the elastomer samples, the adhesion of particles of carbon pigment to the silica replica enabled the morphology and the size-distribution characteristics of the discontinuous phase to be directly evaluated.

RESULTS

The silica replica of the brittle-fractured paint film shows the distribution of the particles as situated in the cured resin vehicle, Figure 1*A*. The single particles of TiO_2 and their small aggregates appear to be well dispersed, and well bonded to the continuous phase. This condition compared favorably with the good hiding characteristics of this particular paint formulation. Brittle-fracture was essential for exposing the interior of the paint film. Films that were not brittle-fractured pulled away from the metal strips or broke transversely so that there was insufficient internal surface for replication. Figure 1*B* shows that the size and shape of TiO_2 particles, recovered from the fracture-surface, and smeared onto an inert substrate, agrees with those of the sites of TiO_2 particles depicted in the replica of the paint film. Smearing the pigment particles altered the size and distribution of the aggregates; however, the isolation and identification of the discontinuous phase to validate its texture in the brittle-fracture was the main objective.

Figure 2 is a micrograph which shows the interior of the brittle-fractured sheet of filled silicone elastomer. Most of the particles of filler remained stuck to the positive silica replica. Those particles which were left behind are represented either as cavities or elevations in the replica. The extent to which distorting flow was minimized in another elastomeric material is illustrated in the micrograph (Fig. 3) of the brittle-fracture surface of natural rubber containing carbon black as the reinforcing agent. The gelatin-silica replicating process entrapped some of the carbon particles which fortuitously enabled them to be viewed directly. The pits and elevations, randomly scattered over the field of view, correspond to the distribution of the carbon black particles in the plane of the fracture. The average size of the observed carbon black particles, the discontinuous

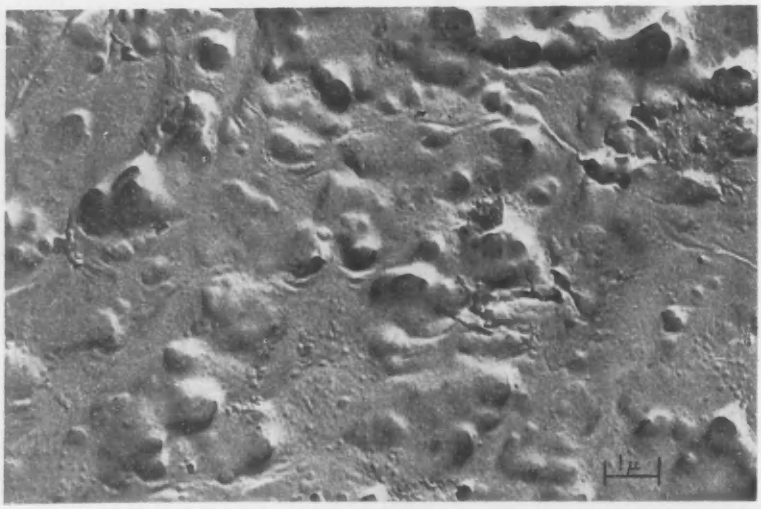

(*A*)

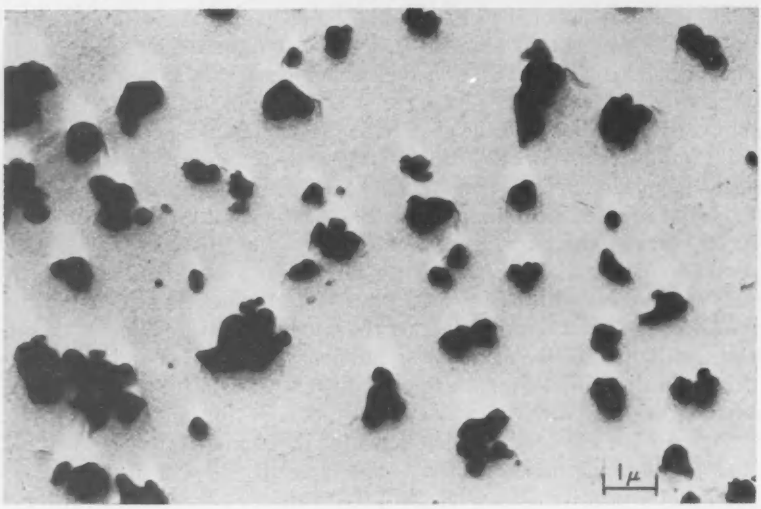

(*B*)

Fig. 1. (*A*) Brittle-fracture surface of paint film showing dispersion of TiO_2 pigment; silica replica. (*B*) TiO_2 particles recovered from paint film.

phase, is 500 A. The continuous rubber phase has a fine granular texture, the fundamental units of which are less than 90 A. in size and probably represent the rubber macromolecules.[9]

The results of the application of these techniques to the resinous test bars can now be evaluated. The importance of embrittlement to minimize

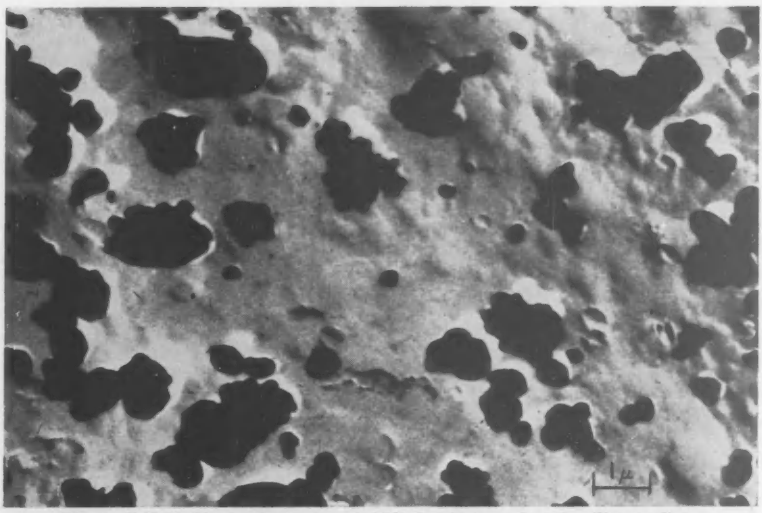

Fig. 2. Filled silicone elastomer; brittle-fracture surface;[9] silica replica.

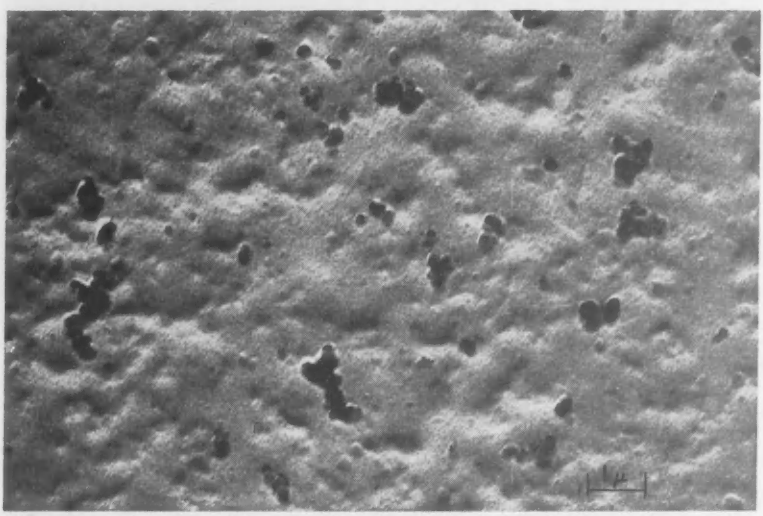

Fig. 3. Natural rubber reinforced with carbon black; brittle-fracture surface;[9] silica replica.

plastic flow through the plane of the fracture is evident from a comparison of the high-impact test-bar, fractured at room temperature and after being cooled to the temperature of dry ice. In the electron micrograph, Figure 4*A*, representing the fracture at room temperature, the unidirectional, poorly defined streaks tend to obliterate the evidence that an equant discrete phase was present in the original piece. The effects of the process of

preparation have overpowered those of the original process of manufacture so that interpretation of the latter is almost impossible.

However, when the same bar was embrittled at about −60°C. and then fractured, the significantly different texture, shown in Figure 4*B*, was observed. The sharply defined oval pits and bumps, and the intervening, randomly shaped, very smooth areas indicate that plastic flow has been

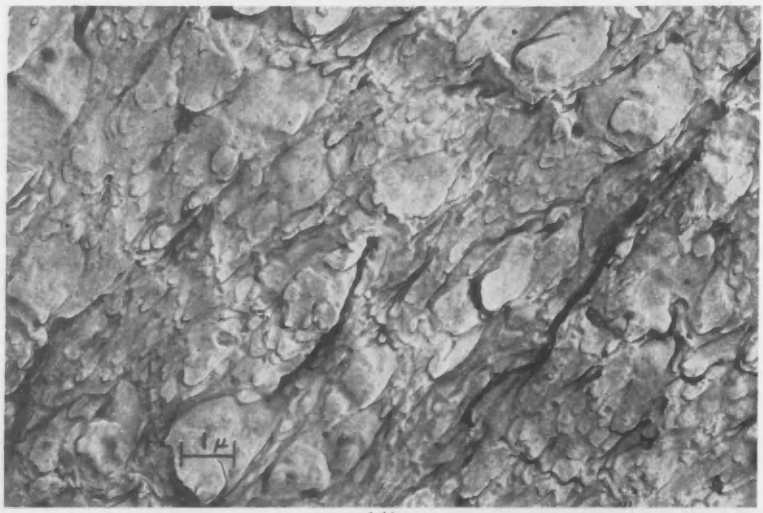

(*A*)

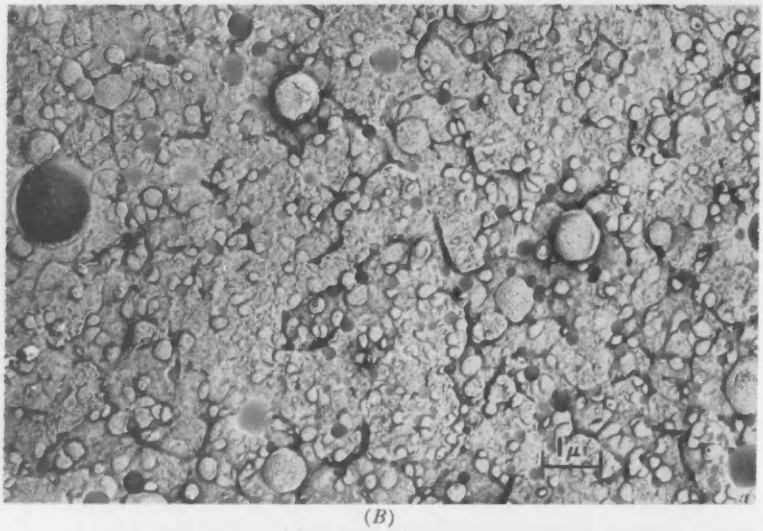

(*B*)

Fig. 4(*A*) and (*B*). See caption on page 159.

minimized. It was assumed that these variations in texture indicated the presence of two or more phases. In particular, the pits and bumps were believed to be related to the discrete phase. Application of the wet-smear technique, which produced the dispersion of particles shown in the electron micrograph, Figure 4*C*, confirmed this interpretation. The size of the individual particles entrapped in the thin film of soluble thermoplastic, i.e., the continuous phase in the molded bar, is in good agreement with the size range of the circular pits associated with the fracture surface.

Further verification of a disperse phase was obtained from UV and electron microscopical examination of thin sections. A section about 0.1 to 0.2 μ thick was cut at room temperature from the broken end of the bar and was viewed with 265 mμ UV emanation. Figure 5*A*, shows that the section had an overall low absorption, but was speckled with areas having significantly greater absorptivity, measuring 1–3 μ in diameter. Occasionally these areas of higher absorptivity reached dimensions of approximately 100 μ. Small areas of very low absorptivity were also occasionally observed.

The electron microscopical examination was conducted on a section about 500 A. thick, also cut at room temperature. In Figure 5*B* many single particles measuring between 500–1000 A. are visible. By number, the fine ultimate particles are more abundant than the compact aggregates. Thus, the observations made of the thin sections with the UV and electron microscopes are substantially in agreement. The overall low absorption seen with the UV microscope was due to the well dispersed, very small,

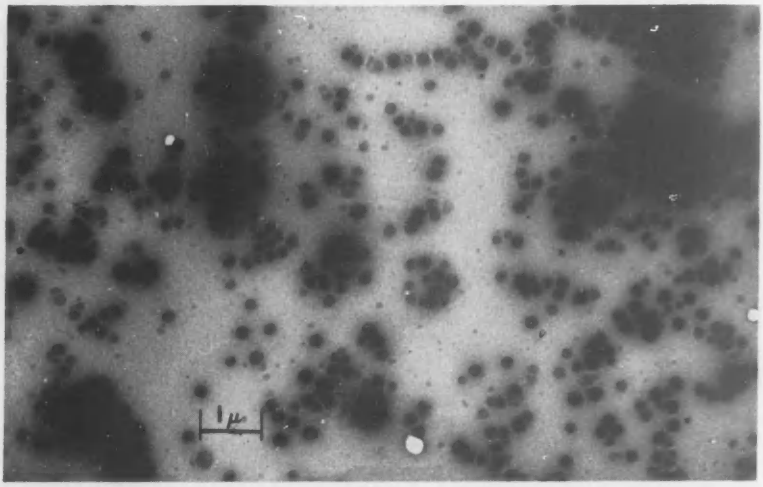

(*C*)

Fig. 4. (*A*) Polyphase, high impact, commercial test specimen fractured at room temperature; silica replica. (*B*) The same specimen as in (*A*) embrittled at about −60°C. and fractured; silica replica. (*C*) Smear of fragment from fractured end of commercial, high impact specimen.

single particles and the areas of higher absorption represented aggregates of these particles. The areas of lowest absorption corresponded to the continuous thermoplastic phase that was devoid of particulate inclusions.

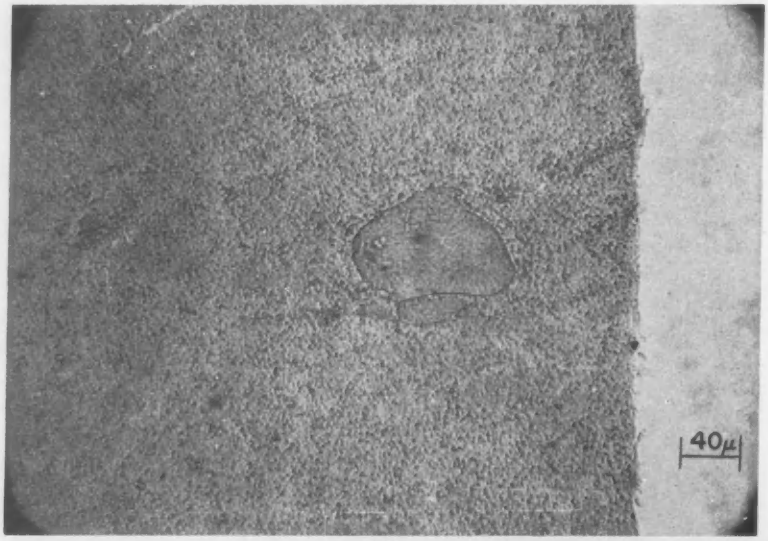

(*A*)

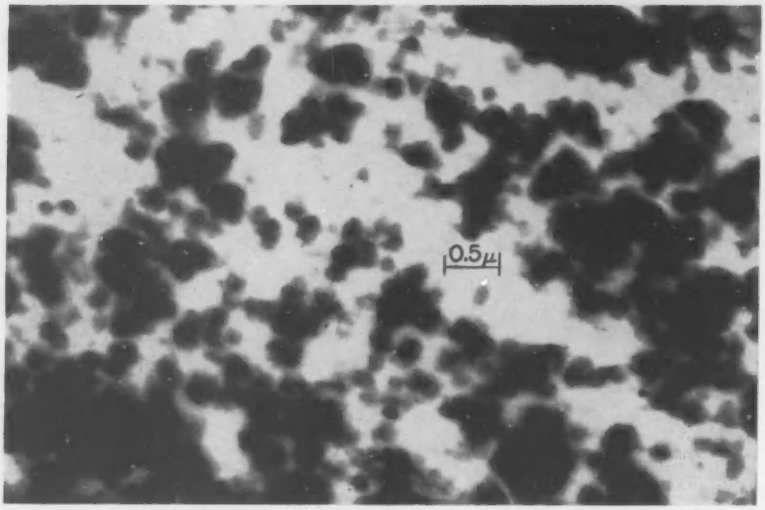

(*B*)

Fig. 5. (*A*) Cross section 0.1–0.2 μ thick, cut from commercial polyphase resin specimen, 265 mμ UV emanation; (*B*) Electron micrograph of section, approximately 500 A. thick, cut from commercial specimen.

These clear and grainy areas also have their counterparts in the replicas of the brittle-fracture surfaces.

The low impact-strength test-bar, consisting only of thermoplastic polymer, was brittle-fractured to determine the extent to which its texture

(*A*)

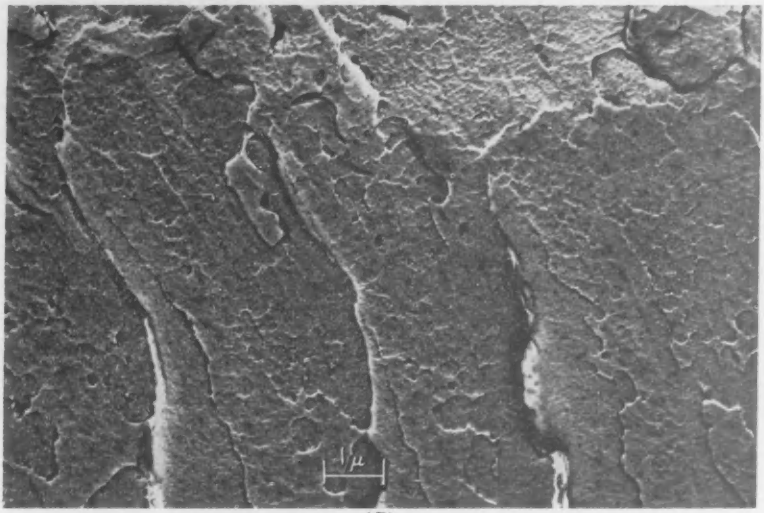

(*B*)

Fig. 6. (*A*) Brittle-fracture surface of low impact-strength, clear, commercial specimen; photomicrograph. (*B*) Brittle-fracture of clear test bar as in (*A*), viewed at high magnification. Silica replica.

might interfere with the detection of the particulate inclusions in the high impact strength bars. Figure 6*A* is a photomicrograph of a relatively large area which shows that the fracture-surface contained many irregularly shaped, patch-like configurations situated between coarse waves. The electron micrograph of this surface at high magnification, Figure 6*B*, shows variation in granular texture within and around these patches, but none of the grainy regions resembled the clearly defined pits and bumps associated with the blended polyphase bar of high impact strength, previously discussed. This type of texture was observed in other clear, unfilled bars that were similarly examined in a related study.

The examination of many polyphase samples by the brittle-fracture method has shown significant variations in phase distribution. By systematically coordinating the microscopical examination with variables introduced during product development, a better understanding of the how and the why of product performance was obtained. The study of soft elastomers and the much more rigid polyphase polymeric materials, as described herein, supports the validity of the brittle-fracture technique to show the internal morphology of polyphase solids.

References

1. Claver, G. C., Jr., and E. H. Merz, *Offic. Dig. Federation Paint Varnish Prod. Clubs*, **28**, 858 (1956).
2. Felton, C. D., E. J. Thomas, and J. J. Clark, *Textile Res. J.*, **32**, 57 (1962).
3. Berry, J. P., *J. Appl. Phys.*, **33**, 1741 (1962).
4. Berry, J. P., *Gen. Elec. Res. Bull.*, **Fall 1962**, p. 13.
5. Ladd, W. A., *Ind. Eng. Chem., Anal. Edition*, **16**, 642 (1944).
6. Evans, R. M., *The Mechanical Behavior and Microstructure of Impact Resistant Thermoplastics*, a thesis at Case Institute of Technology, University Microfilms, Inc., Ann Arbor, Mich., p. 64 (1962).
7. Hock, C. W., and A. N. Abbott, *Rubber Age*, **82**, 471 (1957).
8. Spurr, O. K., Jr., and W. D. Niegisch, *J. Appl. Polymer Sci.*, **6**, 585 (1962).
9. Rochow, T. G., and E. G. Rochow, *Science*, **111**, 271 (1950).

AUTHOR INDEX

Anderson, F.: 123
Berry, J. P.: 91
Botty, M. C.: 151
Bradford, E. B.: 41
Chen Hsia, C. S.: 105
Erath, E. H.: 65
Gillespie, T.: 31
Grabar, D. G.: 105
Hock, C. W.: 139
Keith, H. D.: 121
Moore, L. D., Jr.: 9
Peck, V. G.: 9
Price, F. P.: 117
Richardson, M. J.: 21
Robinson, M.: 65
Sasaguri, K.: 135
Statton, W. O.: 3
Stein, R. S.: 135
Symons, N. K. J.: 109
Vanderhoff, J. W.: 41
Wohnsiedler, H. P.: 77

SUBJECT INDEX

Amorphous polymers, molecular weights, 21
Colloidal particles, in thermosetting resins, 65
Electron microscopy, of molecular weights, 21
High polymers, spherulitic crystallization, 121
Intimate morphology, determination, 3
Matrix rigidity, to determine intimate morphology, 3
Molecular entanglement, in dilute polymer solutions, 31
Molecular weights, of amorphous polymers, 21
Morphology, crystalline polymers, 109
  large molecules in polyethylene, 9
  molded melamine-formaldehyde, 77
  polymer fracture surfaces, 91
  polyphase solids, 151
  pressure-sensitive adhesive films, 139
  synthetic latexes, 41
Polyethylene, isothermally bulk-crystallized linear, 123
  large molecules, 9
Polymerization, in the solid state, morphological aspects, 105
Polyolefins, morphology and deformation mechanisms, 135
Single crystals, grown from molten state, 109
Spherulite formation, kinetics, 117
Spherulitic crystallization, mechanisms and kinetics, 121
Thermosetting resins, colloidal particles, 65
Viscosity data, to assess molecular conformation and entanglement, 31